This is to certify that the
dissertation entitled

TISSUE-SPECIFIC *IN VITRO* AND *IN VIVO* EVALUATION OF TAMOXIFEN-MEDIATED GENE EXPRESSION

presented by

CORA JUNG-YEE FONG

has been accepted towards fulfillment
of the requirements for the

Ph. D degree in Biochemistry and Molecular Biology

Major Professor's Signature

12/7/07

Date

TISSUE-SPECIFIC *IN VITRO* AND *IN VIVO* EVALUATION OF TAMOXIFEN-MEDIATED GENE EXPRESSION

By

Cora Jung-Yee Fong

A DISSERTATION

Submitted to
Michigan State University
in partial fulfillment of the requirements
for the degree of

DOCTOR OF PHILOSOPHY

Department of Biochemistry and Molecular Biology

2007

ABSTRACT

TISSUE-SPECIFIC *IN VITRO* AND *IN VIVO* EVALUATION OF TAMOXIFEN-MEDIATED GENE EXPRESSION

By

Cora Jung-Yee Fong

Estrogenic endocrine disrupting compounds (EEDCs) are an environmental and human health concern and thus have become a focus for risk assessment characterization. The United States Environmental Protection Agency (US EPA) is considering screening 87, 000 chemicals for their potential endocrine disrupting properties and is currently developing assays for this purpose. An *in vitro* hepatic mouse tissue culture model, Hepa-1c1c7, was thus evaluated as a system to examine estrogenic gene expression responses. Hepa-1c1c7 cells exhibit gene expression changes in response to estrogen treatment, which correlate with those of an *in vivo* system, such as cytoskeletal reorganization and cholesterol metabolism. However, the magnitude of the differential gene expression responses did not warrant further examination with less potent estrogenic compounds.

The rodent uterotrophic assay has historically been used to evaluate estrogenic compounds and extensive literature has examined the effects of the potent estrogen mimic, 17α-ethynylestradiol (EE), on the uterus. This provided an excellent foundation for the characterization of tamoxifen (TAM)-mediated effects. The pharmaceutical tamoxifen is an estrogen receptor (ER) ligand which exhibits its anti-breast cancer effects by competing with estradiol for ER binding. In contrast, TAM elicits an estrogenic effect in endometrial tissue by promoting

proliferation. Its seemingly dual nature classifies it as a selective estrogen receptor modulator (SERM). Comprehensive microarray analysis complemented with physiological and histological data illustrated that TAM elicits gene expression changes which closely resembles those of EE, although for the most part muted in magnitude. In addition, EE-specific genes were identified which were consistent with the increased EE-mediated uterotrophic response compared to that of TAM.

Interestingly, historical studies have shown that mixed treatment of EE and TAM results in an inhibition of EE-mediated uterotrophy. An experimental design was developed to examine whether the mixed treatment physiology was due to global inhibition of gene expression. Surprisingly, only 10% of the genes exhibited a mixture-mediated response which differed from that of EE alone. These differential responses represented genes involved in cell growth and proliferation and were consistent with the inhibited physiology observed. These data suggest that TAM only modifies the expression of a subset of genes involved in eliciting a full uterotrophic effect under mixture conditions with EE and warrants investigation into the mechanisms of regulation involved.

ACKNOWLEDGEMENTS

This graduate school experience has shaped me in ways that I would never have anticipated. My anxiousness was soon overwhelmed with frustration, but I look back on this journey with much gratitude and satisfaction. I wouldn't have changed a thing.

To my advisor, Tim Zacharewski, I thank you for taking a chance on a green but eager undergraduate. He has provided me with an abundance of new learning opportunities and his academic, professional and personal guidance has been invaluable. My time at MSU has been incredibly rewarding from all the challenges which were presented to me. Thank your for your patience. My thanks also extend to the Zacharewski family; Jana, Lara and Nicholas, I'm going to miss all of you.

I could not have completed my research without the help and support of the ever changing members of the Zacharewski lab. Thanks to Robert Halgren, Yue-wern Huang, Jason Matthews and Mark Fielden for providing me a good experimental foundation. Darrell Boverhof, Josh Kwekel, Ed Dere, Suntae Kim, Ania Kopec and Qi Ding, without your assistance, this book would not exist. A special thanks to Kirsten Fertuck and Lyle Burgoon for helping me see the humour in everything and maintaining my sanity, particularly at the beginning of the trip. Of course I must acknowledge the endless number of co-op and undergraduate students who have helped out with projects, sought out advice or who were just fun to hang out with; I wish you all the best.

To my committee members, Drs. David Arnosti, Pam Fraker, Patty Ganey and Bill Henry: I am grateful for all your encouragement and patience. The input you have provided over these years have helped me to develop and hone my skills as a scientist. Thanks also to the excellent departmental staff for always being helpful in keeping all sorts of paperwork straight.

A great thank you goes out to my friends, old and new. Thank you, Eugenie, Nadia, Tori, Konrad & Sara, Marina, Len and Tao, for being around for the ride despite my infrequent calls and visits. Yes, I'm done now. Gabby, I am going to miss our coffee, good eating and music appreciation nights; you have been such a great support this past year.

My parents have been rooting for me throughout my entire undergraduate and graduate career; thank you. Many thanks, to my sister, Grace, who has recently become a great source of entertainment. You've been a great help.

Finally, I would like to express my gratitude to Jeremy Burt. Thank you for always being able to make me see the lighter side of things. He has been nothing but supportive, helpful and encouraging. Thanks for sticking it out for the long haul. /hug

TABLE OF CONTENTS

LIST OF TABLES

Chapter 2

Chapter 3

Chapter 4

LIST OF FIGURES

Chapter 1

Chapter 2

Chapter 3

Chapter 4

ABBREVIATIONS

4OH-TAM	4-hydroxytamoxifen
AhR	arylhydrocarbon receptor
AF	activation function
CA	concentration addition
DBD	DNA binding domain
DCC-FBS	dextran charcoal-coated fetal bovine serum
DDT	dichloro-diphenyl-trichloroethane
DES	diethylstilbestrol
DI	displacement index
DMT	*N*-desmethyltamoxifen
E2	17beta-estradiol
EDC	endocrine disrupting compound
EE	17alpha-ethynylestradiol
EEDC	estrogenic endocrine disrupting compound
ELISA	enzyme-linked immunosorbant assay
ER	estrogen receptor
ERE	estrogen response element
ERKO	estrogen receptor knock out
FSH	follicule stimulating hormone
GnRH	gonadotropin releasing hormone
HAT	histone acetylase

HMGB	high mobility group B
KO	knock out
LBD	ligand binding domain
LC/MS	liquid chromatography/mass spectroscopy
LECH	luminal epithelial cell height
LH	luteinizing hormone
MAPK	mitogen-activated protein kinase
MIX	mixture treatment (EE plus TAM)
MTT	3-[4,5-dimethylthiazol-2-yl]-2,5-diphenyl tetrazolium bromide
NERKI	non-classical estrogen receptor knock-in
NR	nuclear receptor
NTC	no template control
PAH	polyaromatic hydrocarbon
PCB	polychlorinated biphenyl
PND	post-natal day
QRT-PCR	quantitative real time-polymerase chain reaction
SERM	selective estrogen receptor modulator
SRC	steroid receptor coactivator
TAM	tamoxifen
TCT	Toxicogenomics Correlation Tool
US EPA	United States Environmental Protection Agency
UWW	uterine wet weight
WT	wild type

CHAPTER 1

GENE EXPRESSION RESPONSES ELICITED BY ESTROGENIC COMPOUNDS IN LIVER AND UTERUS

INTRODUCTION

Estrogenic compounds and their impact on human health are high priorities in the research field. In 1996, enactment of the Food Quality Protection Act (FQPA) and amendments to the Safe Drinking Water Act (SDWA) required the U.S. Environmental Protection Agency (EPA) to develop programs for the screening of endocrine disrupting compounds (EDCs). These have been defined as synthetic or natural chemicals which have an effect on humans that is similar to those produced by naturally occurring hormones—specifically estrogen, androgen and thyroid (1). These legislative changes arose in response to observed wildlife abnormalities due to chemical exposures such as the dichloro-diphenyl-trichloroethane (DDT)-mediated feminization of male gulls (2), increases in female estrogen levels and decreases in male testosterone in alligators exposed to dicofol and DDT (3) and deformities in *Xenopus* embryos associated with high levels of chemical agents (4).

Human exposure to EDCs is also an area of concern. For instance, world-wide polychlorinated biphenyl (PCB) contamination of fish (5-7) and led to studies assessing their toxicity and establishing safe human consumption guidelines (8). However, some compounds are examined due to their potential beneficial properties. Phytoestrogens are natural plant products demonstrated to

have estrogenic properties. Genistein is an isoflavone extracted from soybean. It is structurally similar to E2 and also exerts its mild estrogenic effects through ER binding (9). In Eastern Asia, where there is a high dietary intake of soy products, the incidence of breast cancer in women is lower compared to their Western counterparts (reviewed in (10)). Phytoestrogens have been used as a natural substitute in hormone replacement therapies but have caused concern with respect to being a potential breast cancer promoter (11).

In response to these environmental and health concerns, the Endocrine Disrupter Screening and Testing Advisory Committee (EDSTAC) was formed to aid in the development of an EPA program to make informed regulatory decisions on compounds. A tiered approach was adopted where by Tier 1 screening would aid in the identification of compounds which may interact with the endocrine system. Tier 2 testing would determine any adverse effects caused by the compound as well as characterize the relationship between dose and effect. At this time, compounds are being prioritized for testing and assays are being validated for the screening and testing phases.

ESTROGENIC COMPOUNDS AND THEIR EFFECTS

ESTROGENS AND ESTROGEN SIGNALING

Endogenous estrogens are comprised of a series of steroidal compounds which are primarily associated with the regulation of female growth and development. Deficiency in humans result in ambiguous external genitalia at birth, lack of maturation of reproductive organs, polycystic ovaries (12), and delayed bone structure development with a prolonged linear bone growth (13). Estrogens also play a role in male growth and development. Estrogen deficient males show no early signs of deficiency, but are diagnosed as adults with delayed bone structure development alongside prolonged linear bone growth (reviewed in (14)). Other studies have shown estrogen to be important in the maintenance of the cardiovascular, hepatic, skeletal and renal systems as well as promoting healthy lipid profiles (reviewed in (15)).

17β-Estradiol (E2) is the most abundant estrogen found in females and exerts its effects through the estrogen receptor (ER). In mammalian systems, two ER isoforms have been identified. ERα is found in uterine, ovarian, mammary, vaginal, epididymal, testicular, hepatic, adrenal and renal tissue while ERβ is found in ovarian, prostate, pulmonary and cerebral tissue (16,17). To further characterize the roles of each receptor, transgenic knockout mice have been developed for both receptors—αERKO and βERKO. αERKO females exhibit immature uterine structure, enlarged, polycystic ovaries, poor mammary duct development, and smaller stature, while males experience progressive testicular tubule degradation, nonfunctional sperm, delayed cardiac

depolarization, lower bone density and attenuated aggressive behavior. βERKO animals generally demonstrate normal organ structure and development, although female mice fertility is decreased (reviewed in (18)).

Nuclear Receptor Signaling

The ER belongs to a class of ligand activated transcription factors identified as the nuclear receptor (NR) superfamily. NR superfamily members share five distinct domain structures (19). Domain A/B contains a constitutively active activation function domain (AF1) which interacts with other transcription cofactors. Domain C is a highly conserved DNA-binding domain (DBD) which seeks out specific response elements in DNA enhancer regions. Domain D is a hinge region separating the DBD from the ligand-binding domain (LBD), domain E, and also serves as a ligand-dependent transactivation region, AF2. ER also contains an F domain which has been implicated in ligand-dependent differential transcription activity (20). Domains A/B, D and F have the lowest similarity between ER alpha and beta isoforms, while the DBD is highly conserved with 97% similarity (21) (Figure 1).

The classical mode of action of NRs involves dimerization with a partner protein followed by dimerized-complex binding to specific DNA sequences in the promoter regions of responsive genes. Co-regulating transcription factors and

Figure 1

Estrogen receptor domain structure

Estrogen receptor isoforms alpha and beta contain five major domains where the DNA binding domain (DBD) and ligand binding domain (LBD) share the highest amino acid sequence similarity. Activation function domains, AF1 and AF2, are located in the A/B and E domains, respectively.

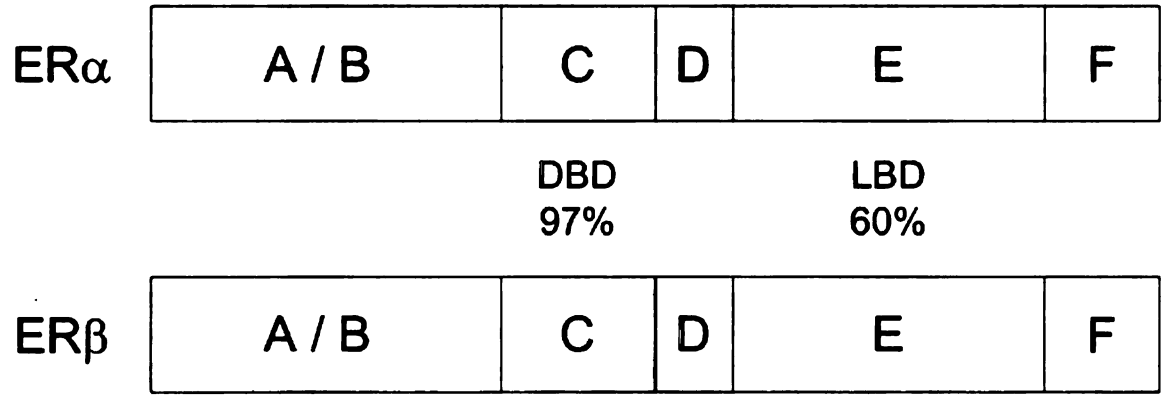

transcriptional machinery may then be recruited to the gene, leading to changes in basal transcriptional activation (Figure 2). Estrogens enter the cell and bind to nuclear residing ER. Ligand binding induces a conformational change causing the release of chaperone proteins such as heat shock protein 90 (Hsp90) (22). Activated ER complexes homodimerize allowing them to bind specific promoter sequences, known as estrogen response elements (EREs), of responsive genes. This DNA-bound complex may then influence changes in the transcriptional state of proximal genes through interactions with the basal transcriptional machinery and transcriptional cofactors (mechanism reviewed in (23)).

DNA-Response Elements

Response elements are short DNA sequences, found in the promoter and enhancer regions of primary responsive genes, which activated NR bind to with high affinity. NR specificity is determined by the nucleotide sequence. Through *in vitro* studies, a consensus ERE sequence (5'-GGTCAnnnTGACC-3', where n represents any nucleotide) has been identified (24). However, examination of other estrogen responsive genes have identified nucleotide substitutions in the ERE (reviewed in (25)). Bioinformatic and high-throughput approaches have also identified putative EREs in the mouse and human genome (26,27).

Interactions between EREs and ligand-bound ER may also induce receptor conformation changes. Peptidase digestion experiments have

Figure 2

Classical mechanism of estrogen receptor signaling

Estrogen receptor ligands diffuse into the cell and bind to the estrogen receptor located in the nucleus. Ligand binding induces a conformational change to release stabilizing chaperone proteins, such as Hsp90, and allow for dimerization of activated receptors. ER dimers may then bind to sequence specific estrogen response elements (ERE) in the promoter region of estrogen responsive genes, recruit co-regulating proteins and transcriptional machinery to drive changes in mRNA expression.

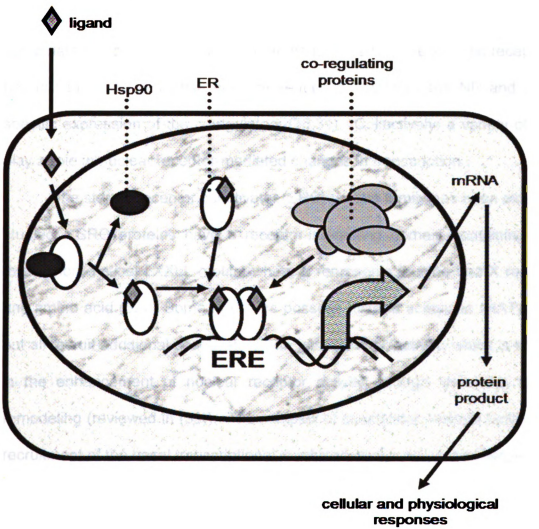

demonstrated that ligand-bound ER, incubated with different ERE sequences, exhibit varied electrophoretic fragment patterns (28). Similarly, phage-display ELISA assays have identified different exposed epitopes on the active ER complex when it is bound to different ERE sequences (29). Thus, ER conformation affects what subset of co-regulating proteins can be recruited and subsequently influence transcriptional changes to proximal genes.

Co-regulatory Proteins

Co-regulating proteins pose as a bridge between the AF2 domain of DNA-bound nuclear receptors and basal transcriptional machinery. The subset of coregulators recruited to a NR is determined in part by the specific receptor, the bound ligand, the response element sequence bound by the NR and the cell-specific expression of the coregulators (30,31). Collectively, a variety of factors play a role in nuclear receptor-mediated changes in transcription.

The steroid receptor coactivator (SRC) protein family has been extensively studied. SRC proteins have a receptor-interacting domain containing two or three short, helical LXXLL motifs, where L represents leucine and X represents any amino acid (32). Some members possess histone acetylase (HAT) activity, but all recruit additional coactivators with intrinsic HAT activity, which is important in the enhancement of nuclear receptor activity through chromatin structure remodeling (reviewed in (33)). The complex of coactivator proteins facilitates the recruitment of the basal transcriptional machinery to the responsive target genes.

Coregulators have also demonstrated their influence on nuclear receptor binding to specific response elements. Affinity binding assays have demonstrated that the presence of high mobility group B (HMGB) coactivators increases the affinity of estrogen-bound ER to consensus ERE sequences, and that different members of the co-regulatory family also affect the degree of affinity (34).

Non-classical Signaling Mechanisms

In addition to the classical NR signaling, ER can elicit activity using other pathways (23). Growth factors may initiate MAPK signaling pathways to phosphorylate specific serine residues found in the ER AF1 domain, allowing interaction with coactivators to modify gene expression (35). ER activated in this manner is capable of tethering to Fos/Jun complexes at AP-1 sites and Sp1 complexes at GC-rich regions to drive differential transcription (36,37). Recently, it has been proposed that ERs can also exist in a membrane-bound state. This form has been proposed to activate signaling cascades which are too rapid to involve genomic responses, such as the influx of extracellular calcium by mast cells (38).

Estrogen signaling is a complex network and can thus be interrupted at various nodes.

ESTROGENIC ENDOCRINE DISRUPTORS

Xenobiotic compounds which disrupt normal estrogen signaling are known as estrogenic endocrine disruptors (EEDs). EEDs are structurally diverse and found as natural products, pharmaceuticals, industrial compounds, pesticides and other environmental contaminants. Disruption of estrogen signaling may affect enzymes involved in estrogen production or metabolism, influence ER expression levels or compete with endogenous estrogens for ER binding (reviewed in (10,39)).

Although the EPA is focused on EED exposure through food and water (40), some research is focused on pharmaceuticals which are directed at disrupting endocrine systems. For example, 17α-ethnylestradiol (EE) is the main component in female contraceptives. It is structurally similar to E2 and its effects mimic that of endogenous estrogen *in vivo* and *in vitro* (41). Diethylstilbestrol (DES) is another ER-binding pharmaceutical, which was first prescribed to pregnant women in the 1940s to prevent miscarriages. In 1971, it was associated with the development of vaginal cancer in female offspring to women prescribed DES (42) and further research has demonstrated the teratogenic properties of DES.

TAMOXIFEN AS AN ENDOCRINE DISRUPTOR

Tamoxifen (TAM) was first developed in the late 1960s and initially prescribed as a fertility drug (43). TAM was subsequently examined for potential anti-cancer activity, an application for which it proved successful (reviewed in (44)). TAM was approved in 1977 for treatment of ER-positive breast cancer. TAM exerts its effects through direct binding to the ER, thus competing with endogenous estrogens that otherwise promote proliferation and cancer progression (45). Consequently, TAM is less effective against ER-negative breast cancers.

TAM is effective for suppressing cancer recurrence by 50% as well as inhibiting contralateral primary breast cancer. In addition, women identified at high risk for breast cancer have a significantly reduced risk of developing cancer with prophylactic TAM treatment (46).

Three TAM metabolites also exhibit antiestrogenic activity, 4-hydroxytamoxifen (4OH-TAM), *N*-desmethyltamoxifen (DMT) and 4-hydroxy-*N*-desmethyltamoxifen (endoxifen) (Figure 3). 4OH-TAM is a potent metabolite due to its high ER binding affinity (47-50). DMT exhibits low ER binding affinity (51) but is the major human metabolite (52). Recent studies with endoxifen suggest that it my be more potent than 4OH-TAM (53,54). Moreover, human plasma concentrations indicate that endoxifen levels (12.4 ng/mL) are greater than that of 4OH-TAM (1.1 ng/mL) (55).

Figure 3

Metabolism of tamoxifen

Tamoxifen is metabolized into bioactive metabolites 4-hydroxytamoxifen, *N*-desmethyltamoxifen, and 4-hydroxy-*N*-desmethyltamoxifen.

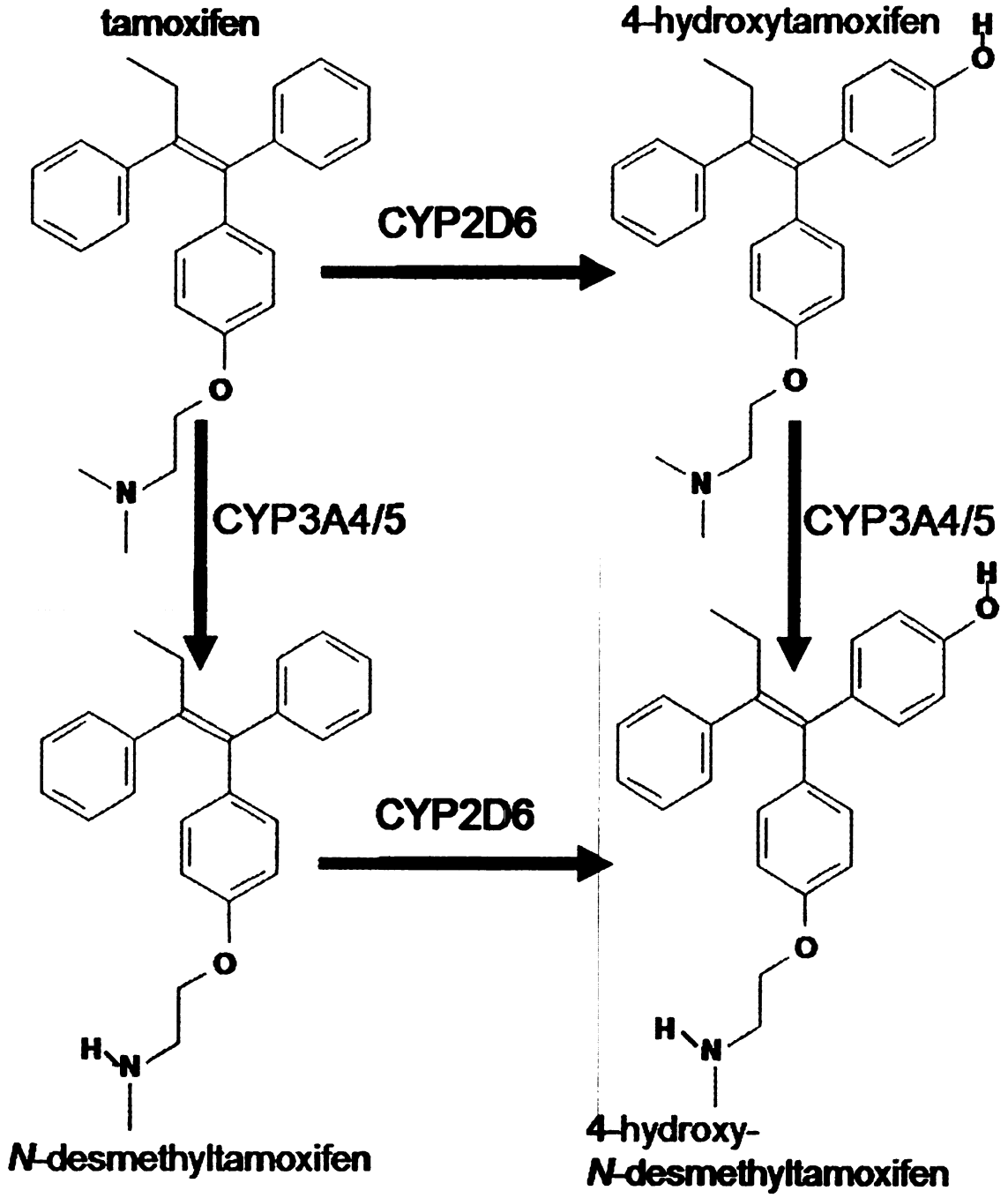

TAM metabolism differs between species. Studies between rodents and humans have shown that TAM *N*-oxide, 4OH-TAM and DMT are the predominant metabolites in the mouse, while DMT is the major human metabolite in microsomal studies (56,57). In rodents, the levels and rates of TAM metabolism to 4OH-TAM and DMT were significantly different in the rat and mouse, where the rat metabolite profile more closely resembles human profiles (52). Such studies illustrate that differences metabolism between models should be considered in extrapolations for risk assessment.

Despite the high therapeutic index of TAM, its adverse effects include a two-fold increase in risk to develop endometrial cancer (58). Cases of endometrial cancer have been reported as early as two years after commencement of treatment (59); however, it is unclear whether TAM is an initiator in the carcinogenesis process. Due to the seemingly opposing effects in mammary and endometrial tissues, TAM is classified as a selective estrogen receptor modulator (SERM).

SERMs are pharmaceuticals with differential tissue effects and are often prescribed for specific conditions. Numerous factors influence the effects of a SERM-bound receptor such as tissue-specific ER isoform expression levels, ligand-induced ER topology, chromatin structure, and coregulator protein expression and distribution (46,60-62). A well studied factor in the SERM property of TAM is the conformation it confers on the ER. The ER-LBD is a 12-helical structure where the position of helix-12 has been identified as a key factor

in differentiating ligand-dependent agonistic and antagonistic effects (63). Helix-12 acts as a lid to encase the bound ligand in the LBD.

Full agonists, such as E2 and EE, induce a conformational change that closes helix-12 over the ligand binding pocket, providing an interface for coregulator protein interactions. Ligands classified as partial agonists typically have bulky side groups that protrude from the pocket displacing helix-12 from its agonist position affecting coactivator docking (64). In the case of full agonist ICI 182,780, binding causes conformational changes exposing hydrophobic surfaces that target the ER for degradation (65). Although TAM-binding causes ER-LBD to adopt a conformation with an unfavourable helix-12 position (66), which may be important in its role as an anti-estrogen in the mammary, it has been suggested that high levels of expressed steroid receptor coactivator 1 (SRC1) in uterine tissue may be a determinant in the agonistic effects of TAM in the uterus (31). However, the influence of these factors on gene expression is poorly understood and warrants further investigation.

RATIONALE, HYPOTHESIS AND SPECIFIC AIMS

The research presented utilizes a microarray approach to comprehensively examine gene expression changes elicited by EE and TAM, alone, as well as in combination.

PROJECT 1: ESTROGENIC ACTIVITY ON THE LIVER

Reproductive tissues have been the focus of the majority of estrogenic studies, although many tissues not classically regarded as targets of estrogen also exhibit gene expression changes in response to estrogens. ERE-mediated transgenic mouse studies that can monitor ER-mediated gene expression have identified the liver to be one of the most estrogen-responsive tissues (67,68). Modulation of lipid transport and metabolism by estrogens in the liver has been well documented (69,70), although its mechanisms have not been fully elucidated. Xenobiotic compounds are delivered to hepatic tissue upon oral exposure; thus, it is important to examine the effects modulated by exposure EEDCs.

THE HEPATIC SYSTEM

Although the liver is not a classical estrogen-responsive tissue, it expresses ER (16) and exhibits changes in gene expression in response to estrogens (67,68). Studies of estrogens on the liver have focused on the biliary system, where primary biliary cirrhosis (autoimmune destruction of liver bile ducts) is more prevalent in females (71), as well as on lipid profiles, where

hormone replacement therapy decreases cholesterol, but increases triglyceride levels (72). Microarray analysis of *in vivo* hepatic responses to estrogen identified changes in gene expression associated with a wide array of pathways including proliferation, cytoskeletal organization, oxidative stress and lipid metabolism (73).

In response to EDSTAC's prioritized chemical screening and testing recommendations, EPA implemented the Endocrine Disruptor Screening Program (EDSP) to develop testing assays. In addition to receptor binding studies, *in vitro* transcriptional assays were to be developed for compound screening. Due to its estrogen responsiveness, investigation of a comparable hepatic *in vitro* model was warranted.

IN VITRO HEPATIC MODEL SYSTEM

Cell culture models are advantageous as they reduce animal experimentation and are amenable to high-throughput testing. Homogeneous cells are expected to exhibit less variability and facilitate the investigation of cell-type specific effects which may otherwise be masked in a heterogeneous tissue.

Mouse Hepa-1c1c7 hepatoma cells were selected as this line is commonly used in the field of toxicology, particularly in aryl hydrocarbon receptor (AhR) mechanism-related studies. (74,75). This model was derived from a BW 7756 hepatoma which arose in a C57L mouse and propagated in C57L/J mice (76). Hepa-1c1c7 cells possess active ERs (77,78) and retain several liver-specific

functions such as synthesis and secretion of albumin (76) and transferrin (79) as well as xenobiotic detoxification activity (80).

Hypothesis:

Estrogenic compounds elicit species conserved time- and dose-dependent hepatic gene expression profiles between *in vitro* hepatoma models.

Specific Aims

The following specific aims were proposed to address the hypothesis:

1) Establish baseline gene expression in response to E2 in mouse, rat and human hepatoma cell lines.

2) Establish an estrogenic expression fingerprint by examining common gene expression changes elicited by structurally diverse EEDCs in a selected hepatoma model.

3) Propose an estrogen receptor-regulated biological response network.

As detailed in Chapter 2, responses associated with proliferation, cytoskeletal reorganization, cholesterol transport and metabolism, fatty acid metabolism, and oxidative stress were well conserved between various models and the Hepa-1c1c7 cells. Some genes demonstrated common activation between estrogen-treated liver of C57BL/6 mice and Hepa-1c1c7 cells and exhibited temporally shifted expression patterns. Despite these similarities, the

magnitudes of gene expression changes elicited by the *in vitro* model were weak and did not warrant further development as a screening or testing system (81).

Although *in vivo* and tissue-culture *in vitro* models demonstrated limited overlap in estrogenic responses, development of other *in vitro* systems may prove to be better *in vivo* predictors such as tissue slices (82). Three-dimensional architecture and signaling between different cell types may be required for accurate gene expression profile responses.

PROJECT 2: THE EFFECT OF TAMOXIFEN ON THE UTERUS

Due to the difficulties encountered in Project 1, a more reliable estrogen responsive model was selected—the immature, ovariectomized mouse uterus. Tamoxifen was selected as an ER ligand of interest due to its SERM properties.

Tamoxifen and its role in breast cancer prevention have been well studied (reviewed in (83)); however, its increased risk in endometrial cancer remains poorly understood. In addition, previous studies have demonstrated that co-treatment of TAM and estrogen result in repression of estrogen-induced, rodent uterotrophy (84,85). However, the molecular basis of the repression has yet to be fully elucidated and a comprehensive experimental design was developed to associate gene expression to the uterotrophic response.

Hypothesis

Tamoxifen antagonizes EE-mediated uterotrophic responses associated with globally antagonized EE-induced gene responses.

Specific Aims

The following specific aims were proposed to address the hypothesis:

1) Establish baseline dose response and temporal gene expression profiles following oral exposure of TAM in the C57BL/6 mouse uterus.

2) Identify the optimal doses of TAM resulting in maximal inhibition of EE-induced uterotrophy.

3) Identify EE-elicited temporal gene expression affected by TAM that may contribute to the inhibition of the induced uterotrophic response.

ESTROGEN ACTIVITY ON THE UTERUS

Estrogen plays an integral role in the maintenance of the female reproductive cycle.

The Menstrual Cycle

In female primates and humans the effects of estrogen signaling on the uterus during the menstrual cycle have been extensively studied. The menstrual cycle is divided into four phases: 1) follicular phase, 2) ovulation, 3) luteal phase and 4) menstruation.

During the follicular phase, gonadotropin releasing hormone (GnRH) is secreted by the hypothalamus to stimulate luteinizing hormone (LH) and follicle stimulating hormone (FSH) release from the anterior pituitary gland. FSH stimulates follicular maturation and positively regulates estrogen release to mediate proliferation of stromal and epithelial cells of the uterine endometrium.

Feedback regulation of estrogen on FSH decreases FSH secretion. This phase is complete once estrogen levels accumulate to cause an LH surge, leading to ovulation. The luteal phase is initiated by the LH surge during which the follicle develops into a corpus luteum. Throughout these phases, uterine endometrium continues to proliferate and progesterone, released by the corpus luteum, aids in its development (86). If no fertilization event occurs, the endometrium is shed during menstruation. Estrogen and progesterone levels decline, releasing inhibitory signals to diminish FSH levels and re-initializing the cycle.

The Estrous Cycle

Other placental mammals undergo an estrous cycle, which differs primarily from the menstrual cycle where the developed endometrium is reabsorbed rather than shed through menstruation. The estrous cycle is also separated into four phases: 1) proestrus, 2) estrus 3) metestrus and 4) diestrus.

Proestrus is analogous to the follicular phase, where by signals are initiated to cause follicle maturation and endometrial proliferation. Estrogen levels peak to stimulate estrus, an LH surge and ovulation. At this stage, the uterus has reached maximal endometrial proliferation and vascularization. Estrus is the phase during which females are most sexually receptive. Decline in estrogen, FSH and LH due to no fertilization leads to metestrus where uterine epithelium begin to degenerate and a corpus luteum begins to develop. Finally, the corpus luteum matures during diestrus releasing progesterone and the uterus reverts back to an atrophic state.

IN VIVO MODEL AND THE UTEROTROPHIC ASSAY

An immature rodent model has long been a gold standard to evaluate compound estrogenicity due to its reproducibility and reliability to identify compounds which exert its effects through an estrogenic mechanism of action (87,88). The specific model utilized in the outlined studies is an estrogen sensitive (89) immature, ovariectomized, C57BL/6 female mouse. An immature mouse provides a low background system in which estrogen treatment can exhibit maximal physiological effects. Ovariectomizing allows continued development of organs for analysis without the confounding effects of circulating estrogens. Moreover, the mouse genome annotation is extensive, comprising approximately 28 000 unique transcripts (90), which aids the construction of estrogen-modulated pathways in gene expression analysis experiments.

The uterotrophic assay consists of three daily doses of compound through subcutaneous injection or oral gavage. Compounds are classified as estrogenic if increases in uterine wet weight (UWW), due to a combination of increased cellular hypertrophy, hyperplasia and water imbibition, are observed. Histological hallmarks of uterotrophy include increased luminal epithelial cell height (LECH), increased luminal circumference, luminal epithelial invagination, stromal edema, and increased glandular epithelium (91).

TRANSGENIC MODELS TO EXAMINE ESTROGEN RECEPTOR SIGNALING

To further elucidate the roles of estrogen signaling in the uterus, several transgenic models have been developed. αERKO mouse uteri maintain all

uterine cell types, however, tissue strata are smaller when compared to wild type (92). These mice are infertile and do not undergo uterotrophy upon estrogen treatment (92). ERβ is not as prominently expressed in the uterus as its alpha counterpart (93,94) and βERKO mice are subfertile, due to diminished ova maturation and subsequent release from the ovaries (95). These models illustrate the importance of ERα in uterine development and function.

More recently non-classical ERα knock-in (NERKI) mice have been developed. A single ER allele mutant, that does not bind DNA, was developed (96) and introduced into embryonic stem cells to create NERKI mice (97). NERKI mice have a double alanine mutation (AA) in the zinc finger region of the ER DBD and were used to characterize non-classical ER signaling where the receptor is required to tether to other DNA bound proteins to influence transcription of estrogen-responsive, non-ERE containing genes (96). NERKI (AA/+) mice exhibit uterotrophy upon E2 and TAM treatment, but a smaller increase in UWW compared to treated WT mice, and NERKI females are infertile (97).

True non-classical signaling cannot be examined in the NERKI mice as a wild type ERα allele is still present. Thus, NERKI (AA/+) males were crossed with ERα +/- females to generate mice with no classical ER signaling capabilities (AA/-) and compared with αERKO (-/-) and wild type (+/+) mice (98). Uteri of AA/- mice demonstrated a physiology intermediate to those of KO and WT mice where AA/- uterine wet weight, radius, inner circular muscle and luminal epithelial height were significantly greater than those of KO mice, but significantly less than

those of WT (98). Responses to estrogen treatment further illustrated the roles of classical and non-classical ER signaling in mouse uterus. Increases in luminal epithelial cell height occurs in AA/- mice suggesting that non-classical signaling is adequate to stimulate this response; however, stromal proliferation was only stimulated in WT mice, indicating its dependency on the classical ER mechanism (98).

CHEMICAL MIXTURES

The field of risk assessment examines the effects of compounds on human health and environmental organisms. Data from these studies provide information to agencies which prioritize these potential hazards and determine methods to regulate high risk factors. Efforts to elucidate the mechanisms of action of individual compounds allows for the association of adverse affects by specific chemicals and classes of chemicals. However, wildlife and human exposure to compounds primarily occur as complex mixtures; thus, efforts to examine mixture effects for risk assessment purposes are warranted. An approach has been developed by the EPA Superfund Program Office which involves the identification and characterization of individual chemicals before examining mixtures (99).

MIXTURE EFFECTS

Effects by mixtures can generally be classified as additive, antagonistic or synergistic. Additive effects are those where the combined treatment results in

an effect which is comparable to the sum of the responses elicited by each individual treatment; for this reason, they are also known as concentration-addition (CA) effects. Additive effects are also considered to be non-interactive as each compound induces an expected degree of response despite the presence of another compound (100). Studies of various species have demonstrated that mixtures of compounds, particularly pesticides, acting through similar modes of action result in additive responses for growth and lethal endpoints (101,102). These studies also demonstrated that the majority of mixtures comprised of compounds with differing modes of action elicit concentration-addition; however, some demonstrated less-than-additive effects while others resulted in greater-than-additive effects (101,102). Although CA predictions are likely adequate for the purposes of risk assessment, identifying and characterizing the combinations of compounds which elicit different-than-additive effects is important.

Synergistic effects are those which exhibit responses greater than the sum of the individual responses. These responses are of interest as the use of the CA theory to risk assessment underestimates the potential adverse affects demonstrated by compound mixtures eliciting synergy. Studies of pesticide mixtures in the environment suggest that atrazine herbicides in combination with organophosphate insecticides resulted in greater-than-additive effects on the locomotive ability of certain invertebrate species (103). Moreover, this mixture represents compounds which exhibit potentiation, in which one compound that

does not exhibit high toxicity, atrazine, increases the expected toxic effect of the second compound, organophosphate.

Other studies have identified compounds that demonstrate synergism through the mechanistic examination of specific signaling pathways. It has been shown that the aryl hydrocarbon receptor (AhR) signaling pathway and its influence on cytochrome P450, family 1 (CYP1A) induction are important mediators in xenobiotic toxicity in mammals (reviewed in (104)). Studies indicate that CYP1A knockdown in killifish and zebrafish embryos result in greater-than-additive effects in the presence of polyaromatic hydrocarbons (PAHs), but not dioxin-like compounds (105). Thus the presence of PAHs with potential CYP1A inhibiting compounds in the environment appears to be a greater hazard for some aquatic species and should be re-evaluated where current risk assessments suggests application of an additive model (106).

Less-than-additive effects are also known as negative interactions or antagonistic effects. Identification of these effects allow for prioritization of compounds with respect to risk assessment. For example, Aroclors are commercial mixtures of PCBs that are immunosuppressive. However, some combinations containing greater concentrations of coplanar PCBs, such as 3,3',4,4'-tetrachlorobipheyl, 2,3,3',4,4'-pentachlorobiphenyl and 2,3',4,4',5'-pentachlorobiphenyl, result in a less-than-additive effect (107). Thus, sites containing high levels of these particular congeners may need to be assessed differently from other PCB contaminated areas with congeners exhibiting additive properties.

Currently, the additive model is still the assumed model for untested chemicals, particularly at concentrations which demonstrate no observable adverse effect (108). It has been recommended that tests should be carried out rather than blindly accepting the assumption (109).

Due to the complexity of chemical mixtures, models to predict the effects of compounds are continually being developed and refined (110-113). These models need to take into consideration the mode of action of the compounds, the dose and temporal range of responses exhibited by each compound (111,114), the pharmacodynamics of the compounds on various tissues (115), and the toxicodynamic and toxicokinetic between the compounds of interest (116).

It is clear that the data collected through mixture studies will be invaluable to the field of risk assessment; however, additional research is necessary in developing study designs to examine effects and generating statistical models for predictive toxicology. Moreover, few studies examine temporal effects of mixture treatments; thus, development of appropriate temporal study designs and establishment of accurate temporal models are warranted. The approach utilized in Chapter 4 offers an experimental design which can be critically evaluated for future studies of mixed-compound affects on gene regulation.

CHAPTER 2

EFFECTS OF CULTURE CONDITIONS ON ESTROGEN-MEDIATED HEPATIC *IN VITRO* GENE EXPRESSION AND CORRELATION TO *IN VIVO* RESPONSES[1].

ABSTRACT

Refinement of *in vitro* systems for predictive toxicology is important in order to develop high-throughput early toxicity screening assays and to minimize animal testing studies. This study assesses the ability of mouse Hepa-1c1c7 hepatoma cell model under differing culture conditions to predict *in vivo* estrogen-induced hepatic gene expression changes. Custom mouse cDNA microarrays were used to compare Hepa-1c1c7 temporal gene expression profiles treated with 10 nM 17β-estradiol (E2) in serum free and charcoal-stripped serum supplemented medium at 1, 2, 4, 8, 12 and 24 hrs. Stripped serum-supplemented medium increased the number gene expression changes and overall responsiveness likely due to the presence of serum factors supporting proliferation and mitochondrial activity. Data from both experiments were compared to a gene expression time course study examining the hepatic effects of 100 μg/kg 17α-ethynylestradiol (EE) in C57BL/6 mice at 2, 4, 8, 12, 18 and 24

[1]Data contained in this chapter have been published.
Fong CJ, Burgoon LD, Zacharewski TR. 2005. Comparative microarray analysis of basal gene expression in mouse Hepa-1c1c7 wild-type and mutant cell lines. Toxicol Sci. 86(2):342-53.

hrs. Only 18 genes overlapped between the serum free and *in vivo* studies, whereas 238 genes were in common between Hepa-1c1c7 cells in stripped serum data and C57BL/6 liver samples. Stripped serum cultured cells exhibited E2-elicited gene expression changes associated with proliferation, cytoskeletal re-organization, cholesterol uptake and synthesis, increased fatty acid β-oxidation and oxidative stress, which correlated with *in vivo* hepatic responses. These results demonstrate that E2 treatment of Hepa-1c1c7 cells in serum supplemented medium modulate responses in selected pathways which appropriately model estrogen-elicited *in vivo* hepatic responses.

INTRODUCTION

Predicting human toxicity typically involves the extrapolation of *in vitro* and non-human model data (117,118). Ideally surrogate models will reflect *in vivo* human responses by replicating appropriate pharmacodynamic and pharmacokinetic interactions. Conventional wisdom suggests that predictive accuracy improves by minimizing the extrapolation to humans, and therefore models that most closely resemble human responses are preferred. Increasing pressure to develop early high-throughput toxicity screening assays and to reduce animal testing has renewed efforts to assess the limitations of existing systems for predicting human toxicity to more accurately define the role of *in vitro* data in decision-making.

Cells in culture have many advantages as well as some significant limitations for toxicity screening early in development. In general, *in vitro* models are amenable to high-throughput screening which can be used to prioritize commerce chemicals and drug candidates requiring further toxicity testing or warranting further development. Cells in culture also provide a homogeneous population that facilitates studies examining the effects of different conditions (i.e., serum free, hypoxia, co-cultures) which are not experimentally feasible using *in vivo* models. In addition, *in vitro* models are expected to be less variable and allow cell-specific effects to be examined that may otherwise be masked in a multicellular target organ. However, they are also sensitive to the culturing environment, which could influence their response and potentially compromise their ability to predict *in vivo* effects. In this study the effects of serum free and

dextran charcoal-coated (DCC) stripped serum supplemented medium on 17□-estradiol (E2)-elicited mouse hepatic Hepa-1c1c7 gene expression were compared to *in vivo* hepatic responses.

Although not considered a classical target organ, the liver is an estrogen-responsive tissue (67,73,119-121). Most hepatic responses are mediated through estrogen receptor (ER) alpha(16), although alternative mechanisms of estrogen activity have been reported (122-127). Hepa-1c1c7 cells possess active ERs (77,78) and retain several liver-specific functions (e.g., synthesis and secretion of albumin (76) and transferrin (79) in addition to xenobiotic detoxification as evidenced by its high aryl hydrocarbon hydroxylase activity (80)).

This study involved time course experiments to identify the effects of culture condition on *in vitro* gene expression following treatment with E2 using cDNA microarrays. Comparisons of *in vitro* data to hepatic gene expression studies of estrogen treated C57BL/6 mice were then conducted to assess whether Hepa-1c1c7 responses are able to model *in vivo* hepatic responses to estrogen.

MATERIALS AND METHODS

Cell viability and growth rate

Hepa-1c1c7 cells (gift from O. Hankinson, UCLA, Los Angeles, CA) were maintained at 37.5°C and 5% CO_2 in phenol red free DMEM/F12 medium (Invitrogen, Carlsbad, CA) supplemented with 5% fetal bovine serum (FBS) (Serologicals Corporation, Norcross, GA), 50 μg/mL gentamycin, 2.5 μg/mL amphotericin B, 100 U/mL penicillin and 100 μg/mL streptomycin (Invitrogen). For the MTT (3-[4,5-dimethylthiazol-2-yl]-2,5-diphenyl tetrazolium bromide) colorimetric assay of cell viability, 10 000 cells were seeded in a 96-well tissue culture plate (Corning, Acton, MA) in 100 μl 5% FBS medium and grown for 48 hrs. Wells containing medium only were used as a blank control. Medium was aspirated and replaced with 5% FBS medium or serum free medium 24 hrs before treatment with 10 nM 17β-estradiol (1,3,5[10]-estratriene-3-17β-diol) (E2) (Sigma, St. Louis, MO) or 0.1% DMSO (JT Baker, Phillipsburg, NJ) treatment. MTT solution (Sigma) was added to cells and absorbencies read 3, 6, 12, 24, 36 and 48 hrs after E2 treatment at 595 nm on an Emax 96-well microplate reader (Molecular Devices, Sunnyvale, CA) and captured using Softmax software (Molecular Devices). Colorimetric readings (n = 4) were normalized to the blank wells. Two-way ANOVA analysis followed by Tukey's HSD *post hoc* test were performed to detect time-matched differences between culture conditions (α = 0.05).

For direct cell counts, 3 x 10^5 cells were seeded in T25 culture flasks (Corning). Medium was changed to 5% FBS or serum free 24 hrs prior to E2 or

DMSO treatment. Cells were then trypsinized and counted, in duplicate, using a hemocytometer (Hausser Scientific Co., Horsham, PA) 6, 12, 24, and 48 hrs after treatment. Experiments were completed in quadruplicate. Statistics were calculated using SAS v.9.1 (Cary, NC). Repeated measures ANOVA was performed followed by a Tukey's HSD *post hoc* test to detect time-matched differences between culture conditions ($\alpha = 0.05$).

Hepa-1c1c7 time course treatment and RNA isolation regimens

Hepa-1c1c7 cells were seeded (1.5×10^6 cells) and grown for 48 hrs in 150 mm culture plates (Corning) in 5% FBS medium. Serum free medium (serum free experiments) or 5% DCC-FBS medium (stripped serum experiments) was then replaced 24 hrs prior to 10 nM E2 or 0.1% DMSO treatment. Cells were harvested by scraping in the presence of Trizol (Invitrogen). RNA was isolated as per manufacturer's instructions at 1, 2, 4, 8, 12, and 24 hrs after treatment and resuspended in RNA Storage Solution (Ambion Inc., Austin, TX). RNA quality and purity was examined by running 2 μg of total RNA on a denaturing 1% agarose gel and by examining an $A_{260/280}$ ratio. Samples were stored at -80°C until further use. Experiments were completed in triplicate using cells between passage 8 and 12.

Animal handling, husbandry and treatment

Animals were treated as previously described (73). Briefly, female C57BL/6 mice, ovariectomized by the vendor on postnatal day (PND) 20, were

obtained from Charles River Laboratories (Raleigh, NC) on PND 26. Groups of five mice were house in polycarbonate cages with cellulose fiber chip bedding (Aspen Chip Laboratory Bedding, Northeastern Products, Warrensberg, NY) at 23°C and 30–40% humidity and a 12 hr light/dark cycle (0700 – 1900 hr). Animals had access to deionized water and Harlan Teklad 22/5 Rodent Diet 8640 (Madison, WI) *ad libitum* and were acclimatized for 4 days prior to treatment. Animals were weighed and orally gavaged with 100 μg/kg 17α-ethynylestradiol (17α-Ethynyl-1,3,5(10)-estratriene-3,17β-diol; EE) (Sigma) dissolved in 0.1 mL sesame oil or vehicle alone. Doses were prepared based on average animal weight. Animals were sacrificed 2, 4, 8, 12, 18 and 24 hrs treatment at which time necropsies were performed to remove hepatic tissues. Tissues were snap frozen in liquid nitrogen and stored at -80°C until further processing. All procedures were performed with the approval of the Michigan State University All-University Committee on Animal Use and Care.

Frozen tissues were homogenized in the presence of Trizol reagent, RNA was isolated as per manufacturer's instructions and resuspended in RNA Storage Solution. RNA quality and purity was examined by running 2 □g of total RNA on a denaturing 1% agarose gel and by examining an $A_{260/280}$ ratio.

Microarray processing

Custom in-house cDNA arrays comprising of 6376 features, representing 4858 unique genes (print version Mm. 6), or 13361 features (print version Mm. 7), representing 7952 unique genes (Unigene Build 144), were spotted on epoxy coated glass slides (SCHOTT Nexterion, Germany) using an Omnigrid arrayer (GeneMachines, San Carlos, CA) and 16 (4 x 4) Chipmaker 2 pins (Mm. 6) or 48 (4 x 12) Telechem Chipmaker 3 pins (Mm. 7) in a TeleChem CHP3 printhead head (Telechem International Inc., Sunnyvale, CA) by the Research Technology Support Facility at Michigan State University (128). Serum free studies were conducted using Mm. 6 arrays, while stripped serum supplemented studies were completed on Mm. 7 arrays, a more comprehensive version of Mm. 6 arrays. Selected clones were obtained from EPAMAC (129), Research Genetics, the National Institute of Aging and Lion Biosciences. Detailed protocols for processing of microarrays are available at the dbZach Home Page (130).

Independent reference study designs were used (Figure 1) to assess three biological replicates of treatment effects. All microarray studies incorporated 6 time points and utilized 12 arrays, including dye swaps, for each biological replicate for a total of 36 microarrays each experiment. Briefly, 20 μg of RNA was reverse transcribed to incorporate Cy3- or Cy5-conjugated dUTP. Cy3 and Cy5 labelled samples were mixed, purified and resuspended in 48 μl of hybridization buffer (56% formamide, 32% 20X SSPE, 8% 50X Denhardt's Solution, 4% 20% SDS, 20 μg poly(A), 20 μg mouse CoT-1 DNA, 10 μg yeast

Figure 1

Independent reference design for microarray hybridization.

Arrows represent a single microarray in which two labelled samples, Cy3 (tail) and Cy5 (arrow head), are hybridized. Directionally opposing arrow pairs represent a dye swap where estrogen-treated (T) and vehicle treated (V) samples are reciprocally labelled and hybridized on two individual arrays. Each replicate temporal study (e.g., samples collected at 1, 2, 4, 8, 12, and 24 hrs) involved 12 hybridizations (2 per time point) for a total of 36 arrays per time course study (n = 3 independent animals). An identical design was used to assess *in vivo* gene expression where samples collected at 2, 4, 8, 12, 18 and 24 hrs were hybridized.

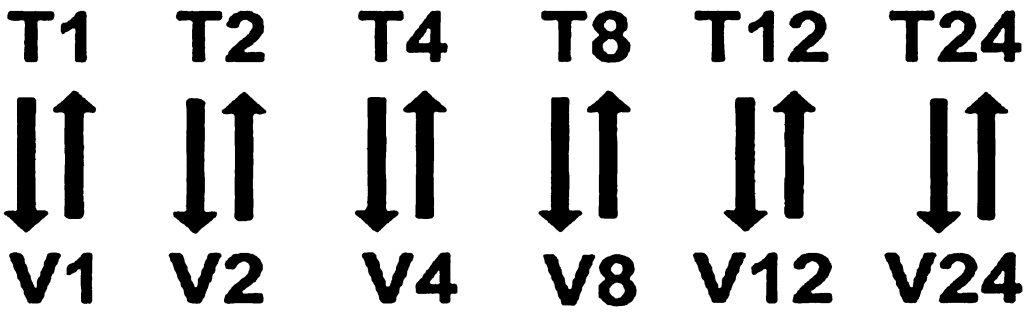

tRNA carrier) for overnight 42°C hybridization on printed arrays. Slides were washed in SSC solutions contain decreasing concentrations of SDS, dried andscanned using a 428 Affymetrix Scanner (Santa Clara, CA). Images were examined, features identified and intensity values determined using GenePix v.5.1 (Molecular Devices). All data was stored in dbZach (130), a Minimum Information About Microarray Experiments (MIAME)-compliant relational database (131) running under Windows 2003/Oracle 10g that currently supports microarray data storage, retrieval, and querying as well as facilitates data analysis, sharing and reporting (132,133)

All arrays within this study were compared to a historical data set of established high quality arrays. Parameters that were assessed included background signal intensity, feature signal intensity, feature vs. background signal intensity ratios, the number of features with background intensities greater than the feature intensity for each array, and relationships between feature and background signal intensities. All arrays met the standards of the quality control parameters (134).

Statistical, filter and cluster analysis of microarray data

Microarray data were analyzed using a semi-parametric approach (135). Model-based t-values were calculated from normalized data, comparing treated and vehicle responses at each time-point. Empirical Bayes analysis was used to calculate posterior probabilities (P1(*t*)-value) of activity on a per gene and time point basis using the model-based t-value (135). A P1(*t*) score cut-off was

initially used to identify differentially expressed transcripts between treatment groups. Feature subsets were associated with functional annotation using Entrez Gene (136) and Gene Ontology (137). General temporal patterns were identified using *k*-means clustering (GeneSpring v7, Silicon Genetics, Redwood City, CA). Temporal gene expression correlations (activity index) and temporal P1(*t*) activity correlations (significance index) between *in vitro* and *in vivo* studies were calculated using Pearson's correlation at overlapping time points (i.e., 2, 4, 8, 12 and 24 hrs). Correlation indices were plotted on a Cartesian plane, to visualize the relationship of the same gene in the two model systems, through an in-house developed Toxicogenomics Correlation Tool (TCT).

A third dimension of information is provided through the Displacement Heat Map function of TCT where time displacement for a gene between the *in vitro* and *in vivo* models is visualized through the color intensity of the point. A Displacement Index (DI) is derived by: i) identifying the number of time points that exhibit opposite activities in between models (e.g. *in vitro* model meets P1(*t*) > 0.9 cut-off whereas *in vivo* does not, or vice versa), ii) identifying the number of time points which are being compared, iii) calculating the quotient by dividing the value of step i by the value of step ii. A range of values representing non-displaced (DI = 0) to highly displaced (DI = 1) results in a gradient from light to dark color intensity, respectively (133). TCT can be licensed through arrangement with the Office of Intellectual Property at Michigan State University.

Quantitative RT-PCR

RNA aliquots from each replicate were set aside for microarray verification by SYBR™ Green quantitative real-time PCR (QRT-PCR). Briefly, 2 μg of RNA were primed by an anchored oligo-dT and reverse transcribed using Superscript II (Invtrogen, Carlsbad, CA) in a 40 μl reaction as described by the manufacturer. The cDNA solution was diluted 4-fold and 3 μl was used in a 30 μl PCR reaction containing 1X SYBR Green PCR buffer, 3 mM $MgCl_2$, 0.33 mM dNTPs, 0.5 IU AmpliTaq Gold (Applied Biosystems, Foster City, CA) and 0.15 mM forward and reverse primer. All primers were designed by submitting clone sequences into Primer3 (138) to obtain an amplicon of approximately 125bp (Table 1). All primer and QRT-PCR reaction conditions were submitted and stored within the Real-Time PCR Subsystem of dbZach (133).

PCR amplification was conducted in 96-well MicroAmp Optical plates (Applied Biosystems) on an Applied Biosystems PRISM 7000 Sequence Detection System under the following conditions: 10 min denaturation and enzyme activation at 95°C, followed by 40 cycles of 95°C for 15 s and 60°C for 1 min. A 30 min dissociation protocol, after amplification, was conducted to assess primer specificity and product uniformity. Each plate contained duplicate standards of purified PCR product of known template concentration over the range of eight orders of magnitude to generate a log template concentration

Table 1. QRT-PCR primer list

Gene Name	Gene Symbol	Entrez Gene ID	RefSeq Accession	Forward Primer	Reverse Primer	Size (bp)
actin, beta, cytoplastmic	Actb	11461	NM_007393	gctacagcttcaccaccaca	tctccagggaggaagaggat	123
antizyme inhibitor 1	Azin1	54375	NM_018754	gaccccagtccattgtcatc	tgccacccttaagttttgg	129
BCL2/adenovirus E1B 19dkDa-interacting protein 1, NIP3	Bnip3	12176	NM_009760	ccgatttaagcagctttgga	accttgggtggtcagttttg	198
cyclin D1	Ccnd1	12443	NM_007631	ggcacctggattgttctgtt	cagcttgctagggaacttgg	150
cyclin G1	Ccng1	12450	NM_009831	tgtgctcagagtctccatgc	cctgtcaaatggttccagcta	117
CD68 antigen	Cd68	12514	NM_009853	tagcccaaggaacagaggaa	tggcagggttatgagtgaca	191
cell division cycle 2 homolog A	Cdc2a	12534	NM_007659	actccactccggttgacatc	tccacttgggaaaggtgttc	192
procollagen, type I, alpha 1	Col1a1	12842	NM_007742	gggcaagacagtcatcgaat	ggtggagggagtttacacga	142
cellular repressor of E1A-stimulated genes 1	Creg1	433375	NM_011804	gaggctcatgcacacttgaa	tccagcaaccacatcttctg	134
cytochrome P450, family 1, subfamily a, polypeptide 1	Cyp1a1	13076	NM_009992	aagtfcagatgcggtcttct	aaagtaggaggcaggcacaa	140
fatty acid binding protein 9, testis	Fabp9	21884	NM_011598	tggagtgcaccatgaacaat	tcttgagcggcaagttcttt	109
fyn-related kinase	Fyn	14302	NM_010237	aagccatggccagtattttg	taagccggttcccttcttct	154
glyceraldehyde 3-phosphate dehydrogenase	Gapd	407972	NM_008084	gtggacctcatggcctacat	tgtgagggagatgctcagtg	125
gem-interacting protein	Gmip	78816	NM_198101	tttacagcaagcaccactgc	tgtgagccacaaatcctctg	119
glutathione S-transferase, mu 2	Gstm2	14863	NM_008183	gcacaacctgtgtggagaga	gtagcaaaccatggccaact	100

Table 1. Continued						
glutathione S-transferase, mu 3	Gstm3	14864	NM_010359	tgtggctcctggttctctct	gtcagggagccaatgaagaa	143
3-hydroxy-3-methylglutaryl-Coenzyme A synthase 1	Hmgcs1	208715	NM_145942	gaaaatggcaaggcaaacat	tcagtgccagcatctttctg	145
hypoxanthine guanine phosphoribosyl transferase	Hprt	15452	NM_013556	aagcctaagatgagcgcaag	ttactaggcagatggccaca	104
insulin-like growth factor 1	Igf1	16000	NM_010512	tggatgctcttcagttcgtg	gcaacactcatccacaatgc	118
lipocalin 2	Lcn2	16819	NM_008491	ctgaatgggtggtgagtgtg	gctctctggcaacaggaaag	101
nuclear receptor subfamily 1, group H, member 2	Nr1h2	22260	NM_009473	gaccctcaccactcttggaa	cagccttggtggtgtcttct	163
nuclear receptor subfamily 1, group H, member 3	Nr1h3	22259	NM_013839	acgcctacgtctccatcaac	agggcaaacacttgctctga	115
nuclear receptor subfamily 3, group C, member 1	Nr3c1	14815	NM_008173	aggccgctcagtgttttcta	cccataatggcataccgaag	148
pitrilysin metalloproteinase 1	Pitrm1	69617	NM_145131	gggtctttggcaatttttga	cctctccgatgagatgaagc	156
sterol carrier protein 2, liver	Scp2	20280	NM_011327	agaatgcaagtcctcaaagca	gtctcgtcgtcagggcttag	147
sterol O-acyltransferase 1	Soat1	20652	NM_009230	gtgtcctggtcctgtgtgtg	catctcagcaaaggcattga	107
sortilin-related receptor, LDLR class A repeats-containing	Sorl1	21244	NM_011436	agagctgacctggcacctta	ggcccaagtcagtgaaggta	103

Table 1. Continued						
signal transducer and activator of transcription 5A	Stat5a	20850	NM_011488	accaagatggcgagtttgac	ggaggtgaagagaccagcag	125
very low density lipoprotein receptor	Vldlr	22359	NM_013703	tcgggctttgtttactggtc	agtagaggcggcttttgaca	148

standard curve. No template controls (NTC) were included on each plate where unknown samples with a Ct value within 2 SD of the mean Ct values of the NTCs were considered below the limits of detection. Plots were visualized and thresholds determined using ABI Prism 7000 SDS Software (Applied Biosystems). Results were normalized to a geometric mean of β-actin (Actb), glyceraldehyde-3-phosphate dehydrogenase (Gapd) and hypoxanthine guanine phosphoribosyl transferase (Hprt) mRNA levels to control for differences in RNA loading, quality and cDNA synthesis. Statistical significance of expression differences were assessed using a factorial ANOVA followed by Tukey's HSD *post hoc* analysis to examine treatment and treatment over time effects using SAS version 9.1. R, version 1.9.1, was used to compute the Pearson's correlation coefficient between DNA microarray data and QRT-PCR results.

RESULTS

Hepa-1c1c7 cell viability and proliferation in serum free medium

E2 effects on Hepa-1c1c7 cells were examined in serum free medium to minimize exposure to serum borne estrogens. Serum starvation synchronizes cells at G_1 and was used in this study to optimize the detection of potential proliferative responses which may otherwise be masked in an asynchronous population. Published reports have demonstrated that estrogen induces synchronized uterine proliferation in the immature, ovariectomized rodent model. However, limiting factors provided by serum may compromise cellular viability and responsiveness. Consequently, medium supplemented with dextran-coated charcoal (DCC) stripped serum was also examined. DCC serum stripping removes steroids and other small molecules that can pass through the dextran coating and bind to the activated charcoal, which is then discarded (139).

Cellular distress may be detected through morphological changes exhibited by the cells. However, no significant morphological differences were observed after four days in either 5% FBS supplemented or serum free medium (data not shown). In addition cell viability and proliferation in serum free medium was assessed, by monitoring mitochondrial activity using the MTT assay, and by direct cell counting. MTT time course assays indicate that Hepa-1c1c7 cells exhibited a 3-fold increase in mitochondrial activity ($p < 0.05$) in 5% FBS supplemented medium over a period of 48 hrs indicative of cellular proliferation (Figure 2A). In serum free conditions, MTT activity was significantly reduced ($p <$

Figure 2

MTT and cell count assessment of Hepa-1c1c7 cells in serum free and stripped serum supplemented medium.

MTT and cell count assays were used to assess the viability of Hepa-1c1c7 cells incubated in a serum free environment. A) Parallel MTT time course assays were conducted in 5% FBS supplemented medium (black bars), serum free medium treated with DMSO (open bars), and serum free medium treated with 10 nM E2 (grey bars). Wells were seeded with 10 000 cells, medium changed after 24 hrs, treated and assayed at 3, 6, 12, 24, 36 and 48 hrs after treatment. Only cells in 5% FBS exhibited a significant increase in mitochondrial activity [a]($p < 0.05$) at all time points beyond 3 hrs. Viability of serum starved cells were significantly different [b]($p < 0.05$) from time-matched 5% FBS cultured cells. B) Parallel direct cell count time course assays were conducted in 5% FBS supplemented medium (squares), serum free medium (triangles), serum free medium treated with DMSO (diamonds) and serum free medium treated with E2 (circles). T25 flasks were seeded with 300 000 cells and directly counted at 6, 12, 24 and 48 hrs. Cells cultured in 5% FBS exhibited a significant increase in number from at 48 hrs relative to 3 hrs [a]($p < 0.05$). Cell numbers of serum starved cells are significantly different [b]($p < 0.05$) from time-matched 5% FBS cultured cells.

Figure 2

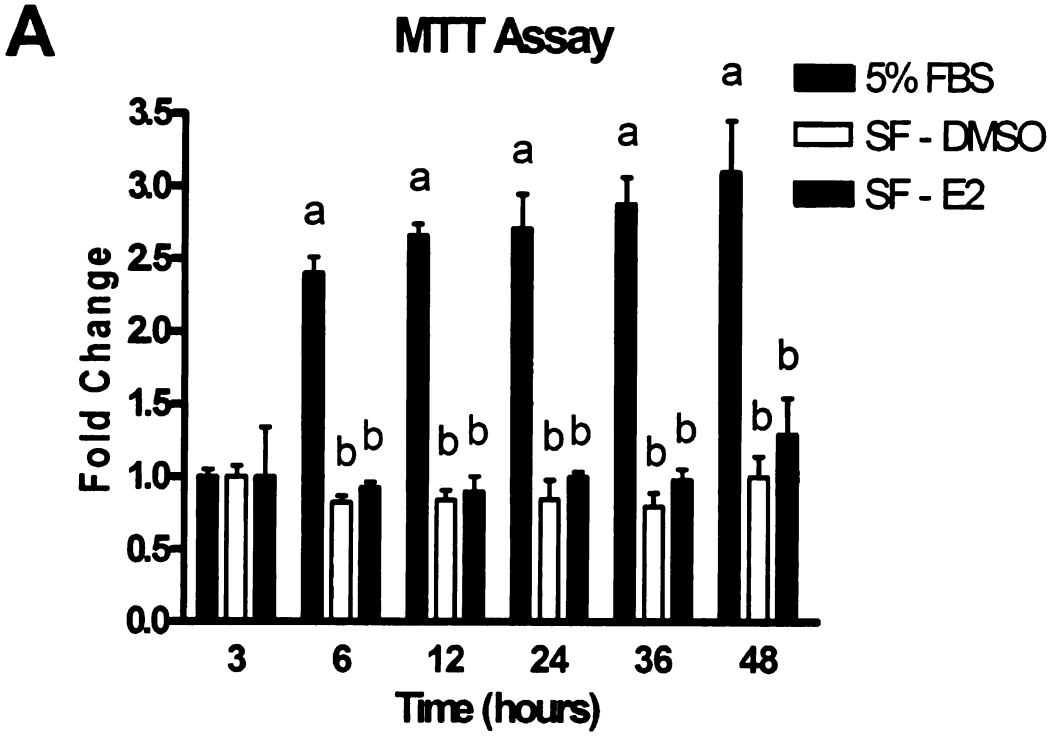
A
MTT Assay
5% FBS
SF - DMSO
SF - E2
Fold Change
3.5
3.0
2.5
2.0
1.5
1.0
0.5
0.0
3
6
12
24
36
48
Time (hours)

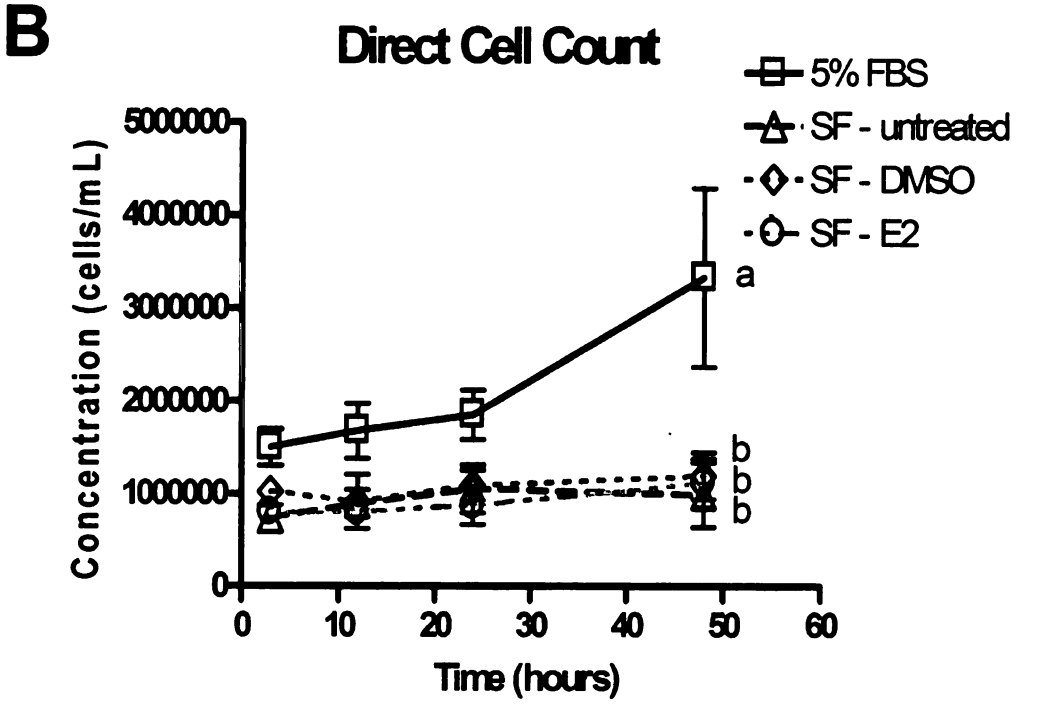
B
Direct Cell Count
5% FBS
SF - untreated
SF - DMSO
SF - E2
Concentration (cells/mL)
5000000
4000000
3000000
2000000
1000000
0
0
10
20
30
40
50
60
Time (hours)

0.05) compared to serum supplemented conditions but no net loss of cells was detected over 48 hrs. E2 did not induce a significant change in MTT activity in a serum free environment when compared to time-matched vehicle treated cells under comparable conditions, although the trend suggested E2 may induce activity beyond 48 hrs.

Direct counts indicate that Hepa-1c1c7 cells cultured in serum supplemented medium are actively proliferating (Figure 2B). This increase in cell number may account for the increased mitochondrial activity observed in the MTT assay by cells in the serum supplemented condition. No increase in cell number was observed using serum free conditions and neither E2 nor DMSO enhanced cell number over time as suggested by the MTT assay.

These results indicate that Hepa-1c1c7 cells maintained in serum free conditions are viable and do not appear to undergo proliferation. Furthermore, viability and proliferation are not affected by E2 treatment, thus concerns regarding E2 induction of proliferation and confluency will not confound gene expression analysis.

Temporal E2-mediated changes of gene expression in a serum free environment

cDNA microarrays were used to investigate E2-elicited Hepa-1c1c7 cell gene expression changes in serum-free and DCC-stripped serum supplemented medium. Empirical Bayes analysis identified 245 active features ($P1(t) > 0.999$, Mm. 6), representing 167 unique Entrez Gene annotated genes following E2

treatment compared to time-matched DMSO treated controls (Supplemental Table S1 (130)). P1(*t*) values were used to rank and prioritize features for further investigation. Gene expression changes ranged from 2.1-fold induction (e.g., decorin - Dcn) to 2.17-fold repression (e.g., chemokine (C-C motif) receptor 5 - Ccr5). Five *K*-means clusters best represented the temporal profiles of these active genes as A) up-regulated beyond 8 hrs, B) down-regulated at 4 hrs, C) down-regulated at 1 and 8 hrs, D) down-regulated at 8 hrs and up-regulated at 12 hrs and E) up-regulated at 4 hrs (Figure 3). Functional annotation for the 167 active genes was identified through Gene Ontology and complemented with reports in the published literature. Genes with roles in transcriptional regulation were most frequently represented in addition to those involved in cell proliferation and differentiation, cytoskeletal organization, and transport and metabolism of lipids and carbohydrates.

The effects of DMSO alone were also examined under serum free conditions where comparisons were made with untreated samples. Interestingly, DMSO elicited transcriptional changes primarily associated with proliferative arrest and increased solute regulation, which were not observed with E2 treatment (Supplemental Table S2) when compared to untreated cells. These results indicate that gene expression differences due to E2 treatment can not be attributed to DMSO.

Figure 3

Temporal gene expression patterns: E2 in serum free medium

Five *k*-means clusters were identified to concisely represent the general temporal patterns exhibited by 246 active features treated with 10 nM E2 in serum free medium. Each line represents a single feature with its fold-change (x = induction; / = repression) determined by comparison to the time-matched vehicle control. Black pseudolines indicate the general profile represented in each cluster.

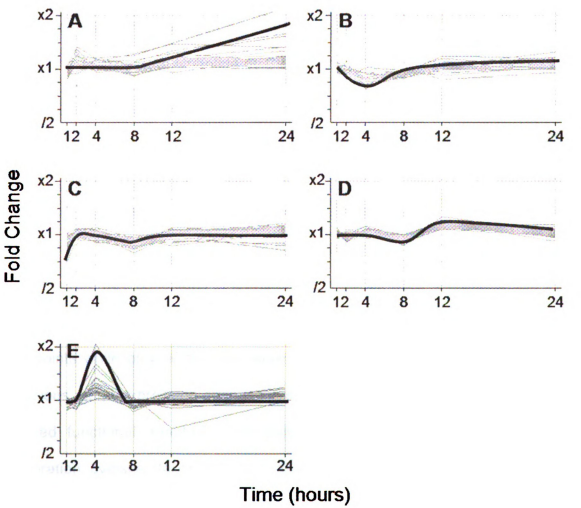

Temporal E2-mediated gene expression changes in stripped serum supplemented medium

Although serum free medium provides a nearly depleted steroid environment and synchronizes the cells at G1, these conditions may compromise responsiveness due to the lack of serum factors that facilitate gene expression (23,140). When E2 elicited gene expression effects were examined in medium supplemented with DCC-stripped serum, 1882 unique features (P1(t) > 0.999; Mm. 7) representing 1134 unique annotated genes were identified as differentially expressed (Supplemental Table S3). The magnitude of transcriptional changes ranged from 2.06-fold induction (e.g., cytochrome P450, family 1, subfamily a, polypeptide 1; *Cyp1a1*) to 2.08-fold repression (Accession ID: CR517543). Five *K*-means clusters best described the temporal gene expression elicited by E2 as A) induced at 2 hrs, B) induced at 8 hrs and repressed at 24 hrs, C) repressed at 24 hrs, D) sustained induction between 2 – 8 hrs and E) repressed at 8 hrs (Figure 4). These clusters exhibited different profiles when compared to the five clusters identified for E2 treated Hepa-1c1c7 cells in serum free conditions in terms of which genes were responsive and their temporal pattern of gene expression. Most genes were induced at one or more time points while only 60 features were repressed. As observed in serum free conditions, gene expression changes in stripped serum supplemented conditions included functional annotation associated with transcriptional regulation, cell proliferation, cytoskeletal organization, and lipid transport and metabolism.

Figure 4

Temporal gene expression patterns: E2 in stripped serum medium

Five *k*-means clusters best represent the temporal expression patterns exhibited by 1882 active features elicited following treatment with 10 nM E2 in stripped serum medium. Each line represents a single feature with its fold-change (x = induction; / = repression) determined by comparison to the time-matched vehicle control. Black pseudolines indicate the general expression profile represented in each cluster. The patterns represented in this study differ from the general patterns exhibited by Hepa-1c1c7 cells treated in serum free medium in genes represented within the cluster and the shape of the temporal expression profile.

Figure 4

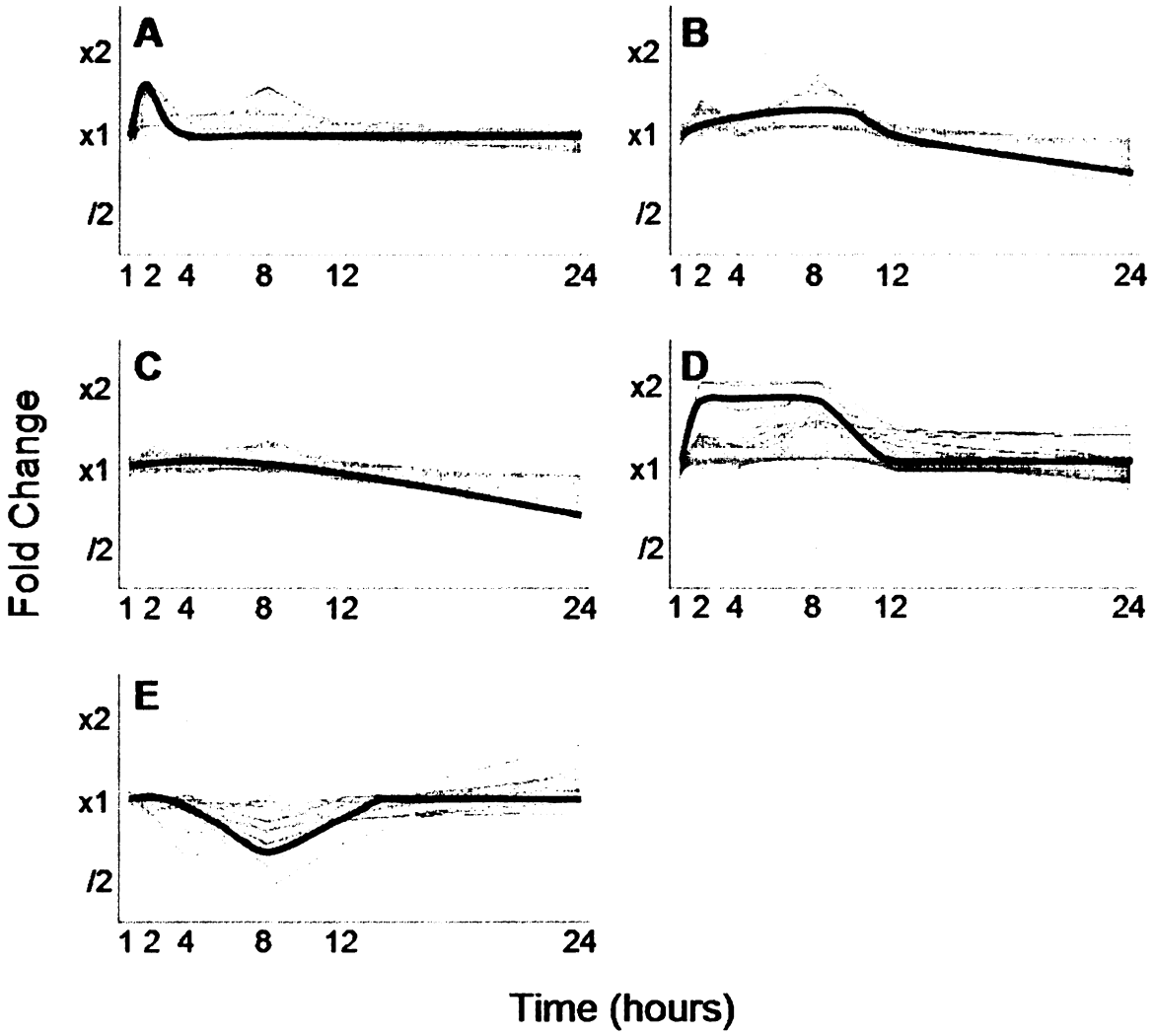

Cells cultured in stripped serum medium exhibited E2-induced changes in a greater number of genes compared to cells cultured in serum free medium. However, this can be attributed to the more comprehensive Mm.7 version of the array. Only 30 unique annotated genes were found to be active between serum free and stripped serum supplemented medium studies suggesting that serum borne factors influence E2-mediated transcription (141,142). Factors influencing gene expression may include the lower mitochondrial activity of Hepa-1c1c7 cells in serum free conditions, and possible non-additive interactions between E2 and serum components such as growth factors, which could activate other signaling pathways.

Quantitative real-time PCR verification

QRT-PCR was used to verify microarray data of selected genes representing different cluster profiles and functional pathways. Pearson's correlations were used to quantitatively assess the level of agreement between microarray and QRT-PCR gene expression profiles. Correlations were classified as either good ($\rho \geq 0.5$), moderate ($0.5 > \rho > 0.1$) or poor ($\rho \leq 0.1$). Of the 32 genes examined (Table 1), 19 were classified as good, 7 as moderate and 6 as poor. In some cases, poor correlations were the result of changes in gene name annotation. Primers were originally designed for a specific gene represented by the clone printed on the array, and not the sequence of the clone. For example, accession numbers for clones may be reassigned upon Unigene database rebuilds, and therefore the initial primer set may no longer amplify the gene of

interest. For example, dbZach Clone ID 87 which was originally identified as representing *Lamb3* (laminin B3), but is not currently associated with an official gene. The correlation for this primer set was classified as poor. Overall, QRT-PCR verified the gene expression changes detected in the microarray assay.

***In vivo* vs. *in vitro* gene expression comparison**

In-life study of temporal hepatic responses to estrogen was conducted in C57BL/6 mice orally gavaged with 100 μg/kg 17α-ethynyl estradiol (EE) for 2, 4, 8, 12, 18 and 24 hrs. EE is an orally active estrogen used in contraceptives that elicits responses comparable to endogenous E2 (143). Empirical Bayes analysis identified 1582 features, representing 1007 active unique annotated genes (P1(*t*) > 0.9999) (Supplemental Table 4). The results were comparable to a previous intralaboratory study using a model-based *t*-test for microarray analysis (73).

Both serum free and stripped serum supplemented conditions were assessed to evaluate the *in vivo* predictive value of Hepa-1c1c7 cells. 6376 features were in common between the serum free (Mm. 6) and *in vivo* (Mm. 7) studies due to different array platform versions (Figure 5). Between the 254 and 1582 active features of the respective studies, only 23, representing 18 annotated genes, were in common between the serum free (Mm. 6) and *in vivo*

Figure 5

Systematic comparison of *in vitro* and *in vivo* active gene lists

Data sets for E2 treated Hepa-1c1c7 in serum free (245 features) and stripped serum (1882 features) (P1(t) ≥ 0.999) were compared to the EE treated C57BL/6 hepatic tissue data set (1582 features; P1(t) ≥ 0.9999). Only 15 annotated genes were active in both serum free *in vitro* and *in vivo* studies; while 238 genes were active in both DCC-treated stripped serum *in vitro* and *in vivo* studies.

Figure 5

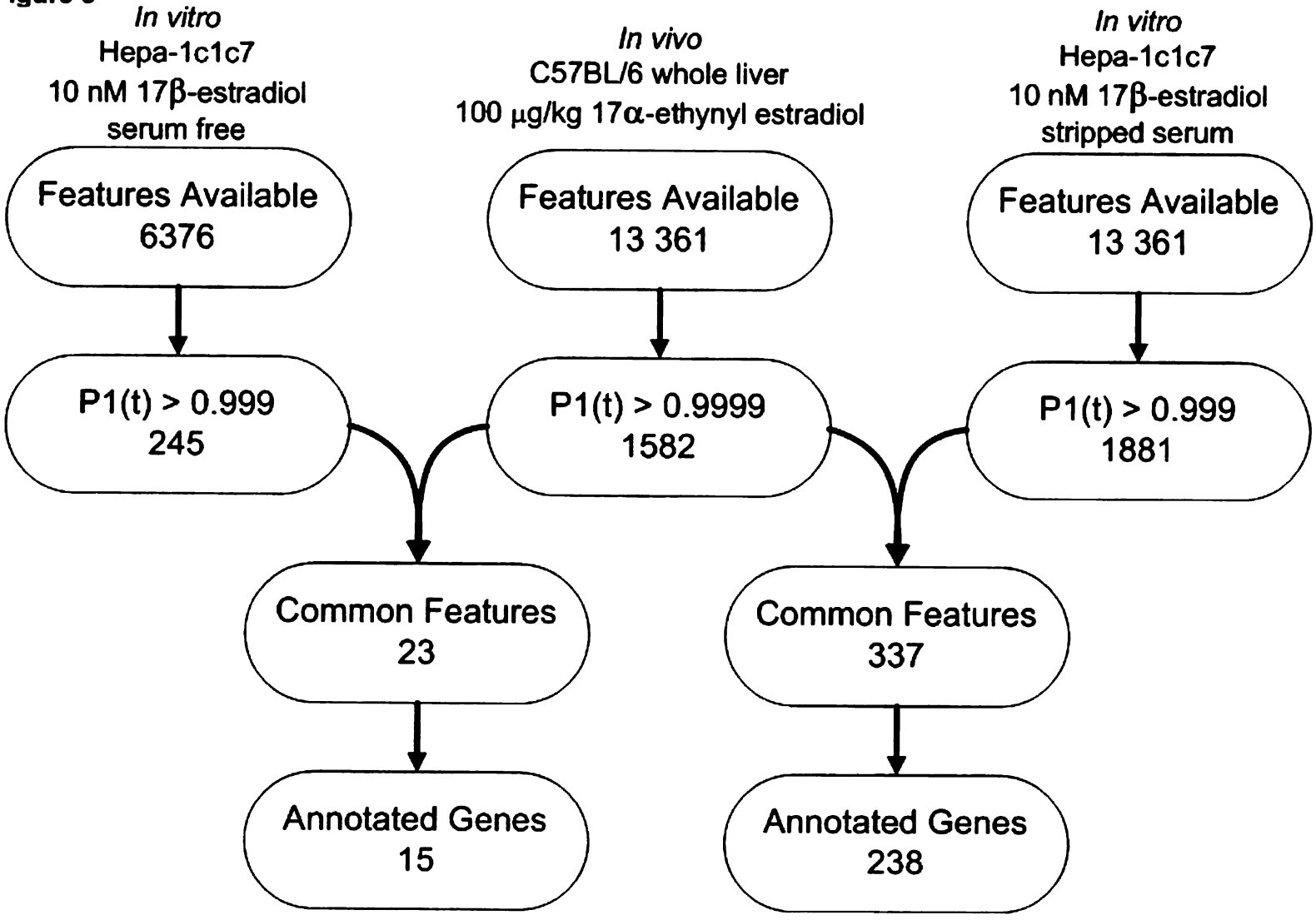
In vitro
Hepa-1c1c7
10 nM 17β-estradiol
serum free
Features Available
6376
P1(t) > 0.999
245
In vivo
C57BL/6 whole liver
100 µg/kg 17α-ethynyl estradiol
Features Available
13 361
P1(t) > 0.9999
1582
In vitro
Hepa-1c1c7
10 nM 17β-estradiol
stripped serum
Features Available
13 361
P1(t) > 0.999
1881
Common Features
23
Annotated Genes
15
Common Features
337
Annotated Genes
238

(Mm. 7) studies indicating that E2-treated Hepa-1c1c7 cells in a serum free environment poorly model EE-elicited hepatic gene expression in C57BL/6 mice.

In contrast, 13,361 features (Mm. 7) were available for comparison between the stripped serum and *in vivo* studies. Microarray studies identified 1881 and 1532 features, in the stripped serum and *in vivo* studies, respectively. Comparing these active gene lists identified 337 active features, representing 238 genes, that were in common between Hepa1c1c7 cells in serum stripped medium and C57BL/6 hepatic tissue. Specific biological pathways were not over-represented by these genes, but associated functions included cellular proliferation, cell signaling, cytoskeletal organization, lipid metabolism, and intracellular communication.

The in-house developed Toxicogenomics Correlation Tool (TCT) was used to identify genes exhibiting similar and different temporal gene expression and P1(*t*) patterns between Hepa-1c1c7 cells in stripped serum medium and C57BL/6 liver. Each data point represents a single gene. Its position on the Cartesian plane represents how the similarity of the temporal response of that gene in the two models as reflected in the gene expression (activity index) and P1(*t*) values (significance index). In general, Pearson's correlations for *in vitro* and *in vivo* gene expression data exhibited a positive relationship (i.e., data point distribution along the positive x-axis, Figure 6A) indicating that these genes respond in similar directions and magnitude over time in estrogen-treated Hepa-1c1c7 cells and C57BL/6 liver. However, P1(*t*) correlations (significance index; y-axis) span both the positive and negative axes indicating variability across time

Figure 6

***In vitro* vs. *in vivo* significance P1(*t*) and activity index correlations**

The TCT plot is a visualization tool which allows groups of genes with similar temporal activity and/or significance between *in vitro* and *in vivo* models to be quickly identified. (A) Plot of significance index (i.e., P1(*t*)) coefficients vs. activity index (i.e., gene expression) coefficients for 337 active clones (238 genes) in E2-treated Hepa-1c1c7 cells maintained in stripped serum (*in vitro*) and EE-treated C56BL/6 mouse hepatic tissue (*in vivo*). Each data point represents a single feature where the *in vitro* and *in vivo* P1(*t*) values and gene expression patterns have been compared through Pearson's correlation analyses. The inset box, upper right, encloses 27 features (17 genes) with the highest P1(*t*) and gene expression correlation coefficients ($\rho \geq 0.5$) (Table 2) identifying *in vitro* and *in vivo* responses with highly similar response profiles and P1(*t*) values across 2, 4, 8, 12 and 24 hrs. Shading intensity of the data point indicates the degree of time displacement of P1(*t*)-values for a single gene when comparing between models. Darker points identify genes with a greater number of time points exhibiting P1(*t*)-value discrepancies between models while lighter points identify genes with fewer time related discrepancies as calculated through a Displacement Index (DI) value. Data points labelled 1 through 4 are graphically described in (B) to further illustrate differences in temporal *in vitro* and *in vivo* activity and significance profiles.

Figure 6A

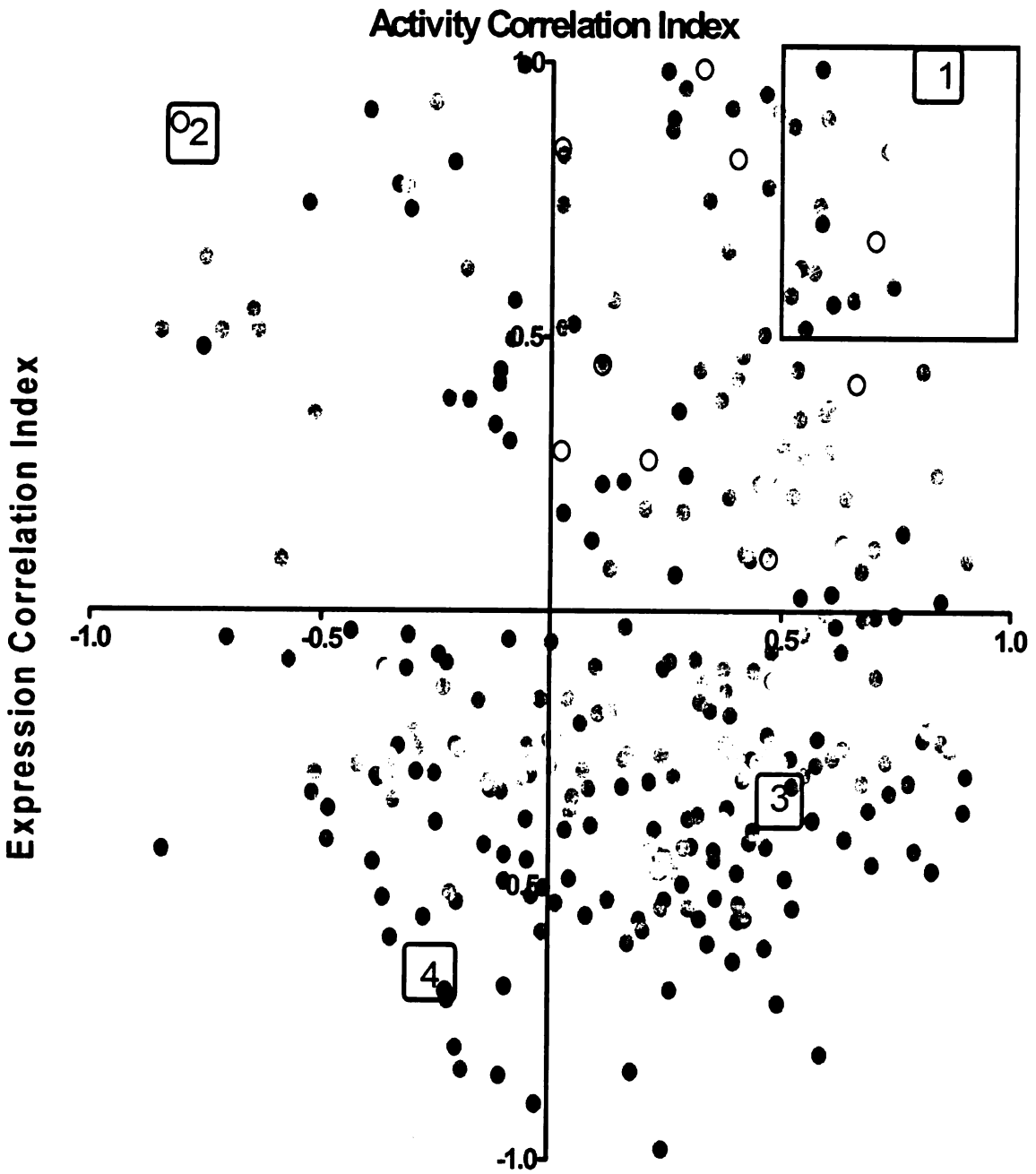
Activity Correlation Index
Expression Correlation Index
1
2
3
4
1.0
0.5
-0.5
-1.0
-1.0
-0.5
0.5
1.0

Figure 6B

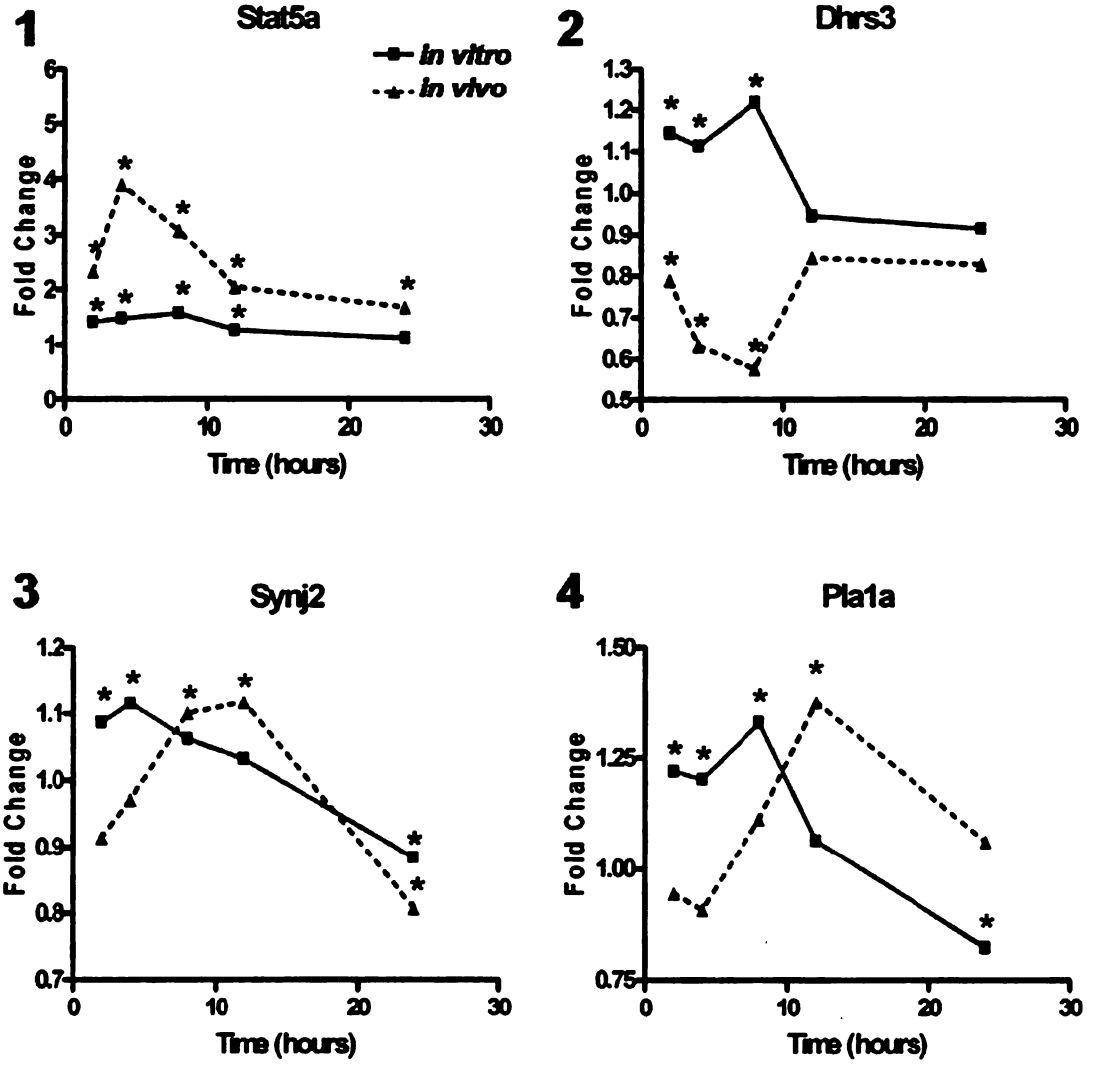
1
Stat5a
in vitro
in vivo
Fold Change
Time (hours)
2
Dhrs3
Fold Change
Time (hours)
3
Synj2
Fold Change
Time (hours)
4
Pla1a
Fold Change
Time (hours)

Table 2. Genes exhibiting high temporal gene expression and activity correlations, ($\rho \geq 0.5$)

Gene Name	Gene Symbol	Entrez Gene ID	Gene Expression Correlation	Activity Correlation
signal transducer and activator of transcription 5A	Stat5a[1]	20850	0.81	0.99
histocompatibility 2, complement component factor B	H2-Bf	14962	0.81	0.57
protein C	Proc	19123	0.76	0.88
uridine monophosphate kinase	Umpk	80914	0.74	0.84
LIM domain only 6	Lmo6	54630	0.73	0.84
syncollin	Sycn	68416	0.70	0.67
PHD finger protein 5A	Phf5a[2]	68479	0.70	0.56
Bcl2-like 10	Bcl2l10	12049	0.66	0.57
enoyl Coenzyme A hydratase domain containing 2	Echdc2	52430	0.60	0.82
FK506 binding protein-like	Fkbpl	56299	0.59	0.71
B-cell leukemia/lymphoma 2	Bcl2[1]	12043	0.57	0.62
fyn-related kinase	Frk	14302	0.54	0.62
Fraser syndrome 1 homolog (human)	Fras1	231470	0.53	0.77
pleckstrin homology, Sec7 and coiled-coil domains 3	Pscd3	19159	0.53	0.88
degenerative spermatocyte homolog 1 (Drosophila)	Degs1	13244	0.52	0.61
voltage-dependent anion channel 1	Vdac1[2]	22333	0.52	0.57
tumor necrosis factor receptor superfamily, member 11b (osteoprotegerin)	Tnfrsf11b	18383	0.51	0.69

[1]Genes containing bone fide, functional ERE sequences.
[2]Genes containing putative ERE sequences as defined by Bourdeau *et al.* 2004.

between model systems. These results suggest some degree of conservation of estrogen-induced signaling pathways where transcript levels exhibit conserved regulation between the stripped serum *in vitro* and *in vivo* systems.

Using a correlation threshold of $\rho \geq 0.5$ for both parameters 27 features, representing 17 annotated genes, were identified with comparable significance and temporal gene expression patterns (Table 2). Generally, these genes were induced between 2-12 hrs and down-regulated by 24 hrs. The functional pathways associated with these genes varied but supported several responses known to be modulated by estrogens (73,144,145). Because these genes exhibited high correlations between models, they were suspected to be primary targets of ER-mediated responses and a search for estrogen response elements (EREs) in their regulatory regions was conducted. *Stat5a* (signal transducer and activator of transcription 5A) and *Bcl2* (B-cell leukemia/lymphoma 2) contain functional EREs, and computational searches identified putative EREs in the regulatory regions of *Phf5a* (PHD finger protein 5A) and *Vdac1* (voltage-dependent anion channel 1) (26). The remaining genes may also be candidates for primary ER-mediated modulation.

Activity indices were spread across both positive and negative axes and appeared to be more heavily distributed into the negative, thus these latter genes were examined to investigate causes contributing to poor temporal P1(t) correlation. Displacement analysis was conducted to identify the degree of non-overlapping significance at similar times between models on a per gene basis. The greater number of time points where a gene does not meet the P1(t) > 0.9

cut-off in both models, a greater displacement index is exhibited by that gene. Displacement indices are displayed as a third dimension (i.e. color) of the TCT plot where features exhibiting greater temporal displacement ($P1(t) > 0.9$) between models are represented by points with greater color intensities, while features with little or no temporal $P1(t)$ displacement are of lighter intensity (Figure 6A). The $P1(t)$ cut-off was lowered to include data approaching significance to achieve a more comprehensive impression of which data were truly incidental, despite the fact that each gene met the initial parameters in both model systems. From the 337 active features in common between models, displacement analysis identified 327 features exhibiting temporally displaced $P1(t)$ values. The trend of color intensity is distributed from light to dark from +1.0 to -1.0 (top to bottom) on the significance index axis. This result is not unexpected since negative significance indices indicate poor correlation of $P1(t)$-values over time.

Selected data points, labeled 1 through 4 (Figure 6A), were examined to further illustrate data represented on the TCT plot. Data point 1 represents *Stat5a,* which demonstrated indices of activity, significance and displacement of 0.807, 0.998 and 0.2, respectively. Graphically, *in vitro* and *in vivo* expression profiles follow similar patterns and attains a $P1(t) > 0.9$ in both models at all but one time point (Figure 6B1). Similarly for data point 2, *Dhrs3* transcripts had similar expression profiles over time but in opposite directions translating to activity, significance and displacement indices of -0.810, 0.885 and 0, respectively (Figure 6B2). However, most genes did not exhibit such stark

similar or opposing responses between models. Data points 3, *Synj2* (DI = 0.8), and 4, *Pla1a* (DI = 1.0), have activity and significance profiles that are temporally displaced (Figure 6B3, 6B4). Interestingly, the expression profiles suggest that an *in vitro* response temporally precedes a similar response *in vivo*. Of the data points demonstrating negative significance indices, 111, representing 80 genes, were first responsive *in vitro* by at least one time point prior to a similar *in vivo* response (Supplementary Table S5). This temporal shift in response may partially be attributed to differences in absorption, distribution and metabolism between *in vitro* and *in vivo* models. However, eight features exhibit *in vivo* gene expression prior to evidence of significant Hepa-1c1c7 expression, while the remaining 87 features had divergent expression patterns between models or do not exhibit temporal displacement. These results indicate that factors beyond differences in pharmacokinetics can also affect *in vitro* and *in vivo* gene expression profiles.

DISCUSSION

In this study the utility of Hepa-1c1c7 cells as a potential *in vitro* model to predict *in vivo* hepatic estrogen responses was examined under serum free and stripped serum conditions. Serum free medium minimizes the effects of serum-borne steroids, synchronizes cells in G_1 arrest and more closely mimics the hormonal milieu of an ovariectomized mouse model. Theoretically, cell synchronization under conditions devoid of steroids should enhance the detection of expression responses for those genes involved in cell cycle and proliferation. However, serum free gene expression was significantly compromised as only 18 genes demonstrated overlap with Hepa-1c1c7 cells cultured in a stripped serum environment. The lack of common responses may be attributed to the lack of serum factors. Epidermal growth factor (EGF) potentiates estrogenic responses in mouse uterus and its signaling pathway has been coupled to several ER-dependent effects (145,146). Furthermore, the promoter regions of classical E2-responsive genes, such as pS2 and lactoferrin, contain active response elements which requires activation by growth factors and other signaling molecules in order to co-operatively elicit a robust response (147,148).

In vivo transgenic reporter models and microarray studies clearly demonstrate that the liver is estrogen responsive, although it does not exhibit the same gross physiology changes as the rodent uterus (67,73). Under stripped serum conditions, Hepa-1c1c7 cells exhibited a more robust gene expression response to E2, when compared to cells maintained in serum free medium, but

did not reflect the diverse response observed *in vivo*. However, specific stripped serum *in vitro* responses associated with proliferation, cytoskeletal reorganization, cholesterol transport and metabolism, fatty acid metabolism, oxidative stress and carbohydrate synthesis, were consistent with reported *in vivo* effects on gene expression.

Cellular proliferation

Several E2-elicited gene expression changes are indicative of proliferation. At 2 hrs *Kit* and *Fos* oncogene transcripts, early proliferation indicators, were up-regulated followed by the induction of genes involved in G1 → S transition such as Calmodulin 3 (*Calm3*), G1 → S phase transition 1 (*Gspt1*), polo-like kinase 2 (*Plk2*), protein phosphatase 3, catalytic subunit, alpha isoform (*Ppp3ca*), and protein kinase, cAMP dependent regulatory, type 1, alpha (*Prkar1a*)). All except *Prkar1a*, which is up-regulated in proliferative cancer lines (149), have been associated with estrogen-mediated action (150-152), and possess putative EREs (26). Moreover, E2 induction of epidermal growth factor receptor (Egfr) (153), c-fos induced growth factor (*Figf*) (154), platelet derived growth factor, alpha (*Pdgfa*) (155) and placental growth factor (*Pgf*) (156) are consistent with cell proliferation. Despite these events no significant E2-induced proliferation was observed, consistent with the lack of proliferation of human HepG2 cells (157) and mouse liver (73), suggesting that these genes are not significant for proliferation or that other signaling responses are involved that negate E2-elicited proliferation signals in hepatic tissue. For example, G1 → S

transition gene integrin beta 1 (*Itgb1*) was down-regulated, contrary to E2 induction seen in MCF-7 cells (158), along with the down regulation of G2 → M transition genes, protein phosphatase 1D magnesium-dependent, delta isoform (*Ppm1d*) and protein kinase, cAMP dependent regulatory, type II beta (*Prkar2b*), which have not been previously reported to be E2 responsive. Interestingly, these responses were also repressed in mouse uterine tissue following the uterotrophic response (159).

Cytoskeletal organization

Proliferation also involves the rearrangement of actin filaments and microtubules for cellular reformation through polymerizing and depolymerizing reactions. Upon estrogen treatment, actin monomer genes, actin, alpha2, smooth muscle, aorta (*Acta2*) (160), and actin polymerizing genes, actin related protein 2/3 complex, subunit 5 (*Arpc5*) were induced along with FYVE, RhoGEF and PH domain containing 1 (*Fgd1*) whose protein product interaction with Cdc42 GTPase may activate actin filament restructuring (161). Some Arpc homologues, which define actin filament polarity, have been shown to be estrogen responsive (162) and may suggest a role for induced actin related protein 2/3 complex subunit transcripts (*Arpc2, Arpc4* and *Arpc5*).

Estrogen has been shown to modulate tubulin polymerization at the protein level (163). This study identifies E2-induction of tubulin monomer transcripts, tubulin, beta 4 (*Tubb4*) and tubulin, gamma 2 (*Tubg2*). These subunits may be remodeled by depolymerizing gene, kinesin family member 2A

(*Kif2a*) and through microtubule interacting organization genes microtubule-actin crosslinking factor 1 (*Macf1*), microtubule-associated protein 1 light chain 3 beta (*Map1lc3b*) and microtubule-associated proteins (*Mtap2* and *Mtap4*) which are induced following estrogen exposure.

Estrogen-induction of keratin (i.e., *Krt1-17, Krt1-19, Krt2-7* and *Krt2-8*) may also be preparatory for morphological changes (164,165). However, all were repressed by 24 hrs, possibly in response to the lack of proliferation. Myosin genes *Myh6, Myl4, Myl7* and *Myo1b* are cytoskeletal components involved in cellular motility and their induction may be a possible morphological determination factor following estrogen exposure. Thus far, estrogen has only been reported to modulate myosin heavy chain expression (166). Despite numerous cytoskeletal reorganization gene expression events, E2 did not induced dramatic changes in cellular morphology (data not shown). It has been suggested that these changes may be in anticipation of pending physiological alterations that require additional signaling (73). In contrast, similar gene expression changes in the uterus yield a dramatic physiological response (144,159).

Cholesterol transport and metabolism

Estrogen lowers serum cholesterol by decreasing LDL:HDL (low density lipoprotein : high density lipoprotein) ratios through increased cellular cholesterol uptake, thus retarding atherosclerotic progression (70). Early induction of LDL receptor transcripts such as *Lrp1, Lrp10* and estrogen responsive *Vldlr* (167)

suggests enhanced cholesterol uptake by Hepa-1c1c7 cells. However, secreted components of the VLDL cholesterol carrier, apolipoproteins *Apoc2* and *Apoe*, are down-regulated, an effect that is contrary to estrogen's anti-atherosclerotic activity, in mouse liver (168), primates and human HepG2 cells (169). Lipoprotein lipase (Lpl) cleavage of VLDL is Apoc2-dependent; however, its repressed transcript levels also suggest reduced VLDL synthesis. These inconsistencies between pro- and anti-atherosclerotic signals may be due to the lack of circulating cholesterol *in vitro,* and therefore its carrier protein expression becomes unnecessary.

Estrogen treatment also affects the cholesterol synthesis pathway. ER-mediated induction of *Hmgcr*, the rate-limiting enzyme involved in cholesterol synthesis, increases buffering by building resistance to dietary cholesterol (170). Although *Hmgcr* was not detected to be significant in this data set, cholesterol synthesis genes 3-hydroxy-3-methylglutaryl-Coenzyme A synthases (*Hmgcs1* and *Hmgcs2*) and phosphomevalonate kinase (*Pmvk*) were up-regulated. However, squalene epoxidase (*Sqle*), a down-stream synthesis gene, was repressed possibly providing feedback to inhibit cholesterol synthesis. Only *Pmvk* and *Sqle* have been reported to be estrogen responsive (171), but all contain a response element in their promoter for sterol regulatory element binding factor 1 (*Srebf1*), which is ER regulated (172). Srebf1 is an endoplasmic reticulum protein that is regulated through Scap cleavage. Scap activity is determined by its release from insulin induced gene 1 (Insig1), which was induced at 2 hr by E2, also reported in the rat uterus (173), and repressed at 24

hr, in the presence of low cholesterol. This potential regulatory network is consistent with the early up-regulation of cholesterol synthesis genes to support cell membrane synthesis for E2 induced growth and proliferation (174).

Fatty acid oxidation

Estrogen is important for lipid homeostasis and regulates a number of β- and ω-oxidation genes as demonstrated by hepatic lipid accumulation in aromatase null mice (175,176). At 8 hrs, several mitochondrial fatty acid oxidation genes were induced. This includes acyl-Coenzyme A dehydrogenase, short chain (*Acads*), which initiates oxidation, acetyl-Coenzyme A dehydrogenase, long-chain (*Acadl*), which breaks down branched and saturated fatty acids, and hydroxyacyl-Coenzyme A dehydrogenase/3-ketoacyl-Coenzyme A thiolase/enoyl-Coenzyme A hydratase (trifunctional protein), beta subunit (*Hadhb*) which hydrates trans double bonds. In addition, peroxisome straight-chain oxidation transcripts acyl-Coenzyme A oxidase 1, palmitoyl (*Acox1*), butyryl Co-enzyme A synthetase 1 (*Bucs1*) and enoyl coenzyme A hydratase 1, peroxisomal (*Ech1*) transcript levels were induced. Although these genes have not been shown to be estrogen responsive, it is consistent with other studies showing that estrogen treatment increases fatty acid oxidation in mice and rats (177,178).

Oxidative stress

E2 hydroxylation and subsequent oxidation to quinines along with the induction of peroxisomal β-oxidation of fatty acids may generate reactive oxygen species (ROS) (179,180). Early E2-induced defensive responses include transaldolase 1 (*Taldo1*), which protects against ROS intermediates, and catalase (*Cat*) which neutralizes peroxide synthesis (175). Furthermore, the elimination of reactive metabolites is facilitated by induced glutathione-S-transferases (*Gsta2, Gsta3* and *Gstm3*) with glutathione replenishment supported by glutathione reductase 1 (*Gsr*) induction, although *in vivo* it was repressed by EE (73). These responses to oxidative stress are accompanied by increases in cytochrome P450 enzymes *Cyp2s1* and *Cyp4b1* for further metabolism and elimination, consistent with reports of other E2-induced isoforms (73,181,182).

Although Hepa-1c1c7 cells maintained in stripped serum conditions are responsive to E2, the transcriptional changes did not reflect the diversity of estrogen-induced responses reported in the mouse liver. Their limited capability to model *in vivo* estrogen elicited responses is not surprising and can be attributed to many factors (e.g., hepatoma vs. normal tissue, 2-D vs. 3-D environment, homogeneous cell population vs. multicellular tissue, lack of systemic immunological effects, and differing pharmacodynamic and pharmacokinetic capacity). Gene-specific discrepancies between models may be a consequence of switch-like responses where treatment triggers a cell from a

gene expression "off" state to an "on" status (183). Consequently, genes may not be identified as active if an insufficient number of cells are triggered. Thus, models may exhibit divergent responses if gene-specific thresholds differ and are not met in both systems. Nevertheless, several responses associated with proliferation, cytoskeletal reorganization, cholesterol transport and metabolism, fatty acid metabolism, and oxidative stress were well conserved. More importantly, most genes commonly expressed between the stripped serum *in vitro* model and C57BL/6 liver samples were temporally co-expressed or exhibited a temporal shift in which *in vitro* responses preceded an equivalent *in vivo* response. Therefore, Hepa-1c1c7 cells in stripped serum conditions can serve as an appropriate model to further investigate selected *in vivo* estrogen-mediated hepatic mechanisms.

CHAPTER 3

COMPARATIVE TEMPORAL AND DOSE-DEPENDENT MORPHOLOGICAL AND TRANSCRIPTIONAL UTERINE EFFECTS ELICITED BY TAMOXIFEN AND ETHYNYLESTRADIOL IN IMMATURE, OVARIECTOMIZED MICE[2].

ABSTRACT

Uterine temporal and dose-dependent histopathologic, morphometric and gene expression responses to the selective estrogen receptor modulator tamoxifen (TAM) were comprehensively examined to further elucidate its estrogen receptor-mediated effects. These results were systematically compared to the effects elicited by the potent estrogen receptor ligand 17α-ethynylestradiol (EE) to identify pathways similarly and uniquely modified by each compound. Three daily doses of 100 μg/kg TAM elicited a dose-dependent increase in uterine wet weight (UWW) in immature, ovariectomized C57BL/6 mice at 72 hrs with concurrent increases in luminal epithelial cell height (LECH), luminal circumference and glandular epithelial tubule number. Significant UWW and LECH increases were detected at 24 hrs after a single dose of 100 μg/kg TAM. cDNA microarray analysis identified 2235 differentially expressed genes following a single dose of 100 μg/kg TAM at 2, 4, 8, 12, 18 and 24 hrs, and at 72

[2] Data contained in this chapter have been published.
Fong CJ, Burgoon LD, Williams KJ, Forgacs AL, Zacharewski TR. 2007. Comparative temporal and dose-dependent morphological and transcriptional uterine effects elicited by tamoxifen and ethynylestradiol in immature, ovariectomized mice. *BMC Genomics* **8**:151.

hrs after three daily doses (3x24 hrs). Functional annotation of differentially expressed genes was associated with cell growth and proliferation, cytoskeletal organization, extracellular matrix modification, nucleotide synthesis, DNA replication, protein synthesis and turnover, lipid metabolism, glycolysis and immunological responses as is expected from the uterotrophic response. Comparative analysis of TAM and EE treatments identified 1209 common, differentially expressed genes, the majority of which exhibited similar profiles despite a temporal delay in TAM elicited responses. However, several conserved and treatment specific responses were identified that are consistent with proliferation (Fos, Cdkn1a, Anapc1), and water imbibition (Slc30a3, Slc30a5) responses elicited by EE. Overall, TAM and EE share similar gene expression profiles. However, TAM responses exhibit lower efficacy, where responses unique to EE are consistent with greater proliferation potential and water imbibition.

INTRODUCTION

Tamoxifen (TAM) treatment is an adjuvant therapy prescribed for estrogen receptor positive breast cancers. TAM and its metabolites, 4-hydroxytamoxifen (4OH-TAM), *N*-desmethyltamoxifen (DMT) and 4-OH-*N*-desmethyltamoxifen (endoxifen), exhibit antiestrogenic activities by competitively inhibiting the binding of potent agonists to the estrogen receptor (ER) thus antagonizing their proliferative effects (53,184-186). Despite the high therapeutic index of TAM for breast cancer, there are concerns regarding the increased occurrence of uterine cancer as early as 2 years after initiating treatment (187). Although there is no direct evidence that it initiates or promotes uterine cancer, TAM exhibits partial ER-agonist activity by inducing uterotrophy in immature and ovariectomized rodents (188,189). Consequently, a more comprehensive comparison to full agonists is warranted to further elucidate the uterine gene expression effects responsible for its partial agonist activity.

TAM is classified as a selective estrogen receptor modulator (SERM) as a result of its differential effects in breast and uterine tissues (190). A number of factors influence the specificity and efficacy of SERM-bound, ER-mediated gene expression, and the subsequent physiological effects. This includes differences in tissue-specific ER isoform expression levels, ligand-induced ER topology, chromatin structure, and coactivator expression and distribution (46,60), thus making the ER an ideal target for drug discovery and development. For example, raloxifene, a second-generation SERM, has been approved for osteoporosis and studies also support its use for breast cancer (191).

The uterotrophic assay is a well established method to evaluate the estrogenicity of a compound as measured by ER-mediated increases in uterine wet weight, making it an ideal model for comparing 17α-ethynylestradiol (EE) and TAM elicited effects (87). The uterotrophic response also provides well characterized phenotypic hallmarks that facilitate the interpretation of gene expression changes and their function. Early studies have shown that TAM elicits a weaker uterotrophic response than 17β-estradiol (E2) in an immature rodent model (47), however, the mechanisms for its partial agonist activity are not well understood.

Genome-wide expression analysis, phenotypically anchored to tissue level effects, provides a comprehensive strategy to identify differential gene expression important in the ER-induction of uterine wet weight. In this report, we extend previous studies examining ER-mediated induction of uterine wet weight (73,144,159) by identifying conserved and divergent uterine tissue and gene expression responses elicited by TAM when compared to EE, an orally active full agonist that mimics the effects of E2 (41). Comparative analysis found conserved gene expression responses that exhibited lower efficacy, consistent with the weak agonist activity of TAM, as well as divergent responses unique to EE that partially explain the lack of TAM-induced water imbibition.

Methods

Animal husbandry and treatment

Female C57BL/6 mice, ovariectomized by the vendor on postnatal day (PND) 20, were obtained from Charles River Laboratories (Raleigh, NC) on PND 25. Groups of five mice were housed in polycarbonate cages bedded with cellulose fiber chips (Aspen Chip Laboratory Bedding, Northeastern Products, Warrensberg, NY) in a 23°C environment with 30-40% humidity and a 12 h light/dark cycle (0700 – 1900 h). Animals had access to deionized water and Harlan Teklad 22/5 Rodent Diet 8640 (Madison, WI) *ad libitum* and acclimatized for 4 days prior to treatment. For the dose response study, animals (n = 5) were orally gavaged with 0.1 mL of 1, 3, 10, 30, 100, 300 or 1000 μg/kg b.w. tamoxifen (≥ 99% pure, *trans*-2-[4-(1,2-Diphenyl-1-butenyl)phenoxy]-*N*,*N*-dimethylethylamine) (Sigma Chemicals, St. Louis, MO), 100 μg/kg b.w. 17α-ethynylestradiol (EE; 17*α*-Ethynyl-1,3,5(10)-estratriene-3,17*β*-diol) (Sigma) or sesame oil vehicle (Sigma) alone. Standard uterotrophic regimen was followed (87), consisting of three daily doses followed by sacrifice 24 hrs after the final treatment, (3 x 24 hrs). Doses were prepared based on average animal weight. For the time course study, animals (n = 5) were orally gavaged once or three times daily (3x24) with 100 μg/kg b.w. TAM or vehicle alone and sacrificed at 2, 4, 8, 12, 18 and 24 hrs after treatment in addition to 3x24 hrs treatment group. Animals were sacrificed by cervical dislocation and animal body weights were recorded. The uterus was transected at the border of the cervix, and stripped of extraneous connective tissue and fat. Whole uterine weights were recorded

before (wet weight) and after blotting (blotted weight) under pressure with absorbent tissue. A 6-8 mm section of uterine horn was not blotted and placed in 10% neutral buffered formalin (NBF) for histological preparation while the remainder was snap frozen in liquid nitrogen and stored at -80°C for RNA extraction. All procedures were performed with the approval of the Michigan State University All-University Committee on Animal Use and Care.

Histological processing, morphometric and pathological analysis

Samples stored in 10% NBF were allowed to fix for at least 24 hrs at room temperature then placed into tissue cassettes and stored in 30% ethanol holding solution at 4°C. Paraffin embedding, 5 μm sectioning, mounting and hematoxylin and eosin staining were completed by the Michigan State University Laboratory for Anatomical Histology and Molecular Sciences according to standard techniques (192). Pathological assessments were evaluated according to standardized National Toxicology Program (NTP) pathology codes.

Morphometric analysis was performed on midhorn uterine cross sections for all animals (n = 5 per treatment group) using Scion Image analysis software (Scioncorp, Frederick, MD). Histological markers of uterotrophy, including luminal epithelial cell height (LECH), luminal circumference and number of endometrial glands were quantified for each slide. Statistical analysis of morphometric data was assessed by Dunnett's or two-way ANOVA followed with Tukey's HSD *post hoc* analysis to examine dose dependent and temporal effects, respectively (SAS version 9.1).

RNA isolation

Briefly, 1.0 mL of Trizol (Invitrogen, Carlsbad, CA) was added to the frozen uterine tissue in a 2.0 mL microfuge tube and homogenized in the presence of steel beads by a Mixer Mill 300 homogenizer (Retsch, Germany). Total RNA was isolated and extracted according to the manufacturer's protocol and resuspended in The RNA Storage Solution (Ambion, Austin, TX). RNA samples were quantified spectrophotometrically (A_{260}) and assessed for quality by A_{260}/A_{280} ratio as well as inspected using denaturing agarose gel electrophoresis.

Microarray hybridization and analysis

Custom in-house cDNA arrays consisting of 13,361 features, representing 7,952 unique genes (Unigene Build 144), were spotted on epoxy coated glass slides (SCHOTT Nexterion, Germany) using an Omnigrid arrayer (GeneMachines, San Carlos, CA) and Telechem Chipmaker 3 pins in a TeleChem CHP3 printhead head (Telechem International Inc., Sunnyvale, CA) by the Research Technology Support Facility at Michigan State University (128). Selected clones were obtained from EPAMAC (129), Research Genetics, the National Institute of Aging and Lion Biosciences. Detailed protocols for processing of microarrays are available at the dbZach Home Page (130).

An independent reference study design was used to assess treatment effects (73). For the dose response study, each treatment group was hybridized to a single vehicle pool utilizing 14 arrays, including dye swaps, and 3 biological

replicates for a total of 42 arrays. For the time course study, each time-matched treated and vehicle sample was competitively hybridized utilizing 14 arrays, including dye swaps with 3 biological replicates for a total of 42 arrays. The Genisphere 900 3DNA Array Detection (Genisphere Inc., Hatfield, PA) indirect incorporation kit was used to generate cDNA samples for hybridization. Briefly, 1 μg of RNA was reverse transcribed in the presence of an oligo-tagged primer specifically targeted for Cy3- or Cy5- conjugated dendrimers. The cDNA was resuspended in 58 μL of 2X Formamide-Based Hybridization Buffer and hybridized overnight on arrays sealed in a light-shielded, humid chamber submerged in a 42°C water bath incubation. Slides were then washed in SSC solutions containing decreasing concentrations of SDS, spin-dried and re-hybridized with a Cy3:Cy5 (1:1) dendrimer mixture in formamide based buffer to indirectly incorporate dyes at the Cy3- and Cy5-dendrimer-tagged cDNA hybridized on the first day. Slides were washed and dried as previously described, and scanned at 635 nm (Cy3) and 532 nm (Cy5) using a 428 Affymetrix Scanner (Santa Clara, CA). Images were examined, features identified and intensity values recorded using GenePix v.5.1 (Molecular Devices).

Microarray quality control, statistical analysis and gene list filtering

All arrays in this study were compared to a historical data set of high quality arrays. Parameters assessed included background signal intensity, feature signal intensity, feature vs. background signal intensity ratios, the number of features with background intensities greater than the feature intensity for each array, and relationships between feature and background signal intensities. All

arrays surpassed the quality control parameters established in this laboratory (193).

Data were normalized using a semi-parametric approach (194) and model-based *t*-values were calculated comparing time-matched treated and vehicle samples. Posterior probabilities of activity [P1(*t*)-value] were then calculated on a per-gene and per-time point basis using an Empirical Bayes analysis (135). Gene lists were initially filtered based on posterior probability (P1(*t*) > 0.999) and fold-change cut-off (|fold change| > ± 1.5) resulting in an active gene list on which further functional analysis was conducted. All raw and analyzed data were stored in dbZach (130), a Minimum Information About Microarray Experiments (MIAME)-supportive relational database (131) running under Linux/Oracle 10g. dbZach currently supports microarray data storage, retrieval, and querying as well as facilitates data analysis, sharing and reporting (133).

Active gene lists exclusive to TAM and EE were also generated. Data for the EE time course has previous been published (159). The TAM unique gene list was generated based on relaxed criteria (P1(*t*) > 0.9 and |fold change| > ± 1.4 cut-off) to obtain a liberal EE-mediated gene list which was then excluded from the original TAM unique gene list using P1(*t*) > 0.999 and |fold change| > ± 1.5 criteria. The EE unique gene list was generated using a reciprocal approach (i.e., relaxed criteria (P1(*t*) > 0.9 and |fold change| > ± 1.4 cut-off) to obtain a liberal TAM-mediated gene list which was then excluded from the original EE unique gene list using P1(*t*) > 0.999, and |fold change| > ± 1.5 criteria). This

approach ensured that genes marginally missing the cut-offs were not included in the compound-unique list.

Estrogen response element searches were completed by comparing Gene Symbols to the computationally identified list compiled by Bourdeau et al. (26).

Quantitative RT-PCR

Aliquots of RNA isolated from each of the five replicates were set aside for SYBR™ Green quantitative real-time PCR (QRT-PCR) verification. EE-treated, temporal mouse uteri RNA were previously isolated (159). An oligo-dT anchored Superscript II (Invitrogen) reverse transcriptase reaction was carried out on 1 μg of RNA, in a 20 μL reaction, from each biological sample as per manufacturer's instructions. Samples were diluted four-fold and 3 μL used in a 30 μL real-time reaction mix containing 1X SYBR Green PCR buffer, 3 mM $MgCl_2$, 0.33 mM dNTPs, 0.5 IU AmpliTaq Gold (Applied Biosystems, Foster City, CA) and 0.15 mM forward and reverse primer. All primers were designed by submitting cDNA microarray clone sequences into Primer3 (138) to obtain an amplicon of approximately 125bp (Supplemental Table 6). PCR amplification was conducted in 96-well MicroAmp Optical plates (Applied Biosystems) on an Applied Biosystems PRISM 7000 Sequence Detection System under the following conditions: 10 min denaturation and enzyme activation at 95°C, followed by 40 cycles of 95°C for 15 s and 60°C for 1 min. After amplification, a 30 min dissociation protocol was conducted to assess primer specificity and product uniformity. Each plate contained duplicate standards of purified PCR product of

known template concentration over eight orders of magnitude to generate a log template concentration standard curve. No template controls (NTC) samples were included on each plate such that experimental samples within 2 standard deviations of the NTCs are considered below the limits of detection. Plots were visualized and thresholds determined using ABI Prism 7000 SDS Software (Applied Biosystems). Results were normalized to a geometric mean of beta-actin (Actb), glyceraldehyde-3-phosphate dehydrogenase (Gapd) and hypoxanthine guanine phosphoribosyl transferase (Hprt) mRNA levels to control for differences in RNA loading, quality and cDNA synthesis. Statistical significance of expression differences between vehicle and TAM treated samples were assessed by two-way ANOVA followed by Tukey's HSD *post hoc* analysis to examine treatment and treatment over time effects (SAS version 9.1). Correlation analyses of QRT-PCR and microarray data generated using the correlation function of R v2.1.0.

Immunohistochemistry

Rabbit polyclonal antibodies specific for PCNA were purchased from Abcam, Inc. (Cambridge, MA) and staining localized using manufacturer's instructions for the Vectastain Elite ABC Kit (Vector Laboratories, Burlingame, CA). Briefly, paraffin-embedded uterine sections were placed on glass slides, deparaffinized in xylene and re-hydrated through a series of decreasing ethanol concentration washes ending in ddH_2O. Endogenous peroxidases were quenched in 0.3% H_2O_2 in methanol solution (30 min) followed by boiling (15

min) in a 10 nM sodium citrate solution (pH 6.0) for antigen retrieval. To minimize nonspecific background staining, sections were blocked with normal goat serum (Vector Laboratories) for 20 min. The slides were incubated for 1 hr with the primary rabbit anti-PCNA polyclonal antibody (1:500 dilution in PBS), followed by 30 min each with biotinylated goat anti-rabbit antibody (Vector Laboratories) (1:400) and ABC reagent (Vector Laboratories). A single PBS rinse was performed between incubations with each antibody. Localization of antigen was obtained using Vector® NovaRED (Vector Laboratories). The sections were counterstained with hematoxylin.

RESULTS

Uterine weight

Increases in uterine wet weight (UWW) in rodents after three daily subcutaneous doses of TAM is well documented (84,195). Dose-dependent increases in uterine weight (EC_{50} = 33.7 μg/kg) were observed following three consecutive daily oral treatments of TAM (Figure 1A), however induction plateaued at 5-fold, compared to 11-fold with an equivalent dose of 100 μg/kg 17α-ethynylestradiol (EE) (159). Comparison of wet and blotted uterine weights indicated no significant water imbibition in TAM-treated uteri. However, blotted EE-treated uteri were larger, consistent with past reports that TAM induces a less efficacious uterotrophic effect (196). In order to establish a temporal profile, the uterotrophic effects of 100 μg/kg TAM were also investigated at 2, 4, 8, 12, 18, 24 and 3x24 hrs. A significant 2.5-fold increase was observed at 24 hrs after a single 100 μg/kg TAM dose (Figure 1B) which was delayed compared to the significant increase seen with 100 μg/kg EE at 18 hrs (159).

Morphometric analysis and histopathology

Luminal epithelial cell height (LECH), luminal circumference and number of endometrial glands are hallmarks of estrogen action in the rodent which correlate with UWW induction (197). Significant dose-dependent increases in LECH and luminal circumference were initially detected at 30 μg/kg TAM (Table 1A). Interestingly, LECH was not significantly different between 100

Figure 1

Tamoxifen-induced dose dependent and temporal changes in uterine weight

Graphs illustrate fold-change increases in uterine wet (open) and blotted (solid) weight. A) Tamoxifen elicits a dose dependent uterotrophic response (EC50 = 33.7 μg/kg) and achieves maximal induction of approximately 5-fold following three daily doses (3 x 24 hrs) of 100 μg/kg TAM. Significant increases ($p < 0.05$, $n = 5$) are denoted by an asterisk (*). In contrast, 100 μg/kg EE (positive control) maximally induced uterine wet weight 11-fold (*, $p < 0.05$, $n = 5$) with significant water imbibition (#; $p < 0.05$, $n = 3$), while TAM only achieved 50% uterotrophic efficacy and no water imbibition. B) A single dose of 100 μg/kg TAM significantly increased uterine wet weight as early as 24 hrs after administration. No significant water imbibition was observed at any time point.

Figure 1

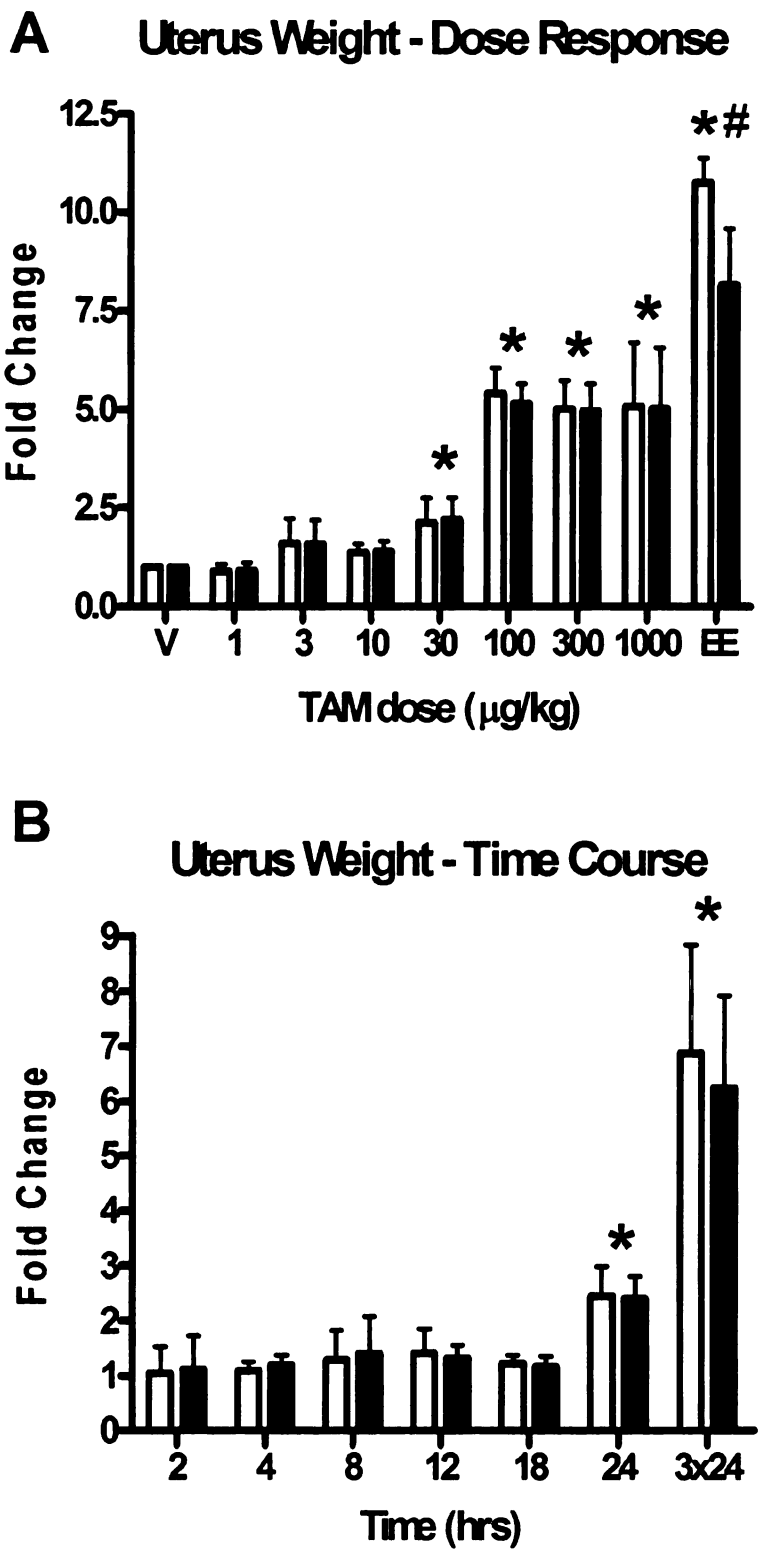
A
Uterus Weight - Dose Response
Fold Change
12.5
10.0
7.5
5.0
2.5
0.0
*#
*
*
*
*
V
1
3
10
30
100
300
1000
EE
TAM dose (µg/kg)
B
Uterus Weight - Time Course
Fold Change
9
8
7
6
5
4
3
2
1
0
*
*
2
4
8
12
18
24
3x24
Time (hrs)

Table 1. TAM- and EE-induced uterine morphometric changes

A)

Dose Response (3 x 24 hr)			
TAM Dose (μg/kg)	Luminal Epithelial Cell Height (μm)	Luminal Circumference (mm)	Avg. Number of Glandular Tubules
0	8.75 ± 0.86	0.77 ± 0.14	1
1	8.99 ± 1.00	0.72 ± 0.12	0
3	10.91 ± 2.97	1.17 ± 0.41	1
10	10.73 ± 1.15	1.17 ± 0.29	3
30	15.12 ± 1.55*	1.87 ± 0.26*	5*
100	24.58 ± 2.79*	3.60 ± 0.27*	10*
300	27.08 ± 3.79*	2.68 ± 1.19*	5*
1000	31.30 ± 2.25*	3.05 ± 0.73*	5*
100 EE	28.94 ± 3.35*	+++[a]	4

B)

Time Course (100 μg/kg)		
Time (hrs)	Luminal Epithelial Cell Height (μm)	Luminal Circumference (mm)
2	9.98 ± 1.68	0.79 ± 0.19
4	8.61 ± 1.58	0.80 ± 0.06
8	10.06 ± 2.50	0.96 ± 0.29
12	9.46 ± 1.28	0.99 ± 0.21
18	9.18 ± 1.03	1.29 ± 0.42
24	11.08 ± 1.94*	1.22 ± 0.42
3x24	28.61 ± 7.50*	2.85 ± 1.83*

* Statistically different from time matched vehicle ($p < 0.05$)

[a] Lumen larger than 100x field of view, accurate measurements could not be made at 40x magnification

Time course vehicle samples are not significantly different from each other.

μg/kg EE and TAM, although the luminal circumference of EE uteri was greater with more pronounced invagination of the luminal glandular epithelium (Figure 2). There was also mild to moderate hypertrophy in the stromal nuclei at 10 μg/kg TAM with moderate epithelial hypertrophy and hyperplasia at 30 μg/kg TAM, which was marked at higher doses. Mild edema was noted for all samples beginning at 100 μg/kg TAM. Marked to severe stromal nuclei hypertrophy and epithelial hypertrophy and hyperplasia, all with mild edema, was observed at 100 μg/kg EE. Mild to moderate stromal edema was observed as early as 12 hrs following after a single 100 μg/kg TAM dose, while increased UWW and LECH were not significant until 24 hrs (Table 1B). No significant increase in luminal circumference was observed in the first 24 hrs after treatment.

Uterine endometrial glands synthesize and secrete fluids in preparation for conceptus, implantation and growth. Significant increases in the number of glands was observed at 30 μg/kg TAM (Table 1A) in the absence of a dose responsive increase, which may be an artifact of histological sampling of the uterine horn. Similarly, EE-treated uteri exhibited an increased number of endometrial glands that was not statistically significant.

Uterine gene expression changes elicited by tamoxifen

Differentially expressed genes in the dose and time dependent studies were identified based on their empirical Bayes posterior probability of activity [P1(*t*)-value] on a per-gene, per-time point basis. P1(*t*)-values approaching 1.0 indicate a greater likelihood of treatment-related differential gene expression.

Figure 2

Uterine histology

Hematoxylin and eosin stained sections of uterine tissue at 100x magnification after three daily doses of A) sesame oil, B) 1 mg/kg TAM and C) 100 μg/kg EE. TAM and EE treatment induced increases in luminal epithelial cell height. Luminal circumference is increased to a greater degree by EE than TAM. Bars represent 20 μm.

Figure 2

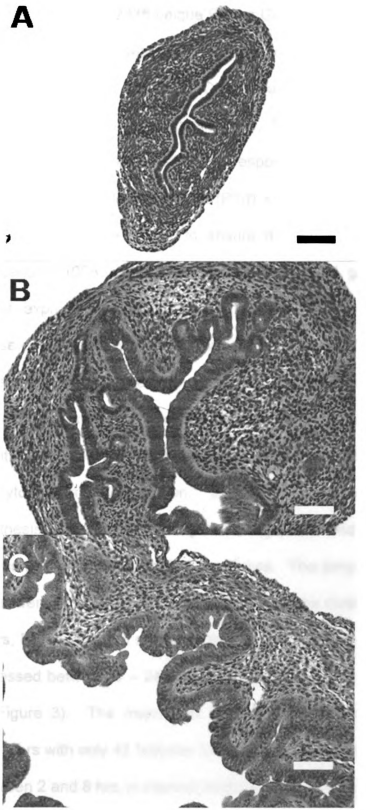

Using P1(t) > 0.999 and |fold change| ≥ 1.5 as selection criteria, a prioritized list of 2941 features, representing 2235 unique Entrez Gene annotated genes, were identified in the temporal study with 55% of the genes exhibiting induction and 45% repression (Supplemental Table 1). Differential expression levels ranged from 14.3-fold repression (tight junction protein 4, *Tjp4*) to 28.1-fold induction (arginase 1, *Arg1*), further demonstrating the responsiveness of the uterus to tamoxifen. Using the same selection criteria (P1(t) > 0.999 and |fold change| of ≥ 1.5) at a minimum of three doses, to ensure dose responsiveness, 1630 features, representing 1036 unique Entrez Gene-annotated genes, exhibited dose dependent expression (Supplemental Table 2). Of the 1036 genes exhibiting a dose-dependent response at 3x24 hrs and of the 738 differentially expressed genes at 3x24 hrs in the time course study, 691 genes (94%) were in common, demonstrating good reproducibility between experiments.

Differentially expressed genes were associated with cell growth and proliferation, cytoskeletal organization, extracellular matrix modification, nucleotide synthesis, DNA replication, protein synthesis and turnover, lipid metabolism, glycolysis and immunological responses. The temporal changes in gene expression were best represented using five k-means clusters: A) induced at 12 and 24 hrs, B) induced and sustained from 24 – 72 hrs, C) induced late at 72 hrs, D) repressed between 8 – 24 hrs and E) repressed and sustained from 24 – 72 hrs (Figure 3). The majority of TAM-elicited differential expression occurred after 12 hrs with only 42 features (26 genes) exhibiting differential gene expression between 2 and 8 hrs, in marked contrast to EE studies where

Figure 3

Tamoxifen-induced temporal gene expression patterns

Five k-means clusters best represent the general temporal patterns for the 2941 features differentially expressed following TAM treatment. Note the 8 hr delay in gene expression response especially in comparison to EE elicited gene expression is speculated to be due to the delayed absorption of TAM. Inset numbers indicate the number of features represented by each cluster. Black pseudolines indicate the general profile represented within each cluster.

Figure 3

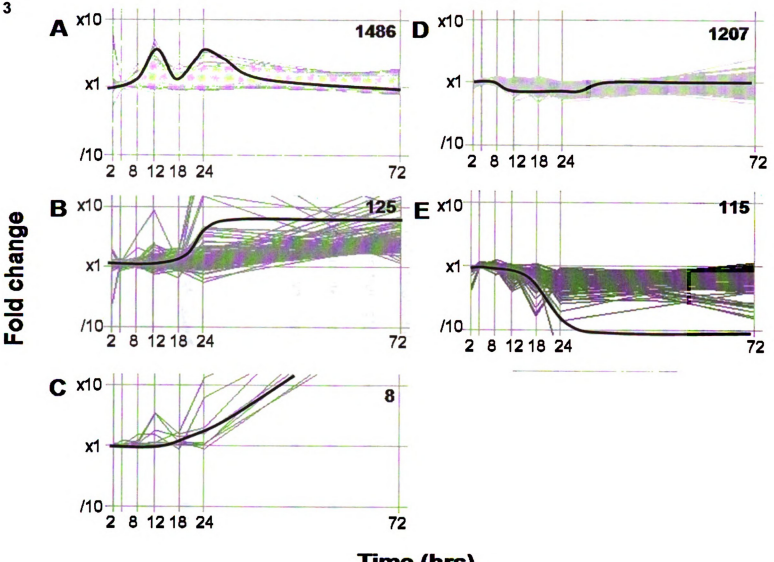
A
x10
x1
/10
1486
2 8 12 18 24 72
D
1207
B
125
E
115
C
8
Fold change
Time (hrs)

significant gene expression changes occurred prior to 8 hrs (144,159,198). The temporal pattern of differential gene expression correlates with the histology results which indicate a delayed response in comparison to EE.

Eleven genes, representative of affected pathways and exhibiting different temporal gene expression patterns (i.e. cytoskeletal organization (*Krt2-4*), signal transduction (*Igf1*), immunological responses (*Il7*), acid-base homeostasis (*Car3*) and lipid transport (*Fabp5, Vldlr*)), were verified by QRT-PCR and exhibited good agreement with microarray results. Correlation coefficients ranged from 0.46 to 0.97 (mean = 0.80) (Figure 4).

Immunohistochemistry (IHC) was also used to assess and localize PCNA protein expression following TAM treatment (Figure 5). Microarray results indicate a 2.5-fold increase in *Pcna* transcript levels between 12 - 18 hrs after treatment with IHC, confirming elevated protein expression in epithelial and stromal cells in 12 hr TAM treated samples when compared to time matched controls.

Comparison of common temporal TAM and EE gene expression data

Temporal TAM data were compared to an analogous EE study using the same immature, ovariectomized C57BL/6 mouse model (159). Employing the $P1(t) > 0.999$ and $|\text{fold change}| \geq 1.5$ criteria, 2657 unique annotated genes were differentially expressed following treatment with 100 μg/kg EE, of which 1209 were also activated by TAM (Supplemental Table 3). Agglomerative hierarchical clustering of common genes by treatment and time indicates that the 12 hr TAM

Figure 4

Quantitative real-time PCR verification of selected TAM-induced genes

Overall, the microarray results for 14 TAM- and EE-induced genes were verified using QRT-PCR. The verified genes represent various affected pathways and different temporal patterns of expression. Overall, there was good correlation (average ρ = 0.8) between microarray (lines) and QRT-PCR (bars) data. Examples for six of the genes are illustrated. Statistically significant QRT-PCR differences ($p < 0.05$, $n = 4$) due to treatment are denoted by an asterisk (*).

Figure 4
Car3
cluster D
QRT-PCR
Microarray
Fold Change
Time (hrs)
Fabp5
cluster C
Igf1
cluster A
Krt2-4
cluster E
Vldlr
cluster B
Il7
cluster B
0 2 4 8 12 18 24 3x24

Figure 5

Immunohistochemical detection of differential Pcna protein levels due to TAM

Twelve-hour vehicle (A) and TAM (B) treated uteri sections were immunohistochemically stained (NovaRED®) with Pcna specific antibodies. Treated samples have darker nuclear staining, indicating greater levels of Pcna protein expression, in agreement with the histological assessment and changes in gene expression associated with cell proliferation. Increased Pcna expression is more pronounced in the luminal and glandular epithelium, and stroma (arrows). Tissues were counter-stained with hematoxylin. Images are representative of four biological replicates. Bars represent 20 μm.

Color representation of this figure may be found in:

Fong CJ, Burgoon LD, Williams KJ, Forgacs AL, Zacharewski TR. 2007. Comparative temporal and dose-dependent morphological and transcriptional uterine effects elicited by tamoxifen and ethynylestradiol in immature, ovariectomized mice. *BMC Genomics* **8:**151.

Figure 5

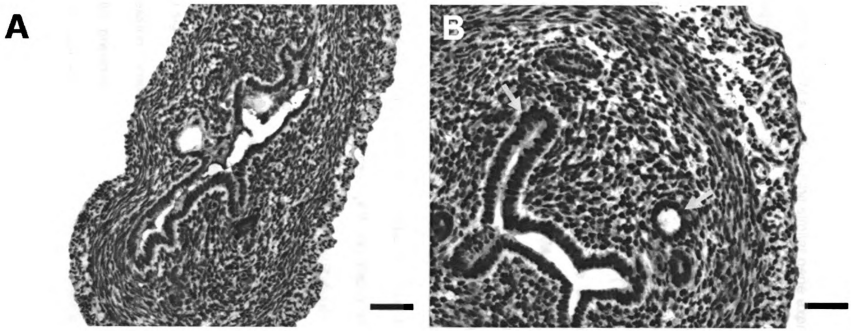

response is most similar to the 4 hr EE response, followed closely by 8 hr TAM (Figure 6). Interestingly, TAM and EE exhibit similar gene expression profiles at 24 and 72 hrs, suggesting that the delay in some TAM-elicited responses is not maintained at later time points.

Expression profiles were compared for the 1209 differentially expressed genes that were regulated by TAM and EE. These genes were categorized as Similar, more Efficacious by EE or TAM, or Ambiguous (Table 2). A total of 793 genes (66%) exhibited expression profiles that were similar in pattern and efficacy when a temporal shift, due to delayed TAM response, was considered. Interestingly, 28 genes that were differentially expressed at least 2-fold more by EE when compared to TAM (i.e., EE Efficacious genes) were associated with cell growth, regulation of transcription and protein metabolism and transport including *Fos* (6.4-fold by EE; 4.1-fold by TAM) and *Inhbb* (7.6-fold by EE; 3.2-fold by TAM). These genes are involved in cell cycle regulation and cellular growth, respectively, and possibly support the greater physiological effect exhibited by EE. In contrast, 19 genes were modulated 2-fold or greater by TAM, including *Sfn* (3.6-fold by EE; 5.5-fold by TAM), which is associated with proliferation inhibition. In general, efficacious TAM elicited responses were associated with receptor-mediated signal transduction, ion transport and protein metabolism.

Gene expression comparisons between the two studies were also verified by QRT-PCR. As previously reported, gene expression data is subject to compression (199), and therefore the sensitivity of QRT-PCR data is often greater when compared to microarray data Thus, some genes classified.

Figure 6

Temporal comparison of genes commonly activated by TAM and EE

Hierarchical clustering of 1209 TAM- and EE-regulated genes (y-axis) identifies subsets of similar profiles according to time and treatment (x-axis). The dendrogram indicates that early responses (4 hrs) to ethynylestradiol (E) are most similar to 8 and 12 hrs tamoxifen (T) responses demonstrating temporally displaced TAM activation consistent with the delayed absorption of TAM. However, temporal displacement of TAM elicited responses is not maintained as EE and TAM responses cluster together at 24 and 72 hrs.

Color representation of this figure may be found in:

Fong CJ, Burgoon LD, Williams KJ, Forgacs AL, Zacharewski TR. 2007. Comparative temporal and dose-dependent morphological and transcriptional uterine effects elicited by tamoxifen and ethynylestradiol in immature, ovariectomized mice. *BMC Genomics* **8:**151.

Figure 6

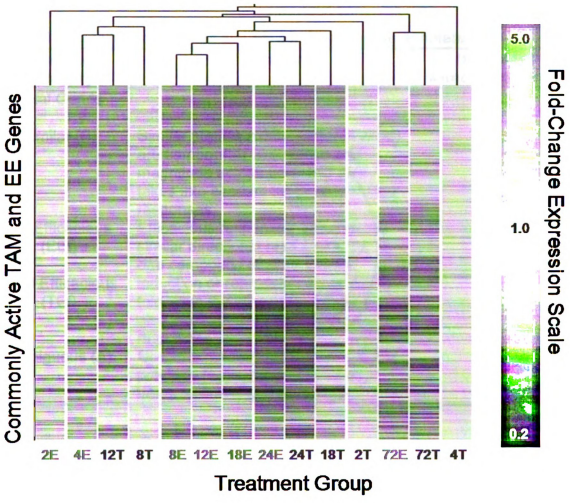
Commonly Active TAM and EE Genes
2E 4E 12T 8T 8E 12E 18E 24E 24T 18T 2T 72E 72T 4T
Treatment Group
5.0
1.0
0.2
Fold-Change Expression Scale

Table 2. Classification of TAM and EE commonly active annotated genes

Classification Category	Definition	Number of Annotated Genes
Total Genes		1209
Similar (S)	Similar profiles exhibit patterns which are comparable in direction and magnitude across time; this also takes into account temporally shifted responses.	793
EE Efficacious (EEf)	Efficacious responses demonstrate similar directional responses, but one compound elicits a greater	28
TAM Efficacious (TEf)	induction or repression, by at least 2-fold, than the other; this category also includes temporally shifted responses.	19
Ambiguous (A)	Gene pairs which did not fall into the previous three categories were labeled as Ambiguous	369

as Similar may also be classified as EE- or TAM-Efficacious. For example, microarray data suggested that Cdkn1a response to TAM and EE were comparable, but through QRT-PCR EE induced an 8-fold response compared to a 3.5-fold induction by TAM (Figure 7).

TAM and EE responsive genes were also examined for estrogen response elements (EREs) in their promoter regions by comparison to a list of computationally identified sequences (26). EREs were found in 176 TAM-active genes and 218 EE-active genes, with 133 regulated by both compounds. Only 10% of TAM or EE differentially expressed genes possessed an ERE suggesting that other *trans*-acting factors may also be involved or that EREs were outside of the search regions. Annotation information in public repositories is constantly evolving, thus gene names may have changed or new genes may have been added since the publication. As a result, some genes may be misclassified regarding their ERE status.

TAM- and EE-specific gene expression data

Gene expression changes unique to either TAM or EE may be another factor contributing to their different uterotrophic responses. An additional filtering method was used to identify genes more likely to be unique to EE treatment which involved excluding an extended list of TAM-regulated genes obtained by relaxing the TAM criteria to $P1(t) > 0.9$ and $|\text{fold change}| \geq 1.4$ from the standard criteria ($P1(t) > 0.999$; $|\text{fold change}| \geq 1.5$) of EE (Figure 8A). The same approach was also used to obtain a list of genes unique to TAM (Figure 8B).

Figure 7

Examples of TAM and EE differential gene expression classifications

Examples of representative genes classified as Similar or Efficacious based on microarray data only. QRT-PCR analysis confirmed the classifications of these genes. In some cases (e.g., Cdkn1a) a gene classified as Similar may also be classified as EE-Efficacious based on QRT-PCR results due to data compression inherent in microarray data. Statistically significant differences ($p < 0.05$, $n = 4$) due to treatment are denoted by an asterisk (*).

Figure 7

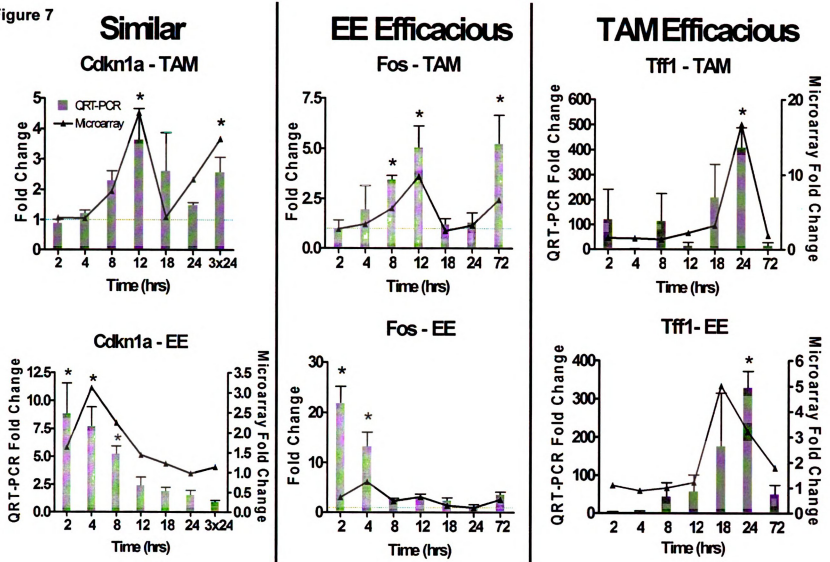
Similar
EE Efficacious
TAM Efficacious
Cdkn1a - TAM
Fos - TAM
Tff1 - TAM
QRT-PCR
Microarray
Fold Change
QRT-PCR Fold Change
Microarray Fold Change
Time (hrs)
2 4 8 12 18 24 3x24
2 4 8 12 18 24 72
Cdkn1a - EE
Fos - EE
Tff1- EE

Figure 8

Identification of unique EE and TAM differentially expressed genes

Treatment specific differentially expressed genes were identified by excluding a list obtained using a more relaxed criteria (P1(t) > 0.9; |fold change| ≥ 1.4) for one treatment from the differentially expressed genes identified using the standard criteria (P1(t) > 0.999; |fold change| ≥ 1.5) of the second treatment to identify gene expression changes that were more likely to be unique to one treatment. (A) A liberal list of TAM-induced genes identified, using a relaxed criteria of P1(t) ≥ 0.9 and |fold change| ≥ ± 1.4, was excluded from the EE differentially expressed gene list using the standard selection criteria of P1(t) ≥ 0.999 and |fold change| ≥ ± 1.5 to identify 240 genes more likely to be differentially expressed by EE alone. (B) Using a similar approach, a list of 60 genes more likely to be differentially expressed by TAM alone was generated. Lists of EE and TAM specific genes are provided in Supplemental Tables 4 and 5.

Figure 8

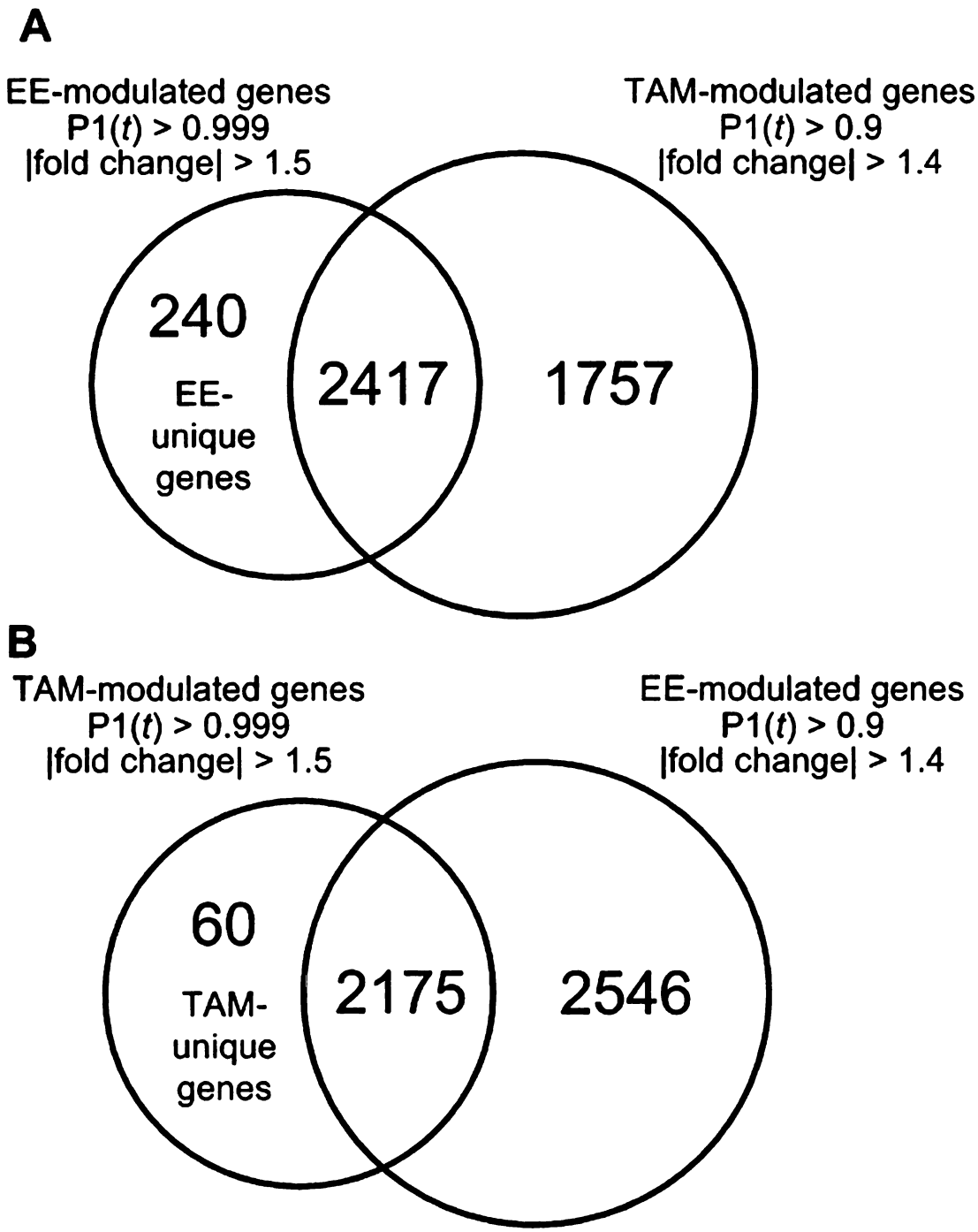
A
EE-modulated genes
P1(t) > 0.999
|fold change| > 1.5
TAM-modulated genes
P1(t) > 0.9
|fold change| > 1.4
240
EE-unique genes
2417
1757
B
TAM-modulated genes
P1(t) > 0.999
|fold change| > 1.5
EE-modulated genes
P1(t) > 0.9
|fold change| > 1.4
60
TAM-unique genes
2175
2546

This ensures that those genes significant in both treatments and approaching significance in the other treatment are not considered as unique, thus increasing the likelihood of identifying treatment-specific differential gene expression responses. For example, to identify unique EE responses, the 2417 differentially expressed TAM genes that satisfy the P1(t) > 0.9 and |fold change| > 1.4 were excluded from the 2657 differentially expressed EE genes (P1(t) > 0.999; |fold change| ≥ 1.5) to identify 240 genes unique to EE treatment (Fig. 8a; Supplemental Table 4). Similarly, genes more likely unique to TAM were identified by excluding the 2175 differentially expressed EE genes with a P1(t) > 0.9 and |fold change| > 1.4 that were in common with the 2235 differentially expressed TAM genes (P1(t) > 0.999; |fold change| ≥ 1.5) to identify 60 genes more likely unique to TAM (Supplemental Table 5). Treatment-specific responses exhibited profiles distinctly different in pattern and magnitude from their counterpart (Figure 9) even when taking delays, due to TAM, into consideration.

The pathways represented within unique EE-responsive genes include apoptosis regulators (*Bok* and *Pdcd6*) and water imbibition (*Aqp8* and *Slc22a7*), consistent with the physiological effects observed. Fewer unique TAM-responsive genes were identified. There was no overrepresentation of any functional pathway consistent with its weaker uterotrophic response. These data suggest that differentially regulated subsets of genes exist that contribute to the distinctive uterotrophic response elicited by each treatment.

Figure 9

Temporal expression profiles of TAM and EE-specific genes

Graphical representation of genes exhibiting compound-specific responses demonstrated profiles which were distinctly different in pattern and magnitude compared to its non-responsive counterpart. These examples further illustrate that the filtering conditions used were adequate to identify differential responses by TAM and EE.

Figure 9

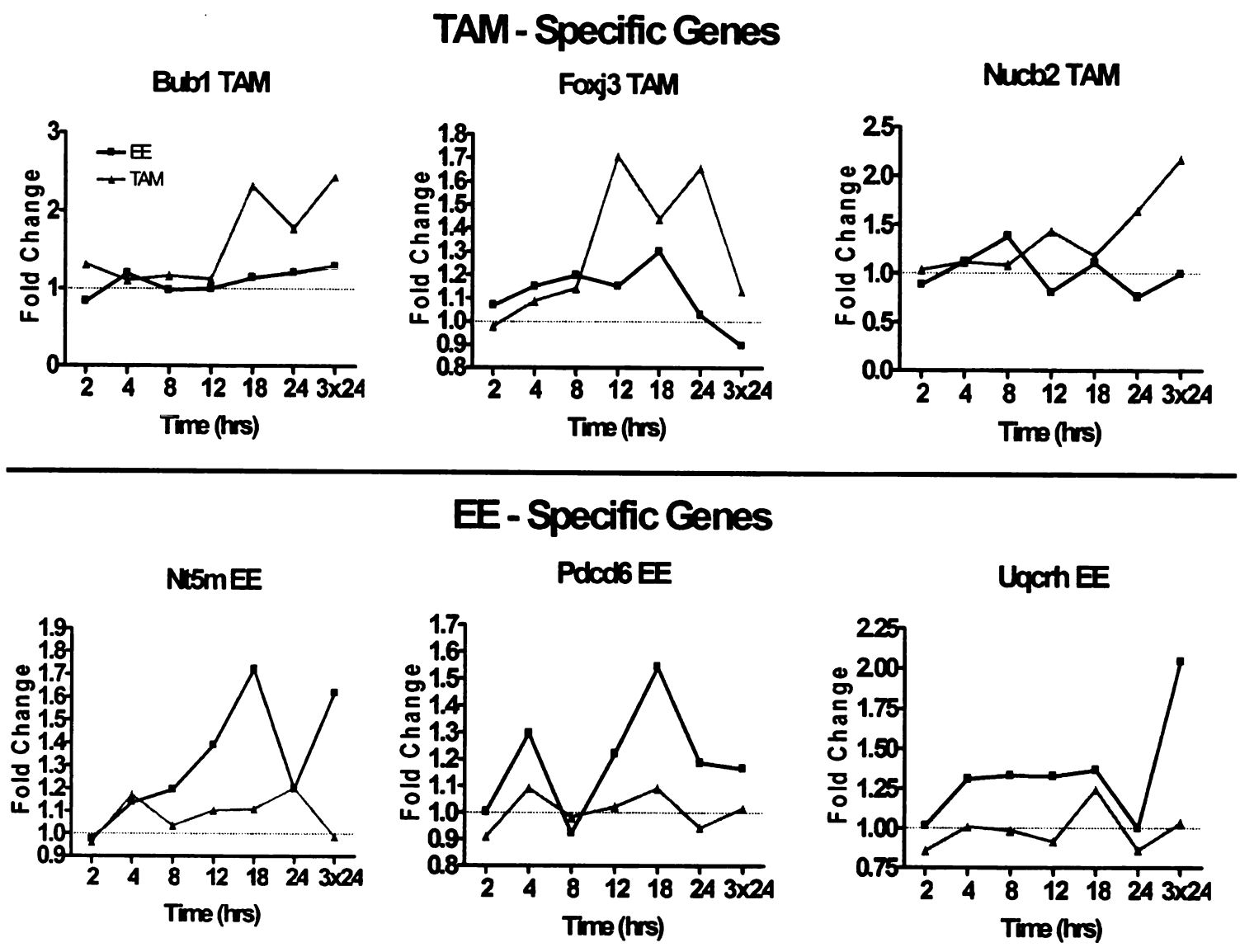
TAM - Specific Genes
Bub1 TAM
Foxj3 TAM
Nucb2 TAM
EE
TAM
Fold Change
Time (hrs)
2 4 8 12 18 24 3x24
EE - Specific Genes
Nt5m EE
Pdcd6 EE
Uqcrh EE

DISCUSSION

A comparative approach was used that integrates the gross organ, histopathological, and morphometric uterine effects of EE and TAM with their dose response and temporal gene expression profiles to further elucidate the molecular basis of the partial agonist activity of TAM. TAM treatment induces a 5-fold increase in gross uterine weight following three daily doses compared to an 11-fold increase with EE. In addition, no significant water imbibition was induced by TAM. These effects are well documented and are the basis for the classification of TAM as a partial agonist (84,195,196,200). Moreover, TAM induces a delayed increase in uterine weight when compared to EE which may be partially attributed to its weaker agonist activity but is more likely a reflection of slower absorption (52,201,202). In contrast, peak serum levels of EE are detected within two hours of treatment (203).

At equi-efficacious doses of TAM and EE (i.e. 100 vs. 20 μg/kg, respectively), comparable effects on UWW, luminal circumference and glandular epithelial were observed (data not shown), suggesting both treatments proceed through similar changes to achieve uterotrophy. However, at higher doses, TAM does not elicit a comparable gamut of responses as seen with higher doses of EE. Surprisingly, TAM increased luminal epithelial thickness (188), due to cellular hypertrophy and hyperplasia, that was not significantly different from EE, but mediated a smaller increase in luminal circumference with more endometrial glands compared to EE. Although these results appear contradictory, glandular epithelium may arise from the luminal epithelium and appear as highly

invaginated regions of the lumen that generate a large secretory surface area (204). Thus, despite fewer endometrial glands in EE samples, its glandular area is greater due to the increased luminal glandular surface area which was not observed in the TAM treated samples.

Temporal tamoxifen-elicited gene expression profiles were examined following a single dose as well as after three daily doses of 100 μg/kg TAM. Only 9 features, representing 6 annotated genes, exhibited differential expression at 2 and 4 hrs after TAM treatment compared to 1234 EE genes at the same time points (159), consistent with the delayed histological effects. Of these early TAM responses, only Esr1 and Car3 have been reported to be induced by estrogen (159,205). At 12 hrs, 683 genes were differentially expressed in response to TAM, of which 541 genes were also affected by EE between 2 and 8 hrs (159). Agglomerative hierarchical clustering suggests that genes affected by TAM and EE exhibited comparable gene expression changes despite the delay in TAM responses.

Genes regulated by TAM and EE represent a variety of pathways including cell cycle regulation, cytoskeletal re-organization, nucleotide metabolism, immune and complement activation and lipid transport and metabolism, and have previously been associated with eliciting the uterotrophic response (144,159,198,206-208). Similarities in their gene expression profiles suggest that the uterotrophic response involves a defined subset of genes mediated by the ER. Furthermore, greater than 75% of TAM-activated genes with putative EREs (26), were also activated by EE. However, differences in

efficacy and responsive genes may partially explain uterotrophic response differences.

Despite temporal delays, many genes were regulated by both EE and TAM. Most of these commonly active genes exhibited comparable fold changes suggesting that they do not significantly influence the magnitude of the uterotrophic response. For instance, both treatments equally repressed uterotrophic supportive pro-apoptotic caspases (*Casp2* and *Casp6*) (reviewed in (209)). Although these genes were responsive to EE and TAM, others demonstrated quantitative differences in their expression behavior. Twenty-eight genes, including the proliferation supportive genes *Cdkn1a*, *Fos* and *Inhbb*, exhibited greater EE efficacy consistent with their previously reported estrogen-induced expression (210-212) resulting in a full uterotrophic agonist response. In contrast, 22 genes more highly induced by TAM included G2/M inhibitor (*Sfn/14-3-3σ*), which has been associated with human endometrial carcinomas (213) to reduce proliferation. Many of these quantitative differences in gene expression efficacy are consistent with the potent agonist activity of EE and the weak agonist activity of TAM.

There were also treatment-specific gene expression effects. Tentatively, 240 and 60 modulated genes were identified as unique to EE or TAM, respectively. In general, these responses were consistent with uterotrophic activity elicited by EE and TAM. For example, QRT-PCR verified the early induction of mitotic gene, *Anapc1* by EE (data not shown). Also, the treatment specific repression of pro-apoptotic Bcl-2 member, *Bok*, and the induction of

Pdcd6, an apoptosis regulator, associated with proliferating tissues (214) are consistent with the greater efficacy of EE. *Bok* has previously been shown to be EE responsive in uteri, whereas *Pdcd6* approached the statistical cut-off in a previous study (144). For TAM, QRT-PCR confirmed decreased expression of *Sipa1* (data not shown), a repressed response at 24 hrs associated with decreased proliferation (215) that may reduce hyperplasia.

DNA synthesis and replication pathways were also differentially regulated. Sustained up-regulation of dNDP phosphorylating genes, *Nme1* and *Nme6* (216), suggest salvage pathways are emphasized for nucleotide synthesis rather than *de novo* processes. Consistent with this view *Prps1*, the first step in purine biosynthesis, is repressed during the same period. These genes are similarly modulated by TAM and EE, suggesting that proliferation may deplete resources for *de novo* synthesis. Only *Nme1* has been previously shown to be EE responsive in rodent uteri (144,159). However, EE uniquely inhibited the *de novo* pyrimidine synthesis gene, *Dhodh* [18 – 72 hrs], and induced the nucleotide recycling gene, *Nt5m* [18 and 72 hrs] (217) suggesting an involvement of salvage pathways to support EE-induced proliferation which have not previously been reported to be estrogen responsive.

Water imbibition is a characteristic uterine response to estrogens, involving the increased flow of water to the lumen mediated by aquaporins and ion transporters (218). It does not appear to be a factor in TAM-induced uterine weight increases, as blotted weights were not significantly different from wet weights. *Aqp1* and *Aqp5* are comparably regulated by TAM and EE, while *Aqp8*

induction was specific to EE (QRT-PCR verified, data not shown). *Aqp8* is a known contributor to water imbibition (219) and its EE-specific response suggests it may play a larger role in the process of a full uterotrophic response.

The lack of ion transporter regulation may also be a contributing factor in the absence of TAM-induced water imbibition. The EE induction of zinc transporter, *Slc30a3* [12 hrs], which causes ion uptake into various vesicle compartments (220,221) may facilitate stromal edema and has been shown to be responsive to estrogen where it is down-regulated in brain tissue (222). Organic anion transporter, *Slc22a7*, was repressed by EE from 18 – 72 hrs in the uteri suggesting anion retention in the stroma that may also be important for edema. *Slc22a7* is an importer in the basolateral membrane of kidney tubule epithelia (reviewed in (223)), and is estrogen responsive in the kidney (224).

Differential regulation of ATP production genes is also consistent with the greater uterotrophic efficacy of EE. Transcripts associated with oxidative phosphorylation (OXPHOS) complex I, *Ndufb8* [8 – 24 hrs], and complex III, *Uqcr* [8 – 18 hrs] and *Uqcrh* [4 – 18, 72 hrs], were all up-regulated. Although not previously been reported as responsive, collectively, the EE modulation of OXPHOS components is consistent with greater energy demands required to support increasing hypertrophic and hyperplastic activity induced by EE compared to TAM.

Other TAM gene expression studies have been conducted using *in vitro* breast cancer models, primarily MCF-7 cells. Comparisons of differentially expressed gene lists identified minimal to no overlap of TAM responses between

in vitro human breast tissue and *in vivo* mouse uterus (225,226). Only the induction of *Uqcrb* (227), *Nqo1* (228), *Tff1*, *Mapt* (229), *Pctk3*, *Wnt4* (230), *Myb*, *Cdc6*, *Cdc20*, *Mcm2*, *Fos* and *Mybl2* (231) and repression of *Xrcc1*, *Tgfa* (228), *Rap1ga1*, *Blnk*, *Tm4sf1*, *Matn2*, *Ifi30*, *Tgfb3* and *Smpd1* (229) correlated with the changes observed in the current study. Moreover, there are examples of divergent gene expression changes such as inverse responses for *Pfn2* (228), *Ctsh*, *Selenbp1*, *Nfrkb*, *Cyp1a1* (229), *Prps1* and *Tmsb4x* (230). The long term uterine effects of TAM have also been examined in mice following neonatal exposure. Mice were treated for four consecutive days after treatment and uteri samples examined at various months after dosing (232). *Col1a1* exhibited persistent up-regulation months after treatment and was also induced in our short term study. Several factors, such as model and tissue differences, likely contribute to the minimal overlap including differences in array platforms and genome coverage, study design, and data analysis. For example, E2 and 4OH-TAM were utilized in the *in vitro* studies while EE and TAM were administered to the mice.

Despite the minimal overlap between the models, the activities of TAM, when compared to E2 were comparable. *In vitro* and *in vivo*, the gene expression changes elicited by 4OH-TAM were similar to those mediated by E2 in MCF-7 cells. Furthermore, the magnitude of gene expression changes due to 4OH-TAM was attenuated compared to E2 (229,231). Although 4OH-TAM and EE induced similar cell cycle genes, down-stream mechanisms were also regulated to prevent 4OH-TAM mediated cell cycle progression (231). Some of

these pathways may play a role in the partial uterotrophic response elicited by TAM in treated mice.

Differences in chemical structure may contribute to ligand specific responses. TAM belongs to the stilbene/triphenylethylene family while EE is steroidal. Each has unique binding modes resulting in different ER conformations (186), binding affinities (233,234), ligand-induced binding domain topographies (235), coactivator recruitment capabilities (236,237), gene-specific thresholds of activation, and efficacies (238). Specifically, 4OH-TAM induces a different conformational change in the ER compared to E2, influencing interactions with different coactivators. Electrophoretic mobility shift assay and crystallographic examination (66) have shown that 4OH-TAM-bound ER could not bind a GRIP1 coactivator LXXLL peptide due to helix-12 interference at the binding cleft, which was recruited by E2. Consequently coactivator recruitment may influence receptor complex interactions with response element variants (34) which has been shown with other structurally diverse ligands and nuclear receptors (239,240).

In addition, differences in absorption, distribution, metabolism and excretion (ADME) between ligands and species, likely contribute to divergent physiological and gene expression characteristics. It is well documented that TAM metabolism differs significantly between humans and rodents, for example, TAM *N*-oxide, 4OH-TAM and DMT are the predominant metabolites in the mouse, while DMT is the major human metabolite in microsomal studies (52,56,57). In rodents, the levels and rates of TAM metabolism to 4OH-TAM and

DMT were significantly different in the rat and mouse, where the rat metabolite profile more closely resembles human profiles (52).

A cytochrome P450 2D6 polymorphism in humans further illustrates the potential effects of differences in metabolism on TAM activity. 4-OH-*N*-desmethyltamoxifen (endoxifen) is a recently identified TAM metabolite, found at higher levels than 4OH-TAM in patient serum, generated by CYP2D6 activity. It exhibits similar ER binding affinity, and comparable breast cancer cell proliferation and estrogen-induced pS2 mRNA expression inhibition activities compared to 4OH-TAM (53). However, patients expressing specific CYP2D6 polymorphisms (i.e., CYP2D6*3, *4, *5 and *10) that impaired or abolished CYP2D6 metabolism have a nearly 2-fold higher risk of breast cancer recurrence (241). Collectively, these studies illustrate the significant differences in TAM metabolism between models that compromise the extrapolation of rodent data for use in human risk assessment.

Conclusions

Despite the comprehensive time course and dose response studies, an assessment of the gene expression effects and their roles in uterine responses could not be achieved due to limited genome coverage on our custom cDNA arrays and incomplete functional annotation for the represented genes. However, comparative TAM and EE studies using comparable designs and models identified conserved functionally annotated gene expression changes that are consistent with the measured uterotrophic response. Qualitatively, TAM

and EE gene expression profiles are similar; however, there are quantitative differences in efficacy, consistent with the partial agonist activity of TAM. Despite the evidence for these qualitative and quantitative differences in gene expression, demonstration that these changes have causal roles in the partial uterotrophic response elicited by TAM is required. The relevance of the differences between estrogen and TAM and the association with endometrial cancer (46,242,243) also needs further investigation.

CHAPTER 4

MIXTURE EFFECTS OF TAMOXIFEN AND ETHYNYLESTRADIOL ON GENE EXPRESSION IN IMMATURE, OVARIECTOMIZED MICE UTERUS.

ABSTRACT

Tamoxifen (TAM), the primary treatment for estrogen receptor (ER) positive breast cancer, has been associated with an increased incidence of endometrial cancer in post-, but not pre-menopausal women. TAM elicits a partial ER-mediated uterotrophic response in immature rodents when compared to ethynylestradiol (EE), a potent ER agonist. However, cotreatment with 1000 μg/kg TAM antagonizes the uterotrophic effect induced by 30 μg/kg EE. To further investigate the antiestrogenicity of TAM in the uterus, immature, ovariectomized C57BL/6 mice were treated with a single oral dose of EE, TAM, EE+TAM or vehicle. Uteri were subsequently examined at 2, 4, 8, 12, 18, 24 hrs or after three daily treatments (3x24 hrs). Significant increases in uterine wet weight (UWW) were observed at 18 hrs for EE, TAM, and EE+TAM. However, EE+TAM induction of UWW was significantly lower when compared to EE-induced uterotrophy at 3x24 hrs. This inhibitory effect is also reflected in decreases in luminal circumference, yet EE-induced luminal epithelial cell height was unaffected by cotreatment with TAM. Analysis using a 2x2 factorial cDNA microarray study design identified 290 genes differentially expressed following EE treatment. However, only a subset of EE-elicited changes in gene expression was affected by TAM cotreatment, consistent with the antiestrogenic response.

These data suggest that the mechanism of TAM antagonism of EE-induced UWW involves the selective inhibition EE-induced genes.

INTRODUCTION

Tamoxifen (TAM) is an adjuvant and prophylactic therapy prescribed for estrogen receptor alpha (ERα) positive breast cancers. Due to the opposing effects of TAM in different tissues, it has been classified as a selective estrogen receptor modulator (SERM). In adjuvent therapy, it suppresses breast cancer recurrance by 50% and reduces the occurrence of contralateral primary breast cancer by 50%; when used as a prophylactic, TAM also reduces cancer occurrence in high risk populations (46). Despite its high therapeutic index, TAM also elicits undesirable effects in postmenopausal women including a two-fold risk increase in endometrial cancer (58). TAM and its active metabolites, 4-hydroxytamoxifen (4OH-TAM), *N*-desmethyltamoxifen (DMT), and 4-hydroxy-*N*-desmethyltamoxifen (endoxifene), elicit these effects by directly binding to the ligand binding domain (LBD) of ERα. Interestingly, TAM elicits a gene expression profile similar to estrogen in both MCF-7 cells and uterine tissue, albiet with lower efficacy (229,231,244).

ER conformational changes in response to ligand binding affect its subsequent activities. Structrural resolution of the ligand binding domain occupied with 17β-estradiol (E2) have elucidated a ligand-trapping conformation involving helix-12; whereas selective antagonists, such as raloxifene, position helix-12 in an orientation where the C-terminal domain of the ER interferes with ER transactivation (64,245). Protease sensitivity assays have also demonstrated that different ER surfaces are accessible to degradation depending on the bound ligand (246), while phage display assays that probe for different epitopes indicate

that ligands induce different ER topologies (235). In addition, FRET analysis demonstrated that different short-peptide fragments prefered to bind to different ligand-bound ER complexes (247).

Ligand induced conformations have been implicated in the spectrum of coactivator proteins which may interact with the active receptor complex. Electrophoretic mobility shift assays have demonstrated the recruitment of GRIP1 co-activator to 17β-estradiol (E2)-bound ER, but not by 4OH-TAM-bound receptor (66). Colorimetric phage ELISA assays have demonstrated that ER conformation may be influenced by both the ligand and the sequence of the gene-specific estrogen response element (ERE) (29). Moreover, coactivator recruitment may influence which activated receptors bind to specific promoter sequences. For example, DNA footprinting has shown that high mobility group B (HMGB) coactivator proteins enhance ER binding to EREs (34). It is evident that ligand-induced topology influences the gene-specific transcriptional activation of a number of steroid hormone receptors including the ER (reviewed in (33)). However, elucidating the influence of ligand structure on receptor conformation and transcriptional activitiy warrants further investigation.

Although TAM and estrogen individually induce agonistic effects on the uterus in the immature, ovariectomized rodent, cotreatment at appropraite ratios elicit an antagonistic effect. For example, TAM significantly repressed uterine weight after 28 days in intact adult mice, but did not elicit reductions after daily treatments six months (248). TAM also antagonizes the E2 induction of uterotrophy (51), as well as other endpoints such as progesterone receptor (249)

and *Fos* expression (211), reporter gene assays (250) and peroxidase enzyme activity (51).

Collectively, these studies demonstrate that TAM elicits a unique ER complex conformation affecting its tissue-specific agonist and antagonist activities. This report extends our previous studies examining the ER-mediated changes in gene expression elicited by EE and TAM alone that are associated with the induction of uterine wet weight (144,159,244), by examining their effects following cotreatment.

A temporal two-by-two factorial microarray hybridization design, with complementary histopathology, was used to comprehensively examine differential gene expression associated with the antagonism of EE-induced uterine wet weight by TAM cotreatment (Figure 1A) (251). Interestingly, only a select subset of EE-induced genes was affected by TAM cotreatment. Antagonized responses were associated with specific genes within cell growth and proliferation pathways that could be correlated with the anti-uterotrophic effect. Results from this study further elucidate the mechanisms involved in the antagonist activities of TAM.

Figure 1

Microarray hybridization design and uterotrophic assay treatment design

A) Differential gene expression between all treatment combinations was examined using the two by two factorial hybridization design (251) to minimize the number of arrays required per biological replicate. Each arrow represents an array and the Cy3 (head) and Cy5 (tail) dyes incorporated.

B) Preliminary dose finding experiments examined uterine wet weight (UWW) 24 hrs after three orally administered daily doses. Mice (n = 5) were treated with vehicle, 30 μg/kg EE, 1000 μg/kg TAM or 30 μg/kg plus 1000 μg/kg TAM. Animals were sacrificed at 2, 4, 8, 12, 18 and 24 hrs after a single oral gavage or at 72 hrs after three daily doses. TAM was initially dosed 8 hrs before EE to compensate for the delayed TAM-elicited responses associated with metabolism and distribution (244) to facilitate equal competition for ER availability.

Figure 1

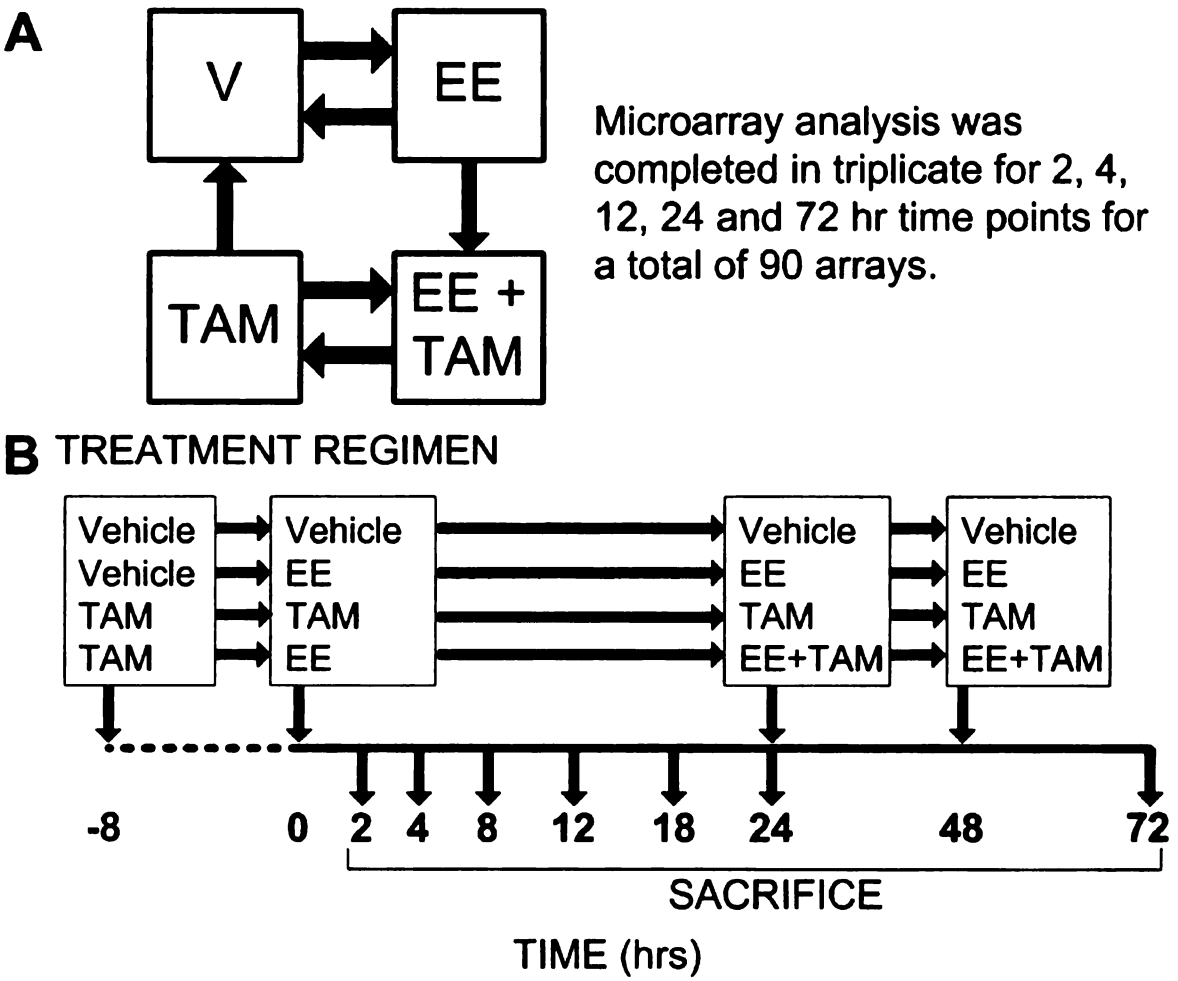
A
V
EE
TAM
EE +
TAM
Microarray analysis was completed in triplicate for 2, 4, 12, 24 and 72 hr time points for a total of 90 arrays.
B TREATMENT REGIMEN
Vehicle
Vehicle
TAM
TAM
Vehicle
EE
TAM
EE
Vehicle
EE
TAM
EE+TAM
Vehicle
EE
TAM
EE+TAM
-8
0
2
4
8
12
18
24
48
72
SACRIFICE
TIME (hrs)

MATERIALS AND METHODS

Animal husbandry and treatment

Female C57BL/6 mice, ovariectomized by the vendor on postnatal day (PND) 20, were obtained from Charles River Laboratories (Raleigh, NC) on PND 25. Animals (n = 5) were housed in polycarbonate cages bedded with cellulose fiber chips (Aspen Chip Laboratory Bedding, Northeastern Products, Warrensberg, NY) in a 23°C environment with 30-40% humidity and a 12 h light/dark cycle (0700 – 1900 h). Animals had access to deionized water and Harlan Teklad 22/5 Rodent Diet 8640 (Madison, WI) *ad libitum* and acclimatized for 4 days prior to treatment. To account for the delayed gene expression responses (244), animals (n = 5 per group) were primed at -8 hrs with 1000 μg/kg TAM (TAM and mixture (MIX) groups) or sesame oil (vehicle and EE groups) (Figure 1B). At 0 hrs, animals were dosed with 30 μg/kg EE (EE and MIX groups) or sesame oil (TAM and vehicle groups). Four groups (n = 5) of mice were also treated with sesame oil, 30 μg/kg EE (Sigma), 1000 μg/kg TAM (Sigma) or 30 μg/kg EE and 1000 μg/kg TAM at 24 and 48 hrs to represent the 3 x 24 hr treatment group. Doses were prepared based on average animal weight. Animals were sacrificed by cervical dislocation and body weights were recorded. The uterus was transected at the border of the cervix, and stripped of extraneous connective tissue and fat. Whole uterine weights were recorded before (wet weight) and after blotting (blotted weight) with absorbent tissue. A 6-8 mm section of unblotted uterine horn was placed in 10% neutral buffered formalin (NBF) for histology. The remainder was snap frozen in liquid nitrogen and stored

at -80°C for RNA extraction. Liver sections from the left lobe were snap frozen for LC/MS/MS analysis. All procedures were performed with the approval of the Michigan State University All-University Committee on Animal Use and Care.

Histological processing, morphometric and pathological analysis

Samples stored in 10% NBF were allowed to fix for at least 24 hrs at room temperature then placed into tissue cassettes and stored in 30% ethanol holding solution at 4°C. Paraffin embedding, sectioning (5 μm), mounting and hematoxylin and eosin staining were completed by the Michigan State University Laboratory for Anatomical Histology and Molecular Sciences (192) using standard techniques. Pathological assessments were evaluated according to standardized National Toxicology Program (NTP) pathology codes.

Morphometric analysis was performed on midhorn uterine cross sections for all animals (n = 5 per treatment group) using Scion Image analysis software (Scioncorp, Frederick, MD). Histological markers of uterotrophy, including luminal epithelial cell height (LECH), luminal circumference and number of endometrial glands were quantified for each slide. Statistical analysis of morphometry data was assessed by Dunnett's or two-way ANOVA followed with Tukey's HSD *post hoc* analysis to examine dose dependent and temporal effects, respectively (SAS version 9.1).

RNA isolation

Briefly, 1.0 mL of Trizol (Invitrogen, Carlsbad, CA) was added to the frozen uterine tissue in a 2.0 mL microfuge tube and homogenized in the presence of steel beads by a Mixer Mill 300 homogenizer (Retsch, Germany). Total RNA was isolated and extracted according to the manufacturer's protocol and resuspended in The RNA Storage Solution (Ambion, Austin, TX). RNA samples were quantified spectrophotometrically (A_{260}) and assessed for quality by A_{260}/A_{280} ratio as well as inspected using denaturing agarose gel electrophoresis.

Microarray hybridization and analysis

Custom in-house cDNA arrays consisting of 13,361 features, representing 7,952 unique genes (Unigene Build 152), were spotted on epoxy coated glass slides (SCHOTT Nexterion, Germany) using an Omnigrid arrayer (GeneMachines, San Carlos, CA) and Telechem Chipmaker 3 pins in a TeleChem CHP3 printhead head (Telechem International Inc., Sunnyvale, CA) at the DNA Sequencing and Gene Expression Analysis facility at Michigan State University (128)). Selected clones were obtained from EPAMAC (129), Research Genetics, the National Institute of Aging and Lion Biosciences. Detailed protocols for processing of microarrays are available at the dbZach Home Page (130).

A two by two factorial hybridization design was used to assess treatment effects (251) such that all treatment groups could be compared to each other

(Figure 1A). Four time-matched samples, of each treatment group, were hybridized to six slides to generate a single replicate of data. Three biological replicates were completed for 2, 4, 12, 24 and 3 x 24 hr time points for a total of 90 arrays. The Genisphere 900 3DNA Array Detection (Genisphere Inc., Hatfield, PA) indirect incorporation kit was used to generate cDNA samples for hybridization. Briefly, 1 μg of RNA was reverse transcribed in the presence of an oligo-tagged primer specifically targeted for Cy3- or Cy5- conjugated dendrimers. The cDNA was resuspended in 58 μL of 2X Formamide-Based Hybridization Buffer and hybridized overnight on arrays sealed in a light-shielded, humid chamber submerged in a 42°C water bath. Slides were then washed in SSC containing decreasing concentrations of SDS, spin-dried and re-hybridized with a Cy3:Cy5 (1:1) dendrimer mixture in formamide based buffer to indirectly incorporate dyes at the Cy3- and Cy5-dendrimer tagged cDNA hybridized on the first day. Slides were washed and dried as previously described, and scanned at 635 nm (Cy3) and 532 nm (Cy5) using a Molecular Devices Genepix 4100A scanner (Sunnyvale, CA). Images were examined, features identified and intensity values recorded using GenePix v.5.1 (Molecular Devices).

Microarray quality control, statistical analysis and gene list filtering

All arrays were compared to a historical data set of high quality arrays. Parameters assessed included background signal intensity, feature signal intensity, feature vs. background signal intensity ratios, the number of features

with background intensities greater than the feature intensity for each array, and relationships between feature and background signal intensities (134).

Data were normalized using a semi-parametric approach (194). Model-based *t*-values were calculated comparing all time-matched treated and vehicle samples. Posterior probabilities of activity [P1(*t*)-value] were then calculated on a per-gene and per-time point basis using an Empirical Bayes analysis (135). Gene lists were filtered to identify genes which demonstrate differential expression between EE and mixture treatment. At each time point, both EE vs. V (EV) and MIX vs. V (MV) lists were identified based on posterior probability (P1(*t*) > 0.9999) and fold-change cut-off (|fold change| > 1.5) and then compared to identify differential expression between EV and EE vs MIX (EM) where P1(*t*) > 0.9999). All raw and analyzed data were stored in dbZach (http://dbzach.fst.msu.edu), a Minimum Information About Microarray Experiments (MIAME)-supportive relational database (133).

QRT-PCR

Aliquots of RNA isolated from each of the five biological replicates were set aside for SYBR™ Green quantitative real-time PCR (QRT-PCR) verification. EE-treated, temporal mouse uteri RNA were previously isolated (159). An oligo-dT anchored Superscript II (Invitrogen) reverse transcriptase reaction was carried out on 1 μg of RNA, in a 20 μL reaction, from each biological sample as per manufacturer's instructions. Samples were diluted four-fold and 3 μL used in a 30 μL real-time reaction mix containing 1X SYBR Green PCR buffer, 3 mM

$MgCl_2$, 0.33 mM dNTPs, 0.5 IU AmpliTaq Gold (Applied Biosystems, Foster City, CA) and 0.15 mM forward and reverse primer. All primers were designed by submitting cDNA microarray clone sequences into Primer3 (138) to obtain an amplicon of approximately 125bp (Table 1). PCR amplification was conducted in 96-well MicroAmp Optical plates (Applied Biosystems) on an Applied Biosystems PRISM 7000 Sequence Detection System under the following conditions: 10 min denaturation and enzyme activation at 95°C, followed by 40 cycles of 95°C for 15 s and 60°C for 1 min. After amplification, a 30 min dissociation protocol was conducted to assess primer specificity and product uniformity. Each plate contained duplicate standards of purified PCR product of known template concentration over eight orders of magnitude to generate a log template concentration standard curve. No template controls (NTC) samples were included on each plate such that experimental samples within 2 standard deviations of the NTCs are considered below the limits of detection. Plots were visualized and thresholds determined using ABI Prism 7000 SDS Software (Applied Biosystems). Results were normalized to Rpl7 mRNA levels to control for differences in RNA loading, quality and cDNA synthesis. Expression differences were assessed using a two-way ANOVA followed by Tukey's HSD *post hoc* analysis to examine treatment and treatment over time effects (SAS version 9.1). Correlation analyses of QRT-PCR and microarray data were generated using the correlation function of R v2.1.0.

LC/MS/MS

Liver tissue was homogenized with ddH_2O in a 1:20 dilution using a handheld Polytron homogenizer (Kinematica, Switzerland). One mL ddH_2O, 200 μL 1N NaOH and 1 ng [^{15}N, $^{13}C_2$] tamoxifen (Sigma), as an internal standard, was added to 1 mL of homogenate. The mixture was extracted in an ether:methanol (95:5 v/v) solution and evaporated at 55°C under a stream of N_2. Residue was resuspended in 200 μL acetonitrile:ammonium acetate (65:35 v/v) and stored at -20°C in amber sample vials until use. Appropriate standards were also prepared for quantitative interpolation of TAM and 4OH-TAM concentrations.

Extracted samples were analyzed at the MSU Mass Spectrometry Facility (128). Samples were injected into the LC-20AD (Shimadzu; Columbia, MD) HPLC system with the SIL-5000 Injector (Shimadzu) and separated on an Atlantis dC18 3mm column (Waters Corporation; Milford, MA) using a 60:40 (v/v) methanol:100mm ammonium acetate (pH = 3) solution. Electrospray ionization mass spectrometry was carried out on a Quattro micro API instrument (Waters Corporation) and data analyzed using Mass Lynx v4.0 software (Waters Corporation).

Bioinformatic Promoter Word Search

Regulatory sequences of genes were obtained from the UCSC Genome Browser for mature RefSeq mRNA accessions and stored in the dbZach database (130). The sequences obtained extended from -5000 kb, upstream from the transcriptional start site, through the 5' untranslated region. A sliding window method (252) was implemented to create a library of 5 to 10 nucleotide

words from these sequences. To identify over-represented 5 to 10 nucleotide motifs from the active gene lists determined through microarray analysis, an empirical Bayes implementation of the Wilcoxon's Rank Sum Test was executed to calculate posterior probabilities (135,253). Queries of the Transfac database (254) were conducted to identify potential binding proteins associated with some over-represented short sequences.

RESULTS

Dose finding studies

Preliminary studies were conducted to identify optimal EE and TAM doses to investigate possible additive, synergistic and antagonistic uterotrophic tissue and gene expression responses. We have established that the oral ED_{50} for the uterotrophic response elicited by EE and TAM are 22.1 and 33.7 μg/kg, respectively, and that 100 μg/kg EE induced a maximal uterine wet weight (UWW) response (~10-fold) in the immature, ovariectomized C57BL/6 (159,244). TAM also exhibited a pronounced temporal delay in gene expression when compared to EE (244). In order to accommodate this delay, and to ensure equal competitive binding by TAM and EE for the ER, a modified treatment regimen was used that dosed the animals with TAM 8 hrs prior to EE (Figure 1B).

Preliminary dose range finding studies were conducted at 72 hrs to identify the optimal EE:TAM ratio that would maximize the antagonism of EE-induced uterotrophy by TAM. Cotreatment with 0.1 and 1.0 mg/kg TAM significantly repressed UWW induction by treatments of 0.03 and 0.06 mg/kg EE (Figure 2). Consequently, 0.03 mg/kg EE and 1.0 mg/kg TAM (1:33 ratio) were selected to further investigate the additive, synergistic and antagonistic uterine responses following cotreatment (MIX).

Figure 2

Dose finding: uterotrophic inhibition

EE (0, 10, 30 and 60 μg/kg) was co-treated with TAM (0.1, 1, 100 mg/kg) to determine the optimal doses resulting in inhibition of EE-induced uterotrophy. 30 μg/kg EE and 1 mg/kg TAM (1:33 ratio) were selected for further examination. The asterisk (*) indicates significant ($p < 0.05$) inhibition relative to EE alone.

Figure 2

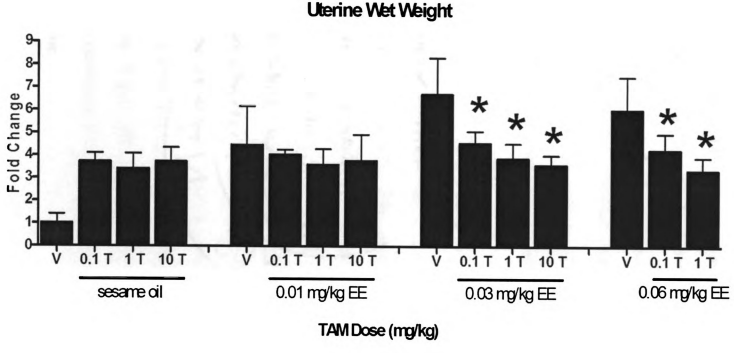
Uterine Wet Weight
Fold Change
0
1
2
3
4
5
6
7
8
9
V
0.1 T
1 T
10 T
sesame oil
0.01 mg/kg EE
0.03 mg/kg EE
0.06 mg/kg EE
TAM Dose (mg/kg)

Treatment Effects on Uterine Weight

Significant ($p < 0.05$) increases in UWW were observed at 18, 24 and 72 hrs after treatment with 0.03 mg/kg EE, and at 8, 18, 24 and 72 hrs with 1.0 mg/kg TAM (Figure 3). However TAM only elicited a 4.0-fold increase compared to the 8.1-fold increase induced by EE at 72 hrs. Although, cotreatment of 0.03 mg/kg EE with 1.0 mg/kg TAM still increased UWW from 12 - 72 hrs compared to vehicle, cotreatment-induced UWW was inhibited approximately 50% at 72 hrs compared to EE treatment alone.

Morphometric analysis and histopathology

Increases in luminal epithelial cell height (LECH) and luminal circumference are hallmarks of estrogenicity in the uterus (88). LECH was significantly induced 3.7-, 3.5- and 3.3-fold by EE, TAM and MIX treatment, respectively, compared to time-matched vehicle controls at 72 hrs (Figure 4A). There was no significant difference in LECH between EE and TAM at 72 hrs, and TAM cotreatment did not antagonize EE induced LECH. Luminal circumference was induced 3.1- and 2.9-fold at 24 hrs, and 8.0- and 4.9-fold at 72 hrs for EE and TAM, respectively (Figure 4B). Mixture treatment repressed luminal circumference by 54% compared to EE alone at 72 hrs, but was not significantly different from TAM alone.

Figure 3

Treatment induced uterotrophy

Uterine wet weight (UWW) was measured at 2, 4, 8, 12, 18, 24 and 72 hrs after treatment (n = 5). "a" indicates a significant increase in UWW compared to the time-matched vehicle control. "b" indicates a significant difference in UWW compared to the time-matched EE-treated sample. TAM inhibited EE-induced UWW only after three daily treatments.

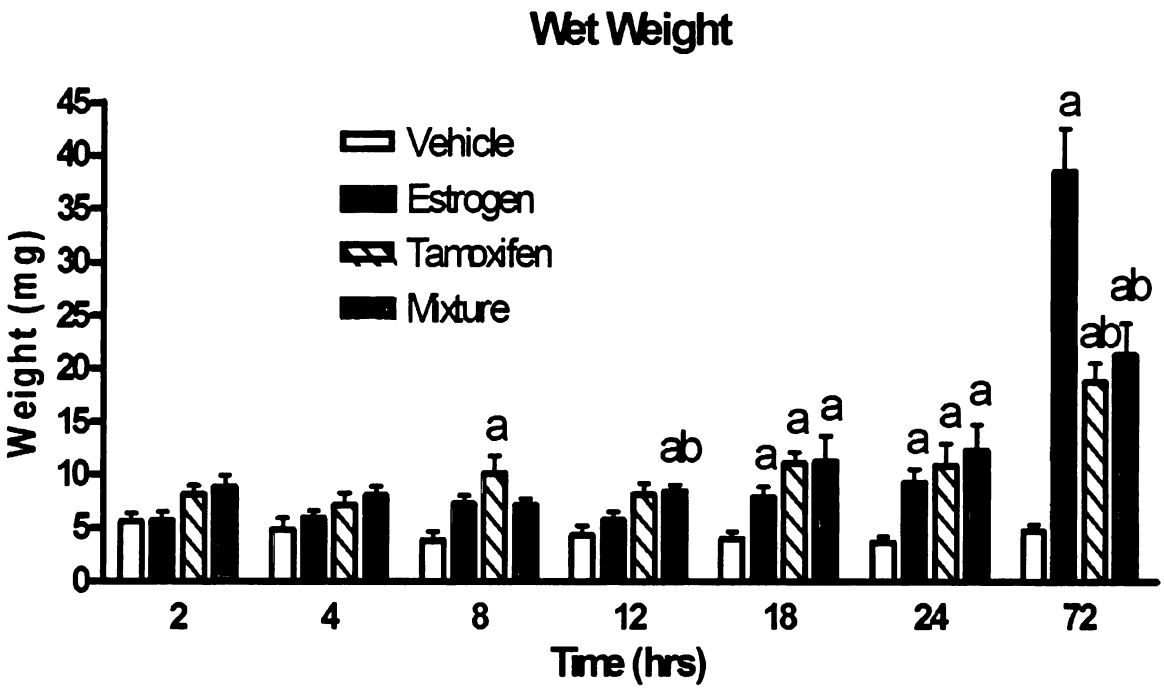

Figure 4

Morphometric changes elicited by EE, TAM and Mixture

Morphometric measurements of luminal epithelial cell height (LECH) and luminal circumference were made on all uteri sections. "a" indicates a significant increase in LECH or luminal circumference compared to the time-matched vehicle control. "b" indicates a significant difference in luminal circumference compared to the time-matched EE-treated sample. TAM inhibited EE-induced luminal circumference only after three daily treatments. There were no significant differences in LECH between treatments at any time point examined.

Figure 4

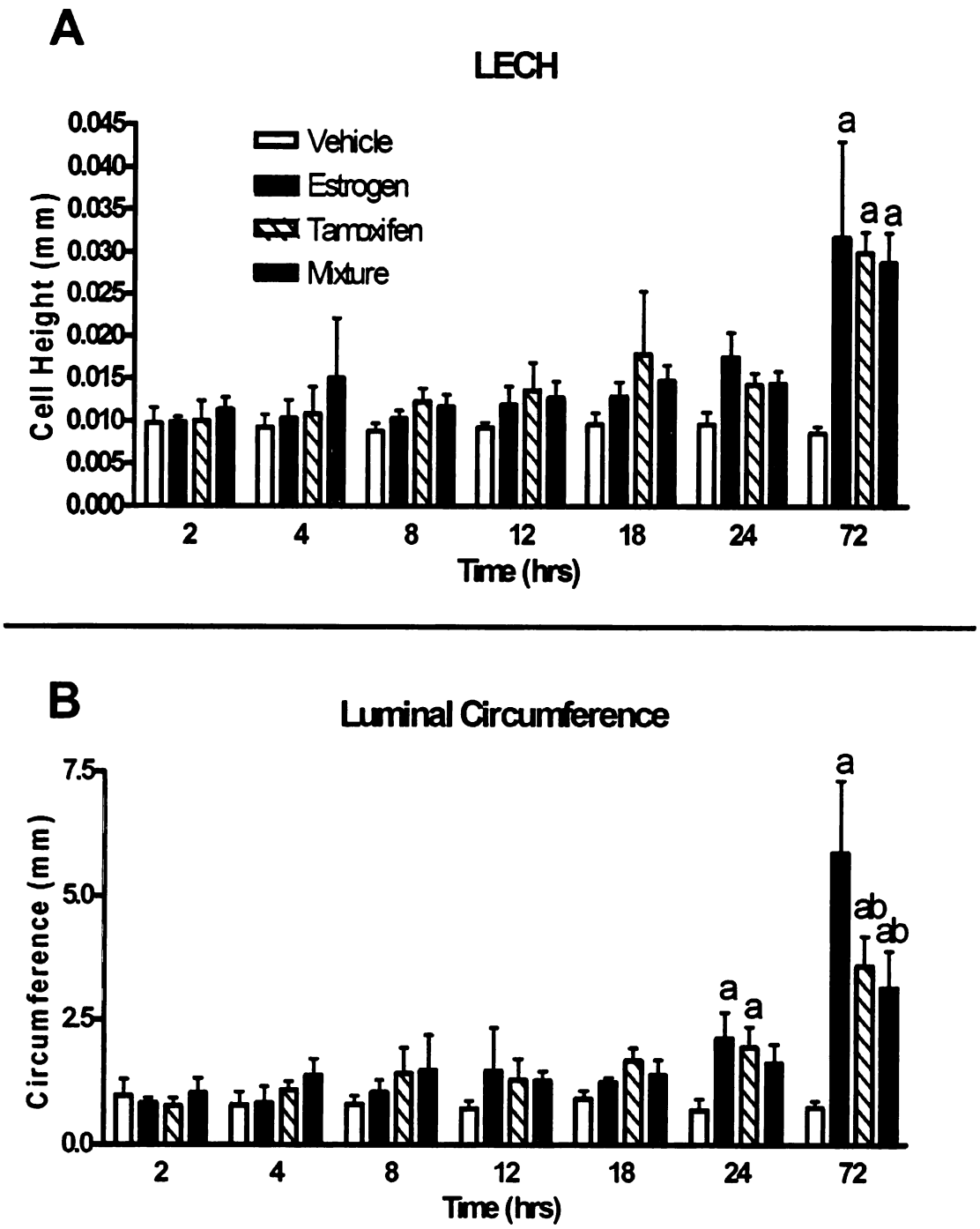
A
LECH
Vehicle
Estrogen
Tamoxifen
Mixture
Cell Height (mm)
0.045
0.040
0.035
0.030
0.025
0.020
0.015
0.010
0.005
0.000
a
a a
2
4
8
12
18
24
72
Time (hrs)
B
Luminal Circumference
Circumference (mm)
7.5
5.0
2.5
0.0
a
ab ab
a a
2
4
8
12
18
24
72
Time (hrs)

Temporal Histological Changes

Temporal- and dose-dependent histological changes in the uterus induced by EE and TAM in the immature, ovariectomized C57BL/6 mouse has been previously reported (159,244) The same assessment was used to characterize the histological changes elicited by vehicle, EE, TAM and EE+TAM treatment using the modified treatment regimen. (Table 1). Mild to moderate stromal edema was observed at 2 hrs in the TAM and MIX groups, likely due to early priming. All treatment groups exhibited mild to moderate hypertrophy in stromal nuclei by 4 hrs, with mild to moderate epithelial hyperplasia in the MIX treatment at 8 hrs. At 12 hrs, EE induced mild to moderate uterine stromal edema, mild stromal cell hypertrophy, and moderate endometrial hyperplasia, while TAM elicited qualitatively similar changes to the uterine architecture. MIX treatment induced comparable uterine morphology relative to EE and TAM treatments alone. After 24 hrs, EE and TAM alone elicited marked increases in uterine edema, stromal cell hypertrophy, and endometrial hyperplasia, and were not histologically distinguishable. Comparable changes were also present 24 hrs after MIX treatment. The severity of the uterotrophic response continued to 72 hrs after EE and TAM treatments alone. In contrast, MIX elicited changes in the uterus were attenuated compared to EE and TAM treatments alone, as evident in the areas of stromal hypertrophy and endometrial hyperplasia (Figure 5). Overall, EE, TAM and MIX treated uteri exhibit similar histological changes. Only at 72 hrs is there evidence of a diminished response elicited by MIX when compared to EE and TAM treatments alone.

Table 1. Histological evaluations of treated uterine sections (n = 5)

Time (hrs)	Treatment group	Stromal edema	Stromal nuclei hypertrophy	Epithelial hyperplasia	Myometrial hypertrophy
2	V	-	-	-	-
	E	-	-	-	-
	T	mild	-	-	-
	M	mild – moderate	none - mild	-	-
4	V	-	-	-	-
	E	mild	none - mild	-	-
	T	moderate	mild	-	-
	M	mild - moderate	moderate	-	-
8	V	-	-	-	-
	E	mild – moderate	mild	-	-
	T	marked	mild	mild - moderate	-
	M	marked – severe	mild	mild - moderate	-
12	V	-	-	-	-
	E	mild – moderate	moderate	mild – moderate	-
	T	moderate	mild	moderate	-
	M	moderate	moderate	moderate	-
18	V	-	-	-	-
	E	mild – moderate	mild – moderate	mild – moderate	-
	T	moderate – marked	mild	moderate	-
	M	moderate	mild	moderate	-
24	V	-	-	-	-
	E	moderate	moderate	marked	mild
	T	moderate	moderate	marked	mild
	M	mild – moderate	mild – moderate	moderate – marked	mild
72	V	-	-	-	-
	E	moderate – marked	marked	severe	mild
	T	moderate	marked	severe	mild
	M	moderate	moderate	marked – severe	mild

Figure 5

Histological observations

Hematoxylin and eosin staining of uteri treated three times daily with (A) vehicle, (B) 30 μg/kg ethynylestradiol, (C) 1000 μg/kg tamoxifen and (D) 30 μg/kg ethynylestradiol plus 1000 μg/kg tamoxifen (MIX). All treatments elicited a uterotrophic effect, however MIX attenuated proliferative effect compared to EE- and TAM-induced responses. Images are representative of five biological replicates; bar represents 30 μm.

Figure 5

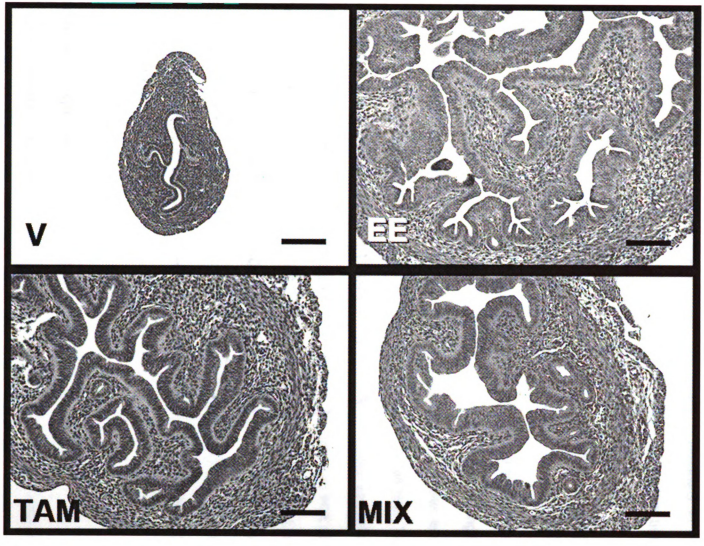

LC/MS/MS analysis of liver TAM and 4OH-TAM levels

TAM and 4OH-TAM levels were determined using LC/MS/MS in liver samples from the same animals due to the limited amount of uterine tissue available. Extracts from a previous study (244) demonstrated that TAM can be detected in hepatic tissues 2 hrs after treatment, with 4OH-TAM reaching a plateau by 4 hrs and decreasing after 12 hrs (Figure 6A). In the current cotreatment study with TAM-priming, comparable levels of TAM and 4OH-TAM were detected in hepatic liver extracts (Figure 6B). Approximately 70 ng/mL TAM were detected at 2 hrs in TAM and MIX treated liver extracts. Peak levels of130 ng/mL were detected at 8 hrs that decreased to 50 ng/mL by 24 hrs. TAM levels were not significantly different between TAM and MIX hepatic extracts at any time point. However, 4OH-TAM levels were significantly higher in MIX (208 ng/mL) compared to TAM (92 ng/mL) at 2 hrs which converged to 100 ng/mL at 4 hrs. 4OH-TAM levels were not significantly different between TAM and MIX groups at any other time point. It was not possible to determine EE levels due to the low doses administered and the inefficiency of EE ionization and detection using LC/MS/MS.

Uterine gene expression changes demonstrating mixture effects

Differentially expressed genes were identified based on their empirical Bayes posterior probability of activity [P1(*t*)-value] on a per-gene, per-time point basis (Supplemental Table 1). P1(*t*)-values approaching 1.0 indicate a greater likelihood of treatment-related differential gene expression. EE-induced gene

Figure 6

Temporal LC/MS/MS analysis of hepatic TAM and 4OH-TAM levels

Hepatic TAM and 4OH-TAM were extracted from a previous study (244) to determine tissue levels using LC/MS/MS. A) TAM was detected (*$p < 0.05$ compared to time-matched vehicle) at 2 hrs after treatment. B) 4OH-TAM levels peaked at 4 hrs (*$p < 0.05$ compared to time-matched vehicle) and plateaued at 12 hrs before steadily decreasing over time. TAM and 4OH-TAM were also extracted from liver samples from the current study to determine hepatic tissue levels using LC/MS/MS. TAM and 4OH-TAM were not significantly different between vehicle and EE treatments. C) TAM levels in TAM and MIX treated samples are significantly different from time-matched vehicle and EE controls ($^{a}p < 0.05$), but not significantly different between TAM and MIX treatments at any time point. D) 4OH-TAM levels are significantly different from time-matched vehicle controls and EE treated animals ($^{a}p < 0.05$). At 2 hrs, TAM and MIX demonstrate significantly different 4OH-TAM levels ($^{b}p < 0.05$) but not beyond 4 hrs after treatment.

Figure 6

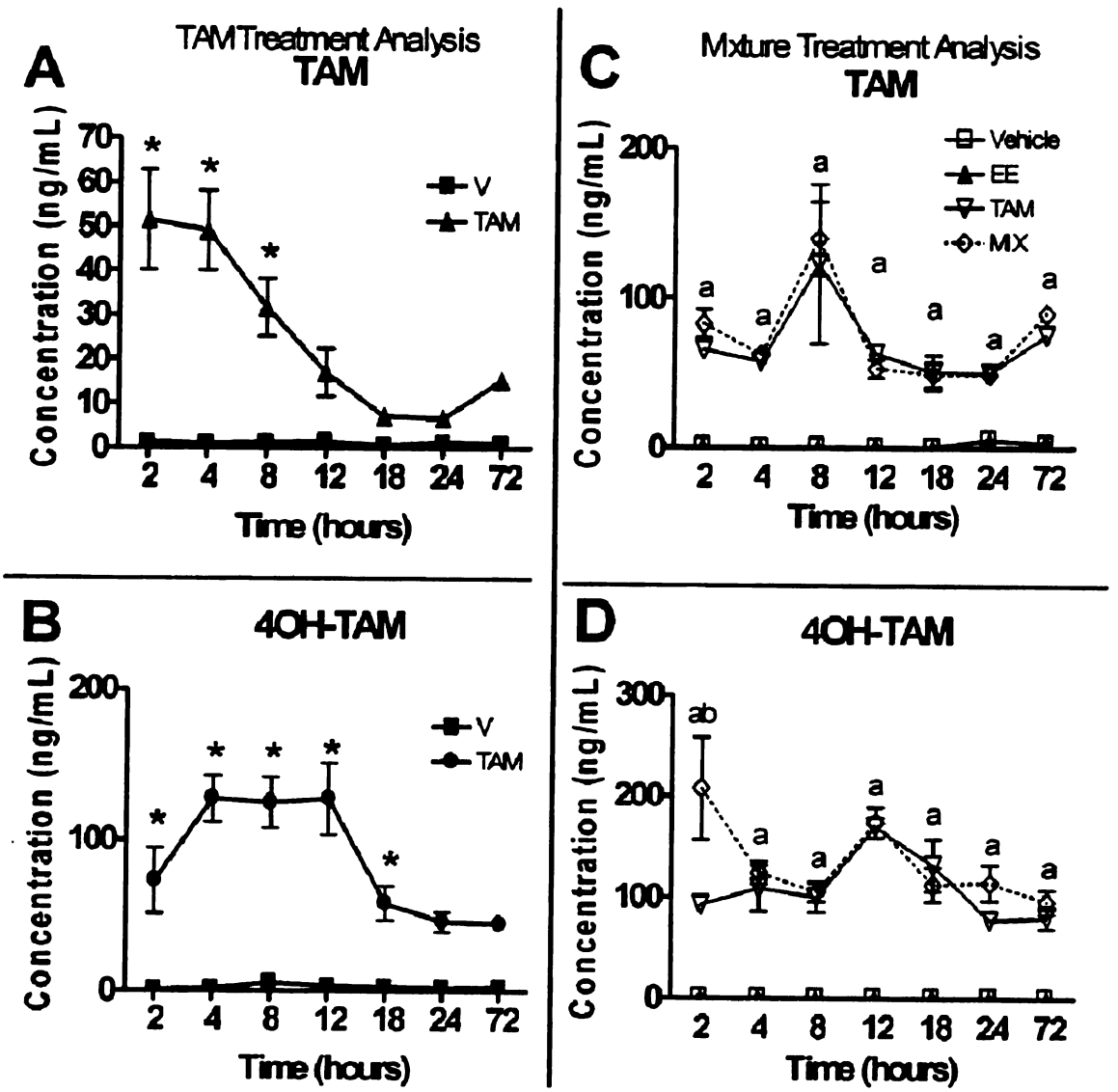
A
TAM Treatment Analysis
TAM
Concentration (ng/mL)
70
60
50
40
30
20
10
0
V
TAM
2 4 8 12 18 24 72
Time (hours)
C
Mixture Treatment Analysis
TAM
Concentration (ng/mL)
200
100
0
Vehicle
EE
TAM
MX
a
2 4 8 12 18 24 72
Time (hours)
B
4OH-TAM
Concentration (ng/mL)
200
100
0
V
TAM
2 4 8 12 18 24 72
Time (hours)
D
4OH-TAM
Concentration (ng/mL)
300
200
100
0
ab
a
2 4 8 12 18 24 72
Time (hours)

expression affected by TAM co-treatment was identified using a two-step process. All genes were first filtered to identify 2518 EE-elicited gene expression changes (EE vs. V: P1(t) ≥ 0.9999; fold change ≥ 1.5) across all time points. These 2518 genes where then screened for modulation by TAM cotreatment (EE vs. MIX: P1(t) ≥ 0.9999) to identify only 290 unique, annotated genes exhibiting a MIX-treatment effect, representing potential non-additive interactions (Table 2).

Gene expression changes were further examined by comparing EE vs. V and MIX vs. V to classify potential non-additive interactions as: A) EE-induced expression repressed by MIX, B) EE-induced expression augmented by MIX, C) EE-repressed expression diminished by MIX , and D) EE-repressed expression further repressed by MIX (Figure 7, Table 3). The distribution of genes across time appears to shift from categories A, B and C (2 – 12 hrs) to primarily categories B and C (24 and 72 hrs). Note that a potential non-additive interaction may occur at several time points. For example, fos-like antigen 2 (*Fosl2*) is a category A gene at 2 and 4 hrs. A gene may also exhibit different non-additive patterns at different times, such as inhibin beta-B (*Inhbb*) which is a category A gene at 2 hrs but is classified as a category B at 24 and 72 hrs.

Functional categorization of microarray data

The majority of EE-elicited differentially expressed genes affected by TAM cotreatment identified at 2 and 4 hrs are associated with cell growth and proliferation including oncogenes such as myelocytomatosis oncogene (*Myc*), Jun oncogene (*Jun*) and FBJ osteosarcoma oncogene (*Fos*). Genes involved in

Table 2. MIX-modified, EE-induced gene list generation

Time (hours)	EE-induced genes * P1(t) ≥ 0.9999 Fold-Change ≥ 1.5	MIX-modified, * EE-induced genes P1(t) ≥ 0.9999
2	49	25
4	336	87
12	1946	128
24	1534	79
72	591	48
Total Unique Genes **	2518	290

* Number of unique, Entrez Gene-annotated genes at indicated time point
** Number of unique Entrez Gene-annotated genes across all time points

NB: Genes may be active across multiple time points, thus the sum of each column is greater than total unique genes in each category.

Figure 7

EE-mediated gene expression affected by TAM cotreatment

Only 209 out of 2518 EE-elicited gene expression changes (P1(*t*) ≥ 0.9999; fold change ≥ 1.5) were affected by TAM cotreatment. These genes were classified as: A) EE-induced expression repressed by MIX, B) EE-induced expression augmented by MIX, C) EE-repressed expression diminished by MIX, and D) EE-repressed expression that is further repressed by MIX. The numbers within each panel indicates the number of genes exhibiting the pattern. Note that some genes exhibited different TAM cotreatment expression patterns at different time points.

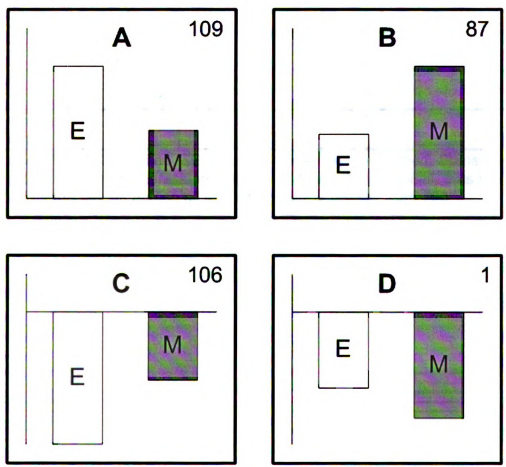

Table 3. MIX-modified, EE-induced gene classifications

Time (hours)	A MIX-repression of EE-induction	B MIX-augmentation of EE-induction	C MIX-diminution of EE-repression	D MIX-augmentation of EE-repression
2	9	15	1	0
4	58	1	28	0
12	48	29	50	1
24	0	45	34	0
72	5	20	23	0
Total Unique Genes*	109	87	106	1

* A total of 290 MIX-modified, EE-mediated genes were identified. Some genes demonstrated different expression patterns at different time points, thus the sum of Total Unique Genes across all four categories is greater than 290.

the cell cycle, cyclin-dependent kinase inhibitor 1A (*Cdkn1a*) and branched chain aminotransferase 1, cytosolic (*Bcat1*), as well as guanine nucleotide binding protein-like 3 (*Gnl3*) and activating transcription factor 4 (*Atf4*) that are associated with proliferation, were also affected by TAM cotreatment. Other affected functional categories included lipid metabolism [peroxisomal trans-2-enoyl-CoA reductase (*Pecr*) and carnitine palmitoyltransferase 2 (*Cpt2*)], immune response [interferon gamma inducible protein 30 (*Ifi30*) and chemokine (C-X-C motif) ligand 12 (*Cxcl12*)], and ion binding and transport [selenoprotein K (*Selk*) and solute carrier family 23 (nucleobase transporters), member 2 (Slc23a2)]. Eleven of these genes, representing different categories of MIX-mediated changes from Table 3, exhibited good correlations between microarray and QRT-PCR data (Figure 8).

Bioinformatic promoter word search analysis

At a single time point, categories A through D adequately describes the relationship between EE and MIX treatment; however, temporal patterns elicited by MIX treatment may also provide insight to its regulation. MIX-modified, EE-mediated genes were categorized according to their MIX vs. V fold-change temporal patterns (Figure 9) and bioinformatic promoter word searches were conducted on each temporal pattern group to identify putative sequence elements over-represented in MIX-mediated, EE-induced genes. Despite seven distinct temporal patterns, only three returned positive TRANSFAC® hits

Figure 8

Quantitative real-time PCR verification

Microarray results for 11 genes were verified using QRT-PCR. These genes represent various affected pathways and different temporal patterns of expression. Overall, there was good agreement between microarray (left) and QRT-PCR (right) data. Examples for four of the genes, A) Fos and Inhbb, B) Ccl21b and Ndufb9, are illustrated demonstrating different patterns of MIX-modified, EE-mediated changes. Statistically significant QRT-PCR differences ($p < 0.05$, $n = 4$) due to treatment are denoted by an asterisk (*).

Figure 8A

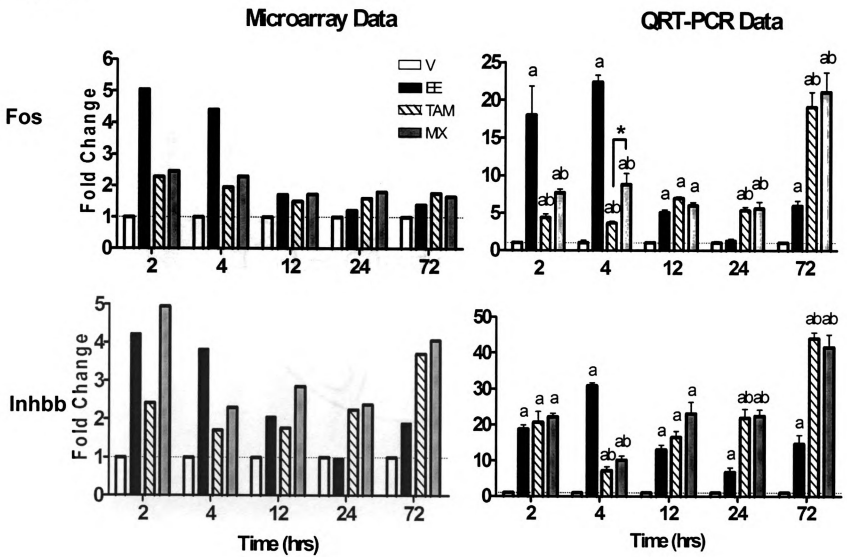
Microarray Data
QRT-PCR Data
Fos
Inhbb
Fold Change
V
EE
TAM
MX
Time (hrs)
2
4
12
24
72

Figure 8B

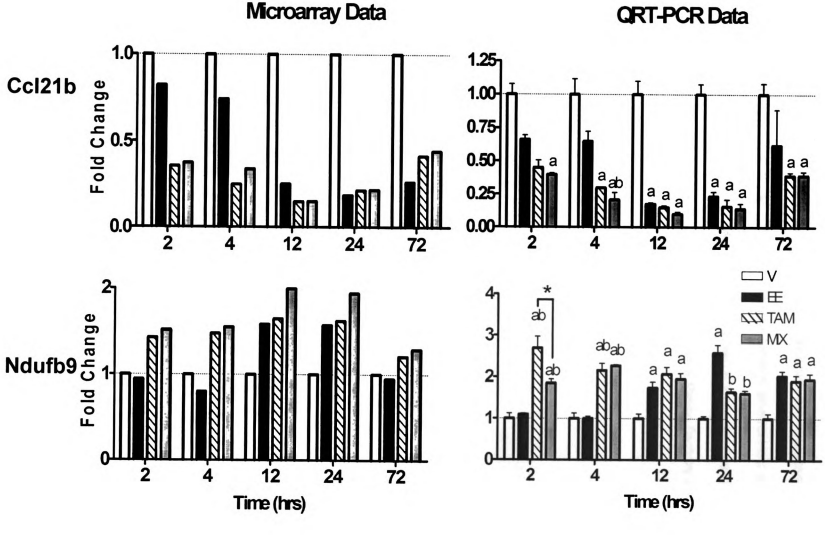
Microarray Data
QRT-PCR Data
Ccl21b
Ndufb9
Fold Change
Time (hrs)
V
EE
TAM
MX

(Supplemental Table 2). These positive hits were associated with known binding factors (posterior probability ≥ 0.95) as reported by experiments reported in the TRANSFAC® database. The most common binding factors associated with the over-represented sequences include C/EBP, Sp1 and hepatocyte nuclear factors (HNFs). Further studies are required to elucidate the role of these factors in MIX-modified, EE-mediated gene transcription.

Figure 9

MIX-modified, EE-mediated gene profiles

Bioinformatic word searches were completed on seven categories of MIX vs. V fold-change, temporal profiles demonstrated by 209 MIX-modified, EE-mediated genes. Three categories returned positive TRANSFAC hits, associated with a binding transcription factor.

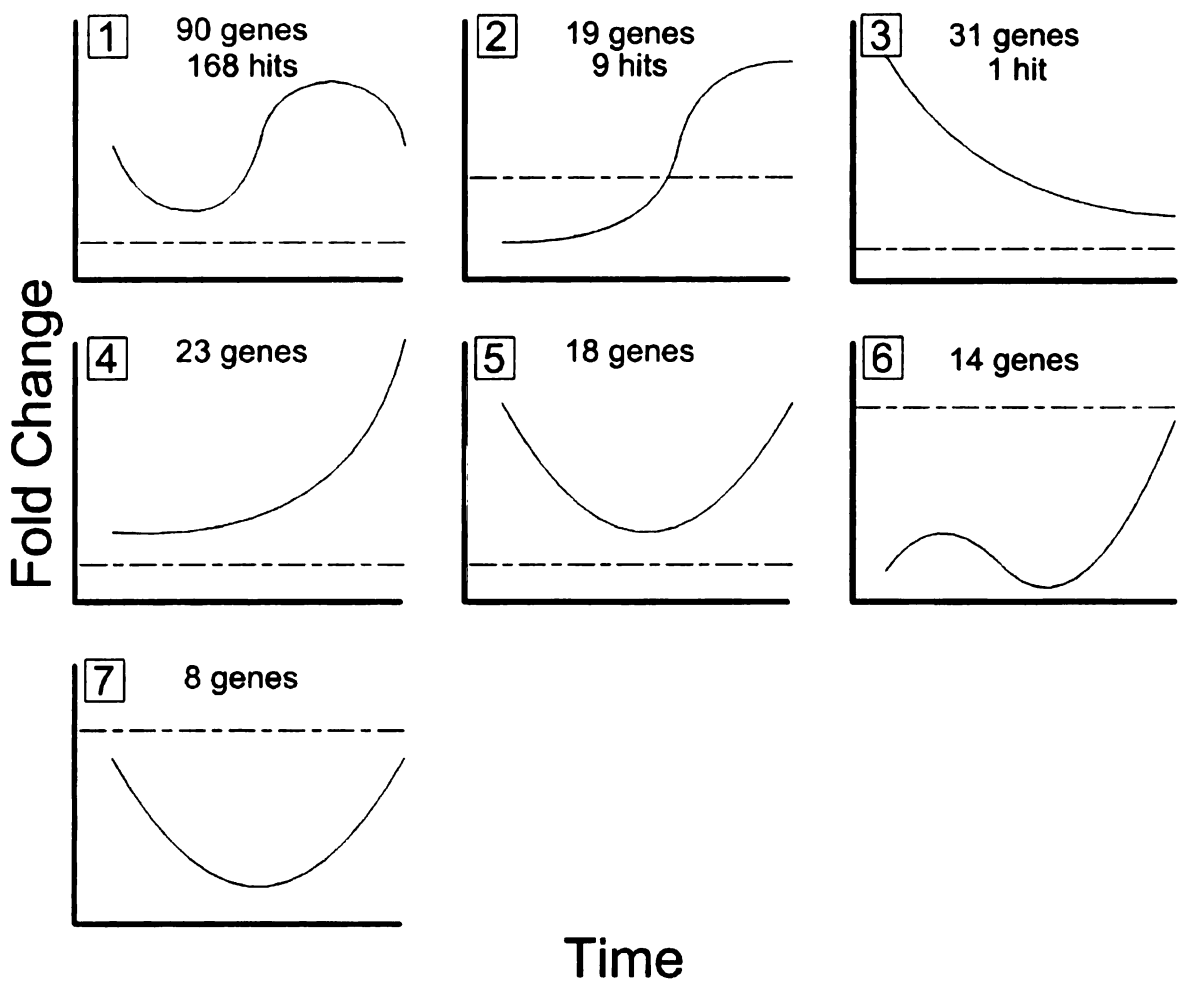

DISCUSSION

The rodent uterotrophic assay is a well established model to study the physiological and morphological effects elicited by estrogenic compounds (91). It has been used to examine the differential uterine gene expression elicited by EE (144,159,198,255) and more recently, the partial agonist effects of TAM (244). Previous studies have demonstrated that TAM inhibits estrogen-induced increases in UWW (84,85), however the effects of cotreatment on gene expression have not been comprehensively examined. In this study, we have used our previously reported EE and TAM differential gene expression data (144,159,244). to further investigate the inhibition of EE-induced uterotrophy by TAM co-treatment using the same model, study design and analysis methods. Moreover, we are also able to re-examine many widely held hypotheses regarding the mechanisms involved in the anti-estrogenicity of TAM.

This study demonstrates that TAM inhibited EE induction of UWW by approximately 50% in immature, ovariectomized C57BL6 mice, comparable to the levels of suppression previously reported (84,200,256). Histologically, TAM co-treatment inhibited EE-induction of luminal circumference but did not antagonize EE-induced LECH, suggesting that the antagonism of proliferation is cell type-specific. Differential gene expression data also indicates that the antagonism is not global since the majority of EE elicited responses were not affected by TAM cotreatment. Of the 2518 EE-elicited differential gene responses, only 290 were affected by TAM cotreatment, with 214 exhibiting

repression and 76 exhibiting enhanced responses, relative to EE treatment alone. Consequently, only a small subset of EE-elicited differential gene expression is affected by TAM, thus indicating that competition for ER binding TAM (51), and down-regulation of ER gene expression (257), does not sufficiently explain the more complex interactions resulting in the inhibition of EE-induced UWW increases (258).

Examination of the functions of EE-elicited gene expression affected by TAM is consistent with the inhibition of EE-induced UWW. For example, several genes associated with growth and proliferation were repressed by TAM at early time points (Figure 9a), including *Myc*, *Jun*, and *Fos*. The proliferation-regulating, uterine-expressed transcription factors, *Fosl2* (259), *Ets1* and *Ets2* (260), as well as estrogen-responsive proliferation-associated *Gtpbp4* (261,262), uterotrophy-associated *Gnl3* (263) and stromal cell differentiation regulator *Socs3* (*Socs3*; 4hrs) (264) were also repressed. Group A proliferation related genes including *Stx2* (265), estrogen responsive *Clu*, mouse uterus-expressed *Popdc2* (266) and *Gja1* found in human myometrium (267) were also all found to be repressed at later time points. The EE elicited repression of some genes was also minimized (Fig. 9c). Growth arrest specific 1 (*Gas1*) expression, which is repressed by *Myc* (268), is consistent with the inhibition of EE-induced *Myc*, thus consistent with the repression of uterotrophy by *Gas1*. In addition, the endometrial expression of *Cirbp,* which exhibits an inverse relationship with proliferation (269), was de-repressed by TAM, also consistent with the antagonism of UWW increases by EE.

Furthermore, TAM enhanced the induction and repression of some EE-elicited gene expression changes (Groups B and D). Although these responses appear counter intuitive, several of these changes are consistent with the repression of the EE-induced uterotrophic effect. For example, over-expression of *Atf4* impairs mammary proliferation and development (270) and *Cdkn1a* is known to promote growth arrest and apoptotic pathways (271). These responses provide further support for a transcriptional role in MIX-repression of EE-induced uterine weight. However, there were also late differential gene expression responses by EE that were enhanced by TAM cotreatment that are consistent with proliferation (Group B). *Crip1*, which is up-regulated in proliferating mammary luminal epithelial cells (272), *Cdc2l1* (273) and endometrium expressed *Tgfa* (274), all exhibited enhanced differential expression at later time points. This enhanced expression may be an attempt to over compensate for the limited induction of UWW in response to the majority of gene expression changes that were otherwise unaffected under TAM co-treatment.

Cytoskeletal reorganization is integral to estrogen-mediated restructuring of proliferating tissue (198). Several genes associated with the cytoskeleton including *Bicd2* (275), *Dctn2* (276) and *Mfap5* (277) were induced by EE and repressed following TAM cotreatment (Group A), consistent with the inhibition of uterotrophy. Although, these genes have not been identified to be ER-regulated, their differential expression serves to prepare the tissue for proliferation.

Binding studies indicate that 33:1 TAM to EE ratio is insufficient to displace greater than 50% of estrogen bound to ER (278). Furthermore,

estrogen is ~200,000-fold more potent than TAM in eliciting a DNA synthesis response in mouse uterus (279). In addition, some genes such as *Fos* and *Ndufb9* (Figure 10), exhibited intermediate behavior where cotreatment induced a response that was greater than TAM alone but less than EE alone. Collectively, these results suggest that the inhibitory effects of TAM are not simply a result of TAM saturation of the ER.

SERM activity is based on the ability to differentially affect various tissue types (31,280). This study is the first to demonstrate that TAM also elicits selective *in vivo* gene expression responses within the uterus. Estrogen and 4OH-TAM cotreatment studies in MCF-7 cells have identified genes that exhibit comparable patterns of antagonism. For example, Group A genes *Fosl2*, *Asns* (225) and *Fos* (229), Group C genes *Il1r1*, *Tm4sf1*, and *Ifi30* (229) exhibited similar gene expression behavior in MCF-7 cells and C57BL/6 uterine tissue. Differences in study design, microarray platforms, gene representation on the arrays, and data analysis are significant factors that limit the number of genes affected by TAM co-treatment in both models. For example, there are significant differences in ER protein levels (31), tissue specific co-regulating factor availability (237,246) as well as gene-specific thresholds of activation (238) that likely confound comparisons between human breast cancer MCF-7 cells and mouse uterine gene expression profiles.

Conclusions:

This study represents the first comprehensive *in vivo* investigation of the anti-estrogenic effects of TAM on uterine gene expression. Repression of EE-induced uterotrophy, by TAM co-treatment, did not globally repress all EE-mediated gene expression. In contrast, only a select subset was affected which include genes associated with cellular growth and proliferation, consistent with an anti-uterotrophic effect. However, comparative studies in the rat or more sophisticated transgenic approaches are required to conclusively demonstrate the importance of these potential targets in uterine proliferation and growth and as critical TAM targets for the inhibition of EE-induced increases in UWW.

CHAPTER 5

SUMMARY AND FUTURE PERSPECTIVES

The preceding studies have examined mouse *in vitro* liver and *in vivo* uterus as models to examine gene expression changes elicited by estrogenic compounds. Although serum deprived Hepa-1c1c7 cells only demonstrated changes of small magnitude to a potent estrogen, the responses under serum-supplemented conditions did correlate with the diverse responses found *in vivo*. Identification of a more appropriate *in vitro* model would facilitate high-throughput screening of less potent estrogenic compounds with respect to risk assessment and pharmaceutical analysis. Furthermore, characterization of suitable rodent and human *in vitro* models would allow comparative analyses not feasible *in vivo*.

The uterus of the immature, ovariectomized mouse is an excellent model to characterize changes elicited by TAM and examine mixture effects between TAM and EE, due to its well characterized physiological, histological and gene expression responses to estrogens. TAM is a known partial agonist, thus it was not surprising to identify numerous differentially expressed genes associated with cell growth and proliferation. These studies also identified genes which may contribute to the limited uterotrophic effect compared to EE, and through genes uniquely activated by TAM.

Foundational microarray studies of EE, as a positive control, on rodent uterine and hepatic systems have established a baseline, which have been extended to included responses elicited by TAM. These results further support the identification and development of estrogen receptor-specific biomarkers

suitable for high-throughput screening. Collecting differential gene expression data elicited by structurally diverse ER ligands may also be used to investigate structure and function relationships important in target-specific pharmaceuticals.

The benefits of intra-lab microarray studies are also demonstrated through these studies. Early establishment of a comprehensive study design minimizes the need to repeat foundational studies, and facilitate comparisons to other compounds of interest. Also, utilizing the same model, experimental procedures, microarray platform, and data analysis methods reduces the variables that may confound comparisons and data interpretation in future studies examining other ligands, tissues or model systems.

The EE and TAM mixture study demonstrated that only a subset of genes exhibit differential expression when compared to independent treatment. Moreover, the transcriptional changes, elicited by the EE and TAM mixture, correlate with the observed physiological changes. These results present new questions regarding the regulation of responsive genes that exhibit differential regulation following treatment of EE alone, TAM alone and EE and TAM cotreatment.

These mixture studies also further elucidated the characteristics of SERMs. SERMs were initially defined as compounds eliciting differing responses between organs. For example, TAM exhibits anti-estrogenic activities in mammary tissue and partial agonist activities in the uterus. These results indicate that TAM elicits differential gene expression regulation within the uterus, many of which are similar to those elicited by full agonist, EE. Thus, the activities

SERMs, and other compounds, can be more accurately classified using microarray technology. These types of data may be beneficial to the development and characterization of new, target-specific drugs.

Executing a mixture study revealed novel experimental considerations. This includes the use of additional concentrations of the compounds as well as alternate ratio combinations in order to more comprehensively assess the effects of a mixture. In addition, there may be different responses if other endpoints, such as rate of DNA replication, were selected, which could be important for risk assessment and drug development. Such considerations are applicable to all mixture studies as standard experimental designs have yet to be defined.

Consequently, this thesis demonstrates the importance of a solid foundation of experimental procedures, based on a comprehensive design, to optimize future comparative efforts. The analysis of TAM data is enriched due to the availability of well-established EE data as a baseline for comparison. Furthermore, the modifications to the experimental design, to facilitate the comparison between two compounds, have resulted in sound, reproducible data. These results demonstrate the utility of the approach that may be used as a basis for future two-compound mixture studies.

REFERENCES

1. U.S.EPA. (1998) *Federal Register* **63**, 71542-71568

2. Fry, D. M., and Toone, C. K. (1981) *Science* **213**, 922-924

3. Guillette, L. J., Jr., Gross, T. S., Masson, G. R., Matter, J. M., Percival, H. F., and Woodward, A. R. (1994) *Environ Health Perspect* **102**, 680-688

4. Burkhart, J. G., Helgen, J. C., Fort, D. J., Gallagher, K., Bowers, D., Propst, T. L., Gernes, M., Magner, J., Shelby, M. D., and Lucier, G. (1998) *Environ Health Perspect* **106**, 841-848

5. Hagel, P., and Tuinstra, L. G. (1978) *Bull Environ Contam Toxicol* **19**, 671-676

6. Watanabe, I., Yakushiji, T., Kuwabara, K., Yoshida, S., Maeda, K., Kashimoto, T., Koyama, K., and Kunita, N. (1979) *Arch Environ Contam Toxicol* **8**, 67-75

7. Schwartz, P. M., Jacobson, S. W., Fein, G., Jacobson, J. L., and Price, H. A. (1983) *Am J Public Health* **73**, 293-296

8. Cordle, F., Locke, R., and Springer, J. (1982) *Environ Health Perspect* **45**, 171-182

9. Cooke, P. S., Selvaraj, V., and Yellayi, S. (2006) *J Nutr* **136**, 704-708

10. Cheek, A. O., Vonier, P. M., Oberdorster, E., Burow, B. C., and McLachlan, J. A. (1998) *Environ Health Perspect* **106 Suppl 1**, 5-10

11. Rice, S., and Whitehead, S. A. (2006) *Endocr Relat Cancer* **13**, 995-1015

12. Ito, Y., Fisher, C. R., Conte, F. A., Grumbach, M. M., and Simpson, E. R. (1993) *Proc Natl Acad Sci U S A* **90**, 11673-11677

13. Conte, F. A., Grumbach, M. M., Ito, Y., Fisher, C. R., and Simpson, E. R. (1994) *J Clin Endocrinol Metab* **78**, 1287-1292

14. Jones, M. E., Boon, W. C., McInnes, K., Maffei, L., Carani, C., and Simpson, E. R. (2007) *Nat Clin Pract Endocrinol Metab* **3**, 414-421

15. Punyadeera, C., Verbost, P., and Groothuis, P. (2003) *J Steroid Biochem Mol Biol* **84**, 393-410

16. Kuiper, G. G., Carlsson, B., Grandien, K., Enmark, E., Haggblad, J., Nilsson, S., and Gustafsson, J. A. (1997) *Endocrinology* **138**, 863-870

17. Harris, H. A. (2007) *Mol Endocrinol* **21**, 1-13

18. Curtis Hewitt, S., Couse, J. F., and Korach, K. S. (2000) *Breast Cancer Res* **2**, 345-352

19. Moras, D., and Gronemeyer, H. (1998) *Curr Opin Cell Biol* **10**, 384-391

20. Nichols, M., Rientjes, J. M., and Stewart, A. F. (1998) *Embo J* **17**, 765-773

21. Saunders, P. T. (1998) *Rev Reprod* **3**, 164-171

22. Sabbah, M., Radanyi, C., Redeuilh, G., and Baulieu, E. E. (1996) *Biochem J* **314 (Pt 1)**, 205-213

23. Hall, J. M., Couse, J. F., and Korach, K. S. (2001) *J Biol Chem* **276**, 36869-36872

24. Klein-Hitpass, L., Schorpp, M., Wagner, U., and Ryffel, G. U. (1986) *Cell* **46**, 1053-1061

25. Klinge, C. M. (2001) *Nucleic Acids Res* **29**, 2905-2919

26. Bourdeau, V., Deschenes, J., Metivier, R., Nagai, Y., Nguyen, D., Bretschneider, N., Gannon, F., White, J. H., and Mader, S. (2004) *Mol Endocrinol* **18**, 1411-1427

27. Carroll, J. S., Meyer, C. A., Song, J., Li, W., Geistlinger, T. R., Eeckhoute, J., Brodsky, A. S., Keeton, E. K., Fertuck, K. C., Hall, G. F., Wang, Q., Bekiranov, S., Sementchenko, V., Fox, E. A., Silver, P. A., Gingeras, T. R., Liu, X. S., and Brown, M. (2006) *Nat Genet* **38**, 1289-1297

28. Klinge, C. M., Jernigan, S. C., Smith, S. L., Tyulmenkov, V. V., and Kulakosky, P. C. (2001) *Mol Cell Endocrinol* **174**, 151-166

29. Hall, J. M., McDonnell, D. P., and Korach, K. S. (2002) *Mol Endocrinol* **16**, 469-486

30. Zhou, G., Cummings, R., Li, Y., Mitra, S., Wilkinson, H. A., Elbrecht, A., Hermes, J. D., Schaeffer, J. M., Smith, R. G., and Moller, D. E. (1998) *Mol Endocrinol* **12**, 1594-1604

31. Shang, Y., and Brown, M. (2002) *Science* **295**, 2465-2468

32. Heery, D. M., Kalkhoven, E., Hoare, S., and Parker, M. G. (1997) *Nature* **387**, 733-736

33. Edwards, D. P. (2000) *J Mammary Gland Biol Neoplasia* **5**, 307-324

34. Das, D., Peterson, R. C., and Scovell, W. M. (2004) *Mol Endocrinol* **18**, 2616-2632

35. Kato, S. (2001) *Breast Cancer* **8**, 3-9

36. Kushner, P. J., Agard, D. A., Greene, G. L., Scanlan, T. S., Shiau, A. K., Uht, R. M., and Webb, P. (2000) *J Steroid Biochem Mol Biol* **74**, 311-317

37. Dong, J., Tsai-Morris, C. H., and Dufau, M. L. (2006) *J Biol Chem* **281**, 18825-18836

38. Zaitsu, M., Narita, S., Lambert, K. C., Grady, J. J., Estes, D. M., Curran, E. M., Brooks, E. G., Watson, C. S., Goldblum, R. M., and Midoro-Horiuti, T. (2007) *Mol Immunol* **44**, 1977-1985

39. Witorsch, R. J. (2002) *Regul Toxicol Pharmacol* **36**, 118-130

40. U.S.EPA. (2005) *Federal Register* **70**, 56449-56465

41. Van den Belt, K., Berckmans, P., Vangenechten, C., Verheyen, R., and Witters, H. (2004) *Aquat Toxicol* **66**, 183-195

42. Herbst, A. L., Ulfelder, H., and Poskanzer, D. C. (1971) *N Engl J Med* **284**, 878-881

43. Klopper, A. (1976) *Br Med J* **2**, 414-416

44. Jordan, V. C., and Brodie, A. M. (2007) *Steroids* **72**, 7-25

45. Omoto, Y., and Hayashi, S. (2002) *Breast Cancer* **9**, 308-311

46. Lewis, J. S., and Jordan, V. C. (2005) *Mutat Res* **591**, 247-263

47. Jordan, V. C., Collins, M. M., Rowsby, L., and Prestwich, G. (1977) *J Endocrinol* **75**, 305-316

48. Brodie, A., Sabnis, G., and Macedo, L. (2007) *J Steroid Biochem Mol Biol*

49. Zheng, A., Kallio, A., and Harkonen, P. (2007) *Endocrinology* **148**, 2764-2777

50. Fritah, A., Redeuilh, G., and Sabbah, M. (2006) *J Endocrinol* **191**, 613-624

51. Robertson, D. W., Katzenellenbogen, J. A., Long, D. J., Rorke, E. A., and Katzenellenbogen, B. S. (1982) *J Steroid Biochem* **16**, 1-13

52. Robinson, S. P., Langan-Fahey, S. M., Johnson, D. A., and Jordan, V. C. (1991) *Drug Metab Dispos* **19**, 36-43

53. Johnson, M. D., Zuo, H., Lee, K. H., Trebley, J. P., Rae, J. M., Weatherman, R. V., Desta, Z., Flockhart, D. A., and Skaar, T. C. (2004) *Breast Cancer Res Treat* **85**, 151-159

54. Garber, K. (2005) *J Natl Cancer Inst* **97**, 412-413

55. Stearns, V., Johnson, M. D., Rae, J. M., Morocho, A., Novielli, A., Bhargava, P., Hayes, D. F., Desta, Z., and Flockhart, D. A. (2003) *J Natl Cancer Inst* **95**, 1758-1764

56. Lim, C. K., Yuan, Z. X., Lamb, J. H., White, I. N., De Matteis, F., and Smith, L. L. (1994) *Carcinogenesis* **15**, 589-593

57. White, I. N. (2003) *Curr Drug Metab* **4**, 223-239

58. Houssami, N., Cuzick, J., and Dixon, J. M. (2006) *Med J Aust* **184**, 230-234

59. Bergman, L., Beelen, M. L., Gallee, M. P., Hollema, H., Benraadt, J., and van Leeuwen, F. E. (2000) *Lancet* **356**, 881-887

60. Smith, C. L., Nawaz, Z., and O'Malley, B. W. (1997) *Mol Endocrinol* **11**, 657-666

61. Badia, E., Duchesne, M. J., Semlali, A., Fuentes, M., Giamarchi, C., Richard-Foy, H., Nicolas, J. C., and Pons, M. (2000) *Cancer Res* **60**, 4130-4138

62. Dowers, T. S., Qin, Z. H., Thatcher, G. R., and Bolton, J. L. (2006) *Chem Res Toxicol* **19**, 1125-1137

63. Celik, L., Lund, J. D., and Schiott, B. (2007) *Biochemistry* **46**, 1743-1758

64. Pike, A. C., Brzozowski, A. M., Hubbard, R. E., Bonn, T., Thorsell, A. G., Engstrom, O., Ljunggren, J., Gustafsson, J. A., and Carlquist, M. (1999) *Embo J* **18**, 4608-4618

65. Wu, Y. L., Yang, X., Ren, Z., McDonnell, D. P., Norris, J. D., Willson, T. M., and Greene, G. L. (2005) *Mol Cell* **18**, 413-424

66. Shiau, A. K., Barstad, D., Loria, P. M., Cheng, L., Kushner, P. J., Agard, D. A., and Greene, G. L. (1998) *Cell* **95**, 927-937

67. Ciana, P., Di Luccio, G., Belcredito, S., Pollio, G., Vegeto, E., Tatangelo, L., Tiveron, C., and Maggi, A. (2001) *Mol Endocrinol* **15**, 1104-1113

68. Ciana, P., Raviscioni, M., Mussi, P., Vegeto, E., Que, I., Parker, M. G., Lowik, C., and Maggi, A. (2003) *Nat Med* **9**, 82-86

69. Williams, C. M. (2004) *Proc Nutr Soc* **63**, 153-160

70. Blum, A., and Cannon, R. O., 3rd. (1998) *Curr Opin Lipidol* **9**, 575-586

71. Alvaro, D., Mancino, M. G., Onori, P., Franchitto, A., Alpini, G., Francis, H., Glaser, S., and Gaudio, E. (2006) *World J Gastroenterol* **12**, 3537-3545

72. Lewis, S. (2007) *Am Heart J* **153**, 182-188

73. Boverhof, D. R., Fertuck, K. C., Burgoon, L. D., Eckel, J. E., Gennings, C., and Zacharewski, T. R. (2004) *Carcinogenesis* **25**, 1277-1291

74. Hoffman, E. C., Reyes, H., Chu, F. F., Sander, F., Conley, L. H., Brooks, B. A., and Hankinson, O. (1991) *Science* **252**, 954-958

75. Reyes, H., Reisz-Porszasz, S., and Hankinson, O. (1992) *Science* **256**, 1193-1195

76. Bernhard, H. P., Darlington, G. J., and Ruddle, F. H. (1973) *Dev Biol* **35**, 83-96

77. Jeong, H. G., and Lee, S. S. (1998) *Cancer Lett* **133**, 177-184

78. Zacharewski, T., Harris, M., and Safe, S. (1991) *Biochem Pharmacol* **41**, 1931-1939

79. Darlington, G. J., Bernhard, H. P., Miller, R. A., and Ruddle, F. H. (1980) *J Natl Cancer Inst* **64**, 809-819

80. Hankinson, O. (1979) *Proc Natl Acad Sci U S A* **76**, 373-376

81. Fong, C. J., Burgoon, L. D., and Zacharewski, T. R. (2005) *Toxicol Sci* **86**, 342-353

82. Werle-Schneider, G., Wolfelschneider, A., von Brevern, M. C., Scheel, J., Storck, T., Muller, D., Glockner, R., Bartsch, H., and Bartelmann, M. (2006) *Int J Toxicol* **25**, 379-395

83. Jordan, V. C. (2006) *Br J Pharmacol* **147 Suppl 1**, S269-276

84. Jordan, V. C., Dix, C. J., Naylor, K. E., Prestwich, G., and Rowsby, L. (1978) *J Toxicol Environ Health* **4**, 363-390

85. Jordan, V. C., and Gosden, B. (1983) *Endocrinology* **113**, 463-468

86. Dassen, H., Punyadeera, C., Kamps, R., Klomp, J., Dunselman, G., Dijcks, F., de Goeij, A., Ederveen, A., and Groothuis, P. (2007) *Cell Mol Life Sci* **64**, 1009-1032

87. Reel, J. R., Lamb, I. J., and Neal, B. H. (1996) *Fundam Appl Toxicol* **34**, 288-305

88. Owens, J. W., and Ashby, J. (2002) *Crit Rev Toxicol* **32**, 445-520

89. Greenman, D. L., Dooley, K., and Breeden, C. R. (1977) *J Toxicol Environ Health* **3**, 589-597

90. (2007)

91. Diel, P., Schmidt, S., and Vollmer, G. (2002) *J Chromatogr B Analyt Technol Biomed Life Sci* **777**, 191-202

92. Lubahn, D. B., Moyer, J. S., Golding, T. S., Couse, J. F., Korach, K. S., and Smithies, O. (1993) *Proc Natl Acad Sci U S A* **90**, 11162-11166

93. Kuiper, G. G., and Gustafsson, J. A. (1997) *FEBS Lett* **410**, 87-90

94. Couse, J. F., Curtis Hewitt, S., and Korach, K. S. (2000) *J Steroid Biochem Mol Biol* **74**, 287-296

95. Krege, J. H., Hodgin, J. B., Couse, J. F., Enmark, E., Warner, M., Mahler, J. F., Sar, M., Korach, K. S., Gustafsson, J. A., and Smithies, O. (1998) *Proc Natl Acad Sci U S A* **95**, 15677-15682

96. Jakacka, M., Ito, M., Weiss, J., Chien, P. Y., Gehm, B. D., and Jameson, J. L. (2001) *J Biol Chem* **276**, 13615-13621

97. Jakacka, M., Ito, M., Martinson, F., Ishikawa, T., Lee, E. J., and Jameson, J. L. (2002) *Mol Endocrinol* **16**, 2188-2201

98. O'Brien, J. E., Peterson, T. J., Tong, M. H., Lee, E. J., Pfaff, L. E., Hewitt, S. C., Korach, K. S., Weiss, J., and Jameson, J. L. (2006) *J Biol Chem* **281**, 26683-26692

99. U.S.EPA. (1989) Vol. 1, United States Environmental Protection Agency, Washington, DC

100. Berenbaum, M. C. (1981) *Adv Cancer Res* **35**, 269-335

101. Deneer, J. W. (2000) *Pest Management Science* **56**, 516-520

102. Broderius, S. J., Kahl, M. D., Elonen, G. E., Hammermeister, D. E., and Hoglund, M. D. (2005) *Environ Toxicol Chem* **24**, 3117-3127

103. Schuler, L. J., Trimble, A. J., Belden, J. B., and Lydy, M. J. (2005) *Arch Environ Contam Toxicol* **49**, 173-177

104. Nebert, D. W., Dalton, T. P., Okey, A. B., and Gonzalez, F. J. (2004) *J Biol Chem* **279**, 23847-23850

105. Billiard, S. M., Timme-Laragy, A. R., Wassenberg, D. M., Cockman, C., and Di Giulio, R. T. (2006) *Toxicol Sci* **92**, 526-536

106. Barron, M. G., Carls, M. G., Heintz, R., and Rice, S. D. (2004) *Toxicol Sci* **78**, 60-67

107. Harper, N., Connor, K., Steinberg, M., and Safe, S. (1995) *Fundam Appl Toxicol* **27**, 131-139

108. U.S.EPA. (2000), United States Environmental Protection Agency, Washington, DC

109. Stork, L. G., Gennings, C., Carchman, R. A., Carter, W. H., Jr., Pounds, J., and Mumtaz, M. (2006) *Risk Anal* **26**, 1601-1612

110. Mowat, F. S., and Bundy, K. J. (2002) *Chemosphere* **49**, 499-513

111. Gennings, C., Carter, W. H., Jr., Carney, E. W., Charles, G. D., Gollapudi, B. B., and Carchman, R. A. (2004) *Toxicol Sci* **80**, 134-150

112. Moser, V. C., Simmons, J. E., and Gennings, C. (2006) *Toxicol Sci* **92**, 235-245

113. Charles, G. D., Gennings, C., Tornesi, B., Kan, H. L., Zacharewski, T. R., Bhaskar Gollapudi, B., and Carney, E. W. (2007) *Toxicol Appl Pharmacol* **218**, 280-288

114. Jonker, M. J., Svendsen, C., Bedaux, J. J., Bongers, M., and Kammenga, J. E. (2005) *Environ Toxicol Chem* **24**, 2701-2713

115. Andersen, M. E., and Dennison, J. E. (2004) *Environ Toxicol Pharm* **16**, 1-11

116. Rider, C. V., and LeBlanc, G. A. (2005) *Toxicol Sci* **87**, 520-528

117. Horrocks, C., Halse, R., Suzuki, R., and Shepherd, P. R. (2003) *Curr Opin Drug Discov Devel* **6**, 570-575

118. Baker, V. A. (2001) *Toxicol In Vitro* **15**, 413-419

119. Diel, P., Walter, A., Fritzemeier, K. H., Hegele-Hartung, C., and Knauthe, R. (1995) *J Steroid Biochem Mol Biol* **55**, 363-373

120. Lemmen, J. G., Arends, R. J., van Boxtel, A. L., van der Saag, P. T., and van der Burg, B. (2004) *J Mol Endocrinol* **32**, 689-701

121. Zajchowski, D. A., Kauser, K., Zhu, D., Webster, L., Aberle, S., White, F. A., 3rd, Liu, H. L., Humm, R., MacRobbie, J., Ponte, P., Hegele-Hartung, C., Knauthe, R., Fritzemeier, K. H., Vergona, R., and Rubanyi, G. M. (2000) *J Biol Chem* **275**, 15885-15894

122. Cato, A. C., Nestl, A., and Mink, S. (2002) *Sci STKE* **2002**, RE9

123. Hammond, G. L. (2002) *Obstet Gynecol Clin North Am* **29**, 411-423

124. Paech, K., Webb, P., Kuiper, G. G., Nilsson, S., Gustafsson, J., Kushner, P. J., and Scanlan, T. S. (1997) *Science* **277**, 1508-1510

125. Revelli, A., Massobrio, M., and Tesarik, J. (1998) *Endocr Rev* **19**, 3-17

126. Watson, C. S., Pappas, T. C., and Gametchu, B. (1995) *Environ Health Perspect* **103 Suppl 7**, 41-50

127. Wong, C. W., McNally, C., Nickbarg, E., Komm, B. S., and Cheskis, B. J. (2002) *Proc Natl Acad Sci U S A* **99**, 14783-14788

128. Research Technology Support Facility [http://www.genomics.msu.edu]

129. Rockett, J. C., and Dix, D. J. (1999) *Environ Health Perspect* **107**, 681-685

130. dbZACH Home Page: Zacharewski Laboratory [http://dbzach.fst.msu.edu]

131. Brazma, A., Hingamp, P., Quackenbush, J., Sherlock, G., Spellman, P., Stoeckert, C., Aach, J., Ansorge, W., Ball, C. A., Causton, H. C., Gaasterland, T., Glenisson, P., Holstege, F. C., Kim, I. F., Markowitz, V., Matese, J. C., Parkinson, H., Robinson, A., Sarkans, U., Schulze-Kremer, S., Stewart, J., Taylor, R., Vilo, J., and Vingron, M. (2001) *Nat Genet* **29**, 365-371

132. Mattes, W. B., Pettit, S. D., Sansone, S. A., Bushel, P. R., and Waters, M. D. (2004) *Environ Health Perspect* **112**, 495-505

133. Burgoon, L. D., Boutros, P. C., Dere, E., and Zacharewski, T. R. (2005) *Toxicol Sci*

134. Burgoon, L. D., Eckel-Passow, J. E., Gennings, C., Boverhof, D. R., Burt, J. W., Fong, C. J., and Zacharewski, T. (2005) *Nucleic Acids Research* **33**, e172

135. Eckel, J. E., Gennings, C., Chinchilli, V. M., Burgoon, L. D., and Zacharewski, T. R. (2004) *J Biopharm Stat* **14**, 647-670

136. Gene Home [http://www.ncbi.nlm.nih.gov/sites/entrez?db=gene]

137. the Gene Ontology [http://www.geneontology.org]

138. Primer3 Input (primer3/input.htm version 0.3.0 modified for WI) [http://frodo.wi.mit.edu/cgi-bin/primer3/primer3_www.cgi]

139. Wilkinson, R. F. (1993) in *Art To Science: In Tissue Culture* (HyClone Laboratories, I., ed) Vol. 12, pp. 1 - 10, HyClone Laboratories, Inc., Logan

140. Ignar-Trowbridge, D. M., Pimentel, M., Parker, M. G., McLachlan, J. A., and Korach, K. S. (1996) *Endocrinology* **137**, 1735-1744

141. Katzenellenbogen, B. S., and Norman, M. J. (1990) *Endocrinology* **126**, 891-898

142. Cappelletti, V., Fioravanti, L., Miodini, P., and Di Fronzo, G. (1996) *Tumour Biol* **17**, 290-298

143. Hyder, S. M., Chiappetta, C., and Stancel, G. M. (1999) *J Pharmacol Exp Ther* **290**, 740-747

144. Fertuck, K. C., Eckel, J. E., Gennings, C., and Zacharewski, T. R. (2003) *Physiol Genomics* **15**, 127-141

145. Curtis, S. W., Washburn, T., Sewall, C., DiAugustine, R., Lindzey, J., Couse, J. F., and Korach, K. S. (1996) *Proc Natl Acad Sci U S A* **93**, 12626-12630

146. Nelson, K. G., Takahashi, T., Bossert, N. L., Walmer, D. K., and McLachlan, J. A. (1991) *Proc Natl Acad Sci U S A* **88**, 21-25

147. Nunez, A. M., Berry, M., Imler, J. L., and Chambon, P. (1989) *Embo J* **8**, 823-829

148. Shi, H., and Teng, C. (1996) *Mol Endocrinol* **10**, 732-741

149. Tortora, G., Budillon, A., Yokozaki, H., Clair, T., Pepe, S., Merlo, G., Rohlff, C., and Cho-Chung, Y. S. (1994) *Cell Growth Differ* **5**, 753-759

150. Woodman, O. L., Missen, M. A., and Boujaoude, M. (2004) *J Cardiovasc Pharmacol* **44**, 155-163

151. Wolf, G., Hildenbrand, R., Schwar, C., Grobholz, R., Kaufmann, M., Stutte, H. J., Strebhardt, K., and Bleyl, U. (2000) *Pathol Res Pract* **196**, 753-759

152. Rider, V., Foster, R. T., Evans, M., Suenaga, R., and Abdou, N. I. (1998) *Clin Immunol Immunopathol* **89**, 171-180

153. Salvatori, L., Ravenna, L., Felli, M. P., Cardillo, M. R., Russo, M. A., Frati, L., Gulino, A., and Petrangeli, E. (2000) *Endocrinology* **141**, 2266-2274

154. Currie, M. J., Hanrahan, V., Gunningham, S. P., Morrin, H. R., Frampton, C., Han, C., Robinson, B. A., and Fox, S. B. (2004) *J Clin Pathol* **57**, 829-834

155. Gray, K., Eitzman, B., Raszmann, K., Steed, T., Geboff, A., McLachlan, J., and Bidwell, M. (1995) *Endocrinology* **136**, 2325-2340

156. Albrecht, E. D., Robb, V. A., and Pepe, G. J. (2004) *J Clin Endocrinol Metab* **89**, 5803-5809

157. Tam, S. P., Archer, T. K., and Deeley, R. G. (1985) *J Biol Chem* **260**, 1670-1675

158. Dabrowska, M., Palka, J., Wolczynski, S., Pietruczuk, M., and Osada, J. (2001) *Gynecol Obstet Invest* **51**, 248-253

159. Kwekel, J. C., Burgoon, L. D., Burt, J. W., Harkema, J. R., and Zacharewski, T. R. (2005) *Physiol Genomics* **23**, 327-342

160. Hsu, C. Y., and Frankel, F. R. (1987) *J Biol Chem* **262**, 9594-9600

161. Whitehead, I. P., Abe, K., Gorski, J. L., and Der, C. J. (1998) *Mol Cell Biol* **18**, 4689-4697

162. Szelei, J., Soto, A. M., Geck, P., Desronvil, M., Prechtl, N. V., Weill, B. C., and Sonnenschein, C. (2000) *J Steroid Biochem Mol Biol* **72**, 89-102

163. Kipp, J. L., and Ramirez, V. D. (2003) *Neuroendocrinology* **77**, 258-272

164. Choi, I., Gudas, L. J., and Katzenellenbogen, B. S. (2000) *Mol Cell Endocrinol* **164**, 225-237

165. Vijayalakshmi, V., and Gupta, P. D. (1994) *Exp Cell Res* **214**, 358-366

166. Piccone, C. M., Brazeau, G. A., and McCormick, K. M. (2005) *Exp Physiol* **90**, 87-93

167. Naciff, J. M., Jump, M. L., Torontali, S. M., Carr, G. J., Tiesman, J. P., Overmann, G. J., and Daston, G. P. (2002) *Toxicol Sci* **68**, 184-199

168. Srivastava, R. A., Srivastava, N., Averna, M., Lin, R. C., Korach, K. S., Lubahn, D. B., and Schonfeld, G. (1997) *J Biol Chem* **272**, 33360-33366

169. Archer, T. K., Tam, S. P., Deugau, K. V., and Deeley, R. G. (1985) *J Biol Chem* **260**, 1676-1681

170. Ness, G. C., and Chambers, C. M. (2000) *Proc Soc Exp Biol Med* **224**, 8-19

171. Watanabe, H., Suzuki, A., Mizutani, T., Khono, S., Lubahn, D. B., Handa, H., and Iguchi, T. (2002) *Genes Cells* **7**, 497-507

172. Lopez, D., Sanchez, M. D., Shea-Eaton, W., and McLean, M. P. (2002) *Endocrinology* **143**, 2155-2168

173. Wu, X., Pang, S. T., Sahlin, L., Blanck, A., Norstedt, G., and Flores-Morales, A. (2003) *Biol Reprod* **69**, 1308-1317

174. Singh, R. P., Kumar, R., and Kapur, N. (2003) *J Environ Pathol Toxicol Oncol* **22**, 75-92

175. Toda, K., Takeda, K., Akira, S., Saibara, T., Okada, T., Onishi, S., and Shizuta, Y. (2001) *J Steroid Biochem Mol Biol* **79**, 11-17

176. Nemoto, Y., Toda, K., Ono, M., Fujikawa-Adachi, K., Saibara, T., Onishi, S., Enzan, H., Okada, T., and Shizuta, Y. (2000) *J Clin Invest* **105**, 1819-1825

177. Hatta, H., Atomi, Y., Shinohara, S., Yamamoto, Y., and Yamada, S. (1988) *Horm Metab Res* **20**, 609-611

178. Grist, M., Wambolt, R. B., Bondy, G. P., English, D. R., and Allard, M. F. (2002) *Can J Physiol Pharmacol* **80**, 1001-1007

179. Dannan, G. A., Porubek, D. J., Nelson, S. D., Waxman, D. J., and Guengerich, F. P. (1986) *Endocrinology* **118**, 1952-1960

180. Liehr, J. G., and Roy, D. (1990) *Free Radic Biol Med* **8**, 415-423

181. Lee, S. S., Jeong, H. G., and Yang, K. H. (1998) *Biochem Mol Biol Int* **45**, 775-781

182. Sakuma, T., Takai, M., Endo, Y., Kuroiwa, M., Ohara, A., Jarukamjorn, K., Honma, R., and Nemoto, N. (2000) *Arch Biochem Biophys* **377**, 153-162

183. Broccardo, C. J., Billings, R. E., Chubb, L. S., Andersen, M. E., and Hanneman, W. H. (2004) *Toxicol Sci* **78**, 287-294

184. Mandlekar, S., Hebbar, V., Christov, K., and Kong, A. N. (2000) *Cancer Res* **60**, 6601-6606

185. Jordan, V. C. (1993) *Br J Pharmacol* **110**, 507-517

186. Wijayaratne, A. L., Nagel, S. C., Paige, L. A., Christensen, D. J., Norris, J. D., Fowlkes, D. M., and McDonnell, D. P. (1999) *Endocrinology* **140**, 5828-5840

187. Fisher, D. E. (1994) *Cell* **78**, 539-542

188. Carthew, P., Edwards, R. E., Nolan, B. M., Tucker, M. J., and Smith, L. L. (1999) *Toxicol Sci* **48**, 197-205

189. Kohlerova, E., and Skarda, J. (2004) *J Vet Med A Physiol Pathol Clin Med* **51**, 209-217

190. Osborne, C. K., Zhao, H., and Fuqua, S. A. (2000) *J Clin Oncol* **18**, 3172-3186

191. Vogel, V. G., Costantino, J. P., Wickerham, D. L., Cronin, W. M., Cecchini, R. S., Atkins, J. N., Bevers, T. B., Fehrenbacher, L., Pajon, E. R., Jr., Wade, J. L., 3rd, Robidoux, A., Margolese, R. G., James, J., Lippman, S. M., Runowicz, C. D., Ganz, P. A., Reis, S. E., McCaskill-Stevens, W., Ford, L. G., Jordan, V. C., and Wolmark, N. (2006) *Jama* **295**, 2727-2741

192. Human Pathology @ Michigan State University [http://www.humanpathology.msu.edu/histology]

193. Burgoon, L. D., Eckel-Passow, J. E., Gennings, C., Boverhof, D. R., Burt, J. W., Fong, C. J., and Zacharewski, T. R. (2005) *Nucleic Acids Res* **33**, e172

194. Eckel, J. E., Gennings, C., Therneau, T. M., Burgoon, L. D., Boverhof, D. R., and Zacharewski, T. R. (2005) *Bioinformatics* **21**, 1078-1083

195. Carthew, P., Edwards, R. E., and Nolan, B. M. (1999) *Toxicol Appl Pharmacol* **158**, 24-32

196. Jordan, V. C., and Dix, C. J. (1979) *J Steroid Biochem* **11**, 285-291

197. Loeb, L., Suntzeff, V., and Burns, E. L. (1938) *Am J Cancer* **34**, 413-427

198. Moggs, J. G., Tinwell, H., Spurway, T., Chang, H. S., Pate, I., Lim, F. L., Moore, D. J., Soames, A., Stuckey, R., Currie, R., Zhu, T., Kimber, I., Ashby, J., and Orphanides, G. (2004) *Environ Health Perspect* **112**, 1589-1606

199. Yuen, T., Wurmbach, E., Pfeffer, R. L., Ebersole, B. J., and Sealfon, S. C. (2002) *Nucleic Acids Res* **30**, e48

200. Black, L. J., and Goode, R. L. (1980) *Life Sci* **26**, 1453-1458

201. Fromson, J. M., Pearson, S., and Bramah, S. (1973) *Xenobiotica* **3**, 693-709

202. Fromson, J. M., Pearson, S., and Bramah, S. (1973) *Xenobiotica* **3**, 711-714

203. Kiriwat, O., and Fotherby, K. (1983) *Contraception* **27**, 153-160

204. Gray, C. A., Bartol, F. F., Tarleton, B. J., Wiley, A. A., Johnson, G. A., Bazer, F. W., and Spencer, T. E. (2001) *Biol Reprod* **65**, 1311-1323

205. Sanyal, A., Riggs, B. L., Spelsberg, T. C., and Khosla, S. (2005) *J Cell Biochem* **94**, 88-97

206. Boverhof, D. R., Burgoon, L. D., Tashiro, C., Chittim, B., Harkema, J. R., Jump, D. B., and Zacharewski, T. R. (2005) *Toxicol Sci* **85**, 1048-1063

207. Naciff, J. M., Overmann, G. J., Torontali, S. M., Carr, G. J., Tiesman, J. P., Richardson, B. D., and Daston, G. P. (2003) *Toxicol Sci* **72**, 314-330

208. Yamashita, S., Takayanagi, A., and Shimizu, N. (1996) *Endocrinology* **137**, 5468-5475

209. Fan, M., Yan, P. S., Hartman-Frey, C., Chen, L., Paik, H., Oyer, S. L., Salisbury, J. D., Cheng, A. S., Li, L., Abbosh, P. H., Huang, T. H., and Nephew, K. P. (2006) *Cancer Res* **66**, 11954-11966

210. Lai, M. D., Jiang, M. J., and Wing, L. Y. (2002) *Endocrine* **17**, 233-239

211. Kirkland, J. L., Murthy, L., and Stancel, G. M. (1993) *Mol Pharmacol* **43**, 709-714

212. Mylonas, I., Jeschke, U., Wiest, I., Hoeing, A., Vogl, J., Shabani, N., Kuhn, C., Schulze, S., Kupka, M. S., and Friese, K. (2004) *Histochem Cell Biol* **122**, 461-471

213. Nakayama, H., Sano, T., Motegi, A., Oyama, T., and Nakajima, T. (2005) *Pathol Int* **55**, 707-715

214. Krebs, J., Saremaslani, P., and Caduff, R. (2002) *Biochim Biophys Acta* **1600**, 68-73

215. Fernandez-Zapico, M. E., Gonzalez-Paz, N. C., Weiss, E., Savoy, D. N., Molina, J. R., Fonseca, R., Smyrk, T. C., Chari, S. T., Urrutia, R., and Billadeau, D. D. (2005) *Cancer Cell* **7**, 39-49

216. Mehus, J. G., Deloukas, P., and Lambeth, D. O. (1999) *Hum Genet* **104**, 454-459

217. Rampazzo, C., Kost-Alimova, M., Ruzzenente, B., Dumanski, J. P., and Bianchi, V. (2002) *Gene* **294**, 109-117

218. Jablonski, E. M., McConnell, N. A., Hughes, F. M., Jr., and Huet-Hudson, Y. M. (2003) *Biol Reprod* **69**, 1481-1487

219. Koyama, N., Ishibashi, K., Kuwahara, M., Inase, N., Ichioka, M., Sasaki, S., and Marumo, F. (1998) *Genomics* **54**, 169-172

220. Suzuki, T., Ishihara, K., Migaki, H., Matsuura, W., Kohda, A., Okumura, K., Nagao, M., Yamaguchi-Iwai, Y., and Kambe, T. (2005) *J Biol Chem* **280**, 637-643

221. McMahon, R. J., and Cousins, R. J. (1998) *J Nutr* **128**, 667-670

222. Lee, J. Y., Kim, J. H., Hong, S. H., Cherny, R. A., Bush, A. I., Palmiter, R. D., and Koh, J. Y. (2004) *J Biol Chem* **279**, 8602-8607

223. Burckhardt, B. C., and Burckhardt, G. (2003) *Rev Physiol Biochem Pharmacol* **146**, 95-158

224. Ljubojevic, M., Balen, D., Breljak, D., Kusan, M., Anzai, N., Bahn, A., Burckhardt, G., and Sabolic, I. (2006) *Am J Physiol Renal Physiol*

225. Inoue, A., Yoshida, N., Omoto, Y., Oguchi, S., Yamori, T., Kiyama, R., and Hayashi, S. (2002) *J Mol Endocrinol* **29**, 175-192

226. del Carmen Garcia Molina Wolgien, M., da Silva, I. D., Villanova, F. E., Yumi Otsuka, A., Borra, R. C., Lima Reis, L. F., Carvalho, A. F., Baracat, E. C., and Gebrim, L. H. (2005) *Eur J Gynaecol Oncol* **26**, 501-504

227. Scafoglio, C., Ambrosino, C., Cicatiello, L., Altucci, L., Ardovino, M., Bontempo, P., Medici, N., Molinari, A. M., Nebbioso, A., Facchiano, A., Calogero, R. A., Elkon, R., Menini, N., Ponzone, R., Biglia, N., Sismondi, P., Bortoli, M. D., and Weisz, A. (2006) *J Cell Biochem*

228. Gadal, F., Starzec, A., Bozic, C., Pillot-Brochet, C., Malinge, S., Ozanne, V., Vicenzi, J., Buffat, L., Perret, G., Iris, F., and Crepin, M. (2005) *J Mol Endocrinol* **34**, 61-75

229. Frasor, J., Stossi, F., Danes, J. M., Komm, B., Lyttle, C. R., and Katzenellenbogen, B. S. (2004) *Cancer Res* **64**, 1522-1533

230. Frasor, J., Chang, E. C., Komm, B., Lin, C. Y., Vega, V. B., Liu, E. T., Miller, L. D., Smeds, J., Bergh, J., and Katzenellenbogen, B. S. (2006) *Cancer Res* **66**, 7334-7340

231. Hodges, L. C., Cook, J. D., Lobenhofer, E. K., Li, L., Bennett, L., Bushel, P. R., Aldaz, C. M., Afshari, C. A., and Walker, C. L. (2003) *Mol Cancer Res* **1**, 300-311

232. Green, A. R., Styles, J. A., Parrott, E. L., Gray, D., Edwards, R. E., Smith, A. G., Gant, T. W., Greaves, P., Al-Azzawi, F., and White, I. N. (2005) *Exp Toxicol Pathol* **56**, 255-263

233. Robertson, D. W., Katzenellenbogen, J. A., Hayes, J. R., and Katzenellenbogen, B. S. (1982) *J Med Chem* **25**, 167-171

234. Dowsett, M., and Haynes, B. P. (2003) *J Steroid Biochem Mol Biol* **86**, 255-263

235. Giambiagi, N., and Pasqualini, J. R. (1988) *J Steroid Biochem* **30**, 213-217

236. McDonnell, D. P., Chang, C. Y., and Norris, J. D. (2000) *J Steroid Biochem Mol Biol* **74**, 327-335

237. Webb, P., Nguyen, P., and Kushner, P. J. (2003) *J Biol Chem* **278**, 6912-6920

238. Geum, D., Sun, W., Paik, S. K., Lee, C. C., and Kim, K. (1997) *Mol Reprod Dev* **46**, 450-458

239. Kazmin, D., Prytkova, T., Cook, C. E., Wolfinger, R., Chu, T. M., Beratan, D., Norris, J. D., Chang, C. Y., and McDonnell, D. P. (2006) *Mol Endocrinol* **20**, 1201-1217

240. Meijer, O. C., Kalkhoven, E., van der Laan, S., Steenbergen, P. J., Houtman, S. H., Dijkmans, T. F., Pearce, D., and de Kloet, E. R. (2005) *Endocrinology* **146**, 1438-1448

241. Goetz, M. P., Knox, S. K., Suman, V. J., Rae, J. M., Safgren, S. L., Ames, M. M., Visscher, D. W., Reynolds, C., Couch, F. J., Lingle, W. L., Weinshilboum, R. M., Fritcher, E. G., Nibbe, A. M., Desta, Z., Nguyen, A., Flockhart, D. A., Perez, E. A., and Ingle, J. N. (2007) *Breast Cancer Res Treat* **101**, 113-121

242. Deligdisch, L., Kalir, T., Cohen, C. J., de Latour, M., Le Bouedec, G., and Penault-Llorca, F. (2000) *Gynecol Oncol* **78**, 181-186

243. Mourits, M. J., De Vries, E. G., Willemse, P. H., Ten Hoor, K. A., Hollema, H., and Van der Zee, A. G. (2001) *Obstet Gynecol* **97**, 855-866

244. Fong, C. J., Burgoon, L. D., Williams, K. J., Forgacs, A. L., and Zacharewski, T. R. (2007) *BMC Genomics* **8**, 151

245. Brzozowski, A. M., Pike, A. C., Dauter, Z., Hubbard, R. E., Bonn, T., Engstrom, O., Ohman, L., Greene, G. L., Gustafsson, J. A., and Carlquist, M. (1997) *Nature* **389**, 753-758

246. McDonnell, D. P., Clemm, D. L., Hermann, T., Goldman, M. E., and Pike, J. W. (1995) *Mol Endocrinol* **9**, 659-669

247. Weatherman, R. V., Chang, C. Y., Clegg, N. J., Carroll, D. C., Day, R. N., Baxter, J. D., McDonnell, D. P., Scanlan, T. S., and Schaufele, F. (2002) *Mol Endocrinol* **16**, 487-496

248. Sourla, A., Luo, S., Labrie, C., Belanger, A., and Labrie, F. (1997) *Endocrinology* **138**, 5605-5617

249. Castellano-Diaz, E., Gonzalez-Quijano, M. I., Liminana, J. M., and Diaz-Chico, B. N. (1989) *J Steroid Biochem* **33**, 133-139

250. McInerney, E. M., and Katzenellenbogen, B. S. (1996) *J Biol Chem* **271**, 24172-24178

251. Yang, Y. H., and Speed, T. (2002) *Nat Rev Genet* **3**, 579-588

252. Tajima, F. (1991) *J Mol Evol* **33**, 470-473

253. Efron, B., and Tibshirani, R. (2002) *Genet Epidemiol* **23**, 70-86

254. Gene Regulation [http://www.gene-regulation.com/pub/databases.html#transfac]

255. Naciff, J. M., Overmann, G. J., Torontali, S. M., Carr, G. J., Khambatta, Z. S., Tiesman, J. P., Richardson, B. D., and Daston, G. P. (2007) *Toxicol Sci* **97**, 467-490

256. Jordan, V. C., Rowsby, L., Dix, C. J., and Prestwich, G. (1978) *J Endocrinol* **78**, 71-81

257. Koibuchi, Y., Iino, Y., Uchida, T., Andoh, T., Horii, Y., Nagasawa, M., Horiguchi, J., Maemura, M., Takei, H., Yokoe, T., and Morishita, Y. (2000) *Oncol Rep* **7**, 135-140

258. Mnif, W., Pascussi, J. M., Pillon, A., Escande, A., Bartegi, A., Nicolas, J. C., Cavailles, V., Duchesne, M. J., and Balaguer, P. (2007) *Toxicol Lett* **170**, 19-29

259. Bamberger, A. M., Milde-Langosch, K., Rossing, E., Goemann, C., and Loning, T. (2001) *J Cancer Res Clin Oncol* **127**, 545-550

260. Kilpatrick, L. M., Kola, I., and Salamonsen, L. A. (1999) *Biol Reprod* **61**, 120-126

261. Laping, N. J., Olson, B. A., and Zhu, Y. (2001) *J Am Soc Nephrol* **12**, 883-890

262. Wang, D. Y., McKague, B., Liss, S. N., and Edwards, E. A. (2004) *Environ Sci Technol* **38**, 6396-6406

263. Beekman, C., Nichane, M., De Clercq, S., Maetens, M., Floss, T., Wurst, W., Bellefroid, E., and Marine, J. C. (2006) *Mol Cell Biol* **26**, 9291-9301

264. Dimitriadis, E., Stoikos, C., Tan, Y. L., and Salamonsen, L. A. (2006) *Endocrinology* **147**, 3809-3817

265. Wang, Y., Wang, L., Iordanov, H., Swietlicki, E. A., Zheng, Q., Jiang, S., Tang, Y., Levin, M. S., and Rubin, D. C. (2006) *J Clin Invest* **116**, 1535-1546

266. Andree, B., Hillemann, T., Kessler-Icekson, G., Schmitt-John, T., Jockusch, H., Arnold, H. H., and Brand, T. (2000) *Dev Biol* **223**, 371-382

267. Cluff, A. H., Bystrom, B., Klimaviciute, A., Dahlqvist, C., Cebers, G., Malmstrom, A., and Ekman-Ordeberg, G. (2006) *Reprod Biol Endocrinol* **4**, 24

268. Lee, T. C., Li, L., Philipson, L., and Ziff, E. B. (1997) *Proc Natl Acad Sci U S A* **94**, 12886-12891

269. Hamid, A. A., Mandai, M., Fujita, J., Nanbu, K., Kariya, M., Kusakari, T., Fukuhara, K., and Fujii, S. (2003) *Int J Gynecol Pathol* **22**, 240-247

270. Bagheri-Yarmand, R., Vadlamudi, R. K., and Kumar, R. (2003) *J Biol Chem* **278**, 17421-17429

271. Qiao, L., McKinstry, R., Gupta, S., Gilfor, D., Windle, J. J., Hylemon, P. B., Grant, S., Fisher, P. B., and Dent, P. (2002) *Hepatology* **36**, 39-48

272. Mackay, A., Jones, C., Dexter, T., Silva, R. L., Bulmer, K., Jones, A., Simpson, P., Harris, R. A., Jat, P. S., Neville, A. M., Reis, L. F., Lakhani, S. R., and O'Hare, M. J. (2003) *Oncogene* **22**, 2680-2688

273. Wilker, E. W., van Vugt, M. A., Artim, S. A., Huang, P. H., Petersen, C. P., Reinhardt, H. C., Feng, Y., Sharp, P. A., Sonenberg, N., White, F. M., and Yaffe, M. B. (2007) *Nature* **446**, 329-332

274. Ejskjaer, K., Sorensen, B. S., Poulsen, S. S., Mogensen, O., Forman, A., and Nexo, E. (2005) *Mol Hum Reprod* **11**, 543-551

275. Hoogenraad, C. C., Wulf, P., Schiefermeier, N., Stepanova, T., Galjart, N., Small, J. V., Grosveld, F., de Zeeuw, C. I., and Akhmanova, A. (2003) *Embo J* **22**, 6004-6015

276. Uetake, Y., Terada, Y., Matuliene, J., and Kuriyama, R. (2004) *Cell Motil Cytoskeleton* **58**, 53-66

277. Lemaire, R., Bayle, J., Mecham, R. P., and Lafyatis, R. (2007) *J Biol Chem* **282**, 800-808

278. Levin, E., Tomchinsky, S., and Lopez, S. (1990) *J Steroid Biochem Mol Biol* **37**, 681-686

279. Zhang, H., McElrath, T., Tong, W., and Pollard, J. W. (2005) *J Endocrinol* **184**, 129-140

280. Jordan, V. C. (2007) *Nat Rev Cancer* **7**, 46-53